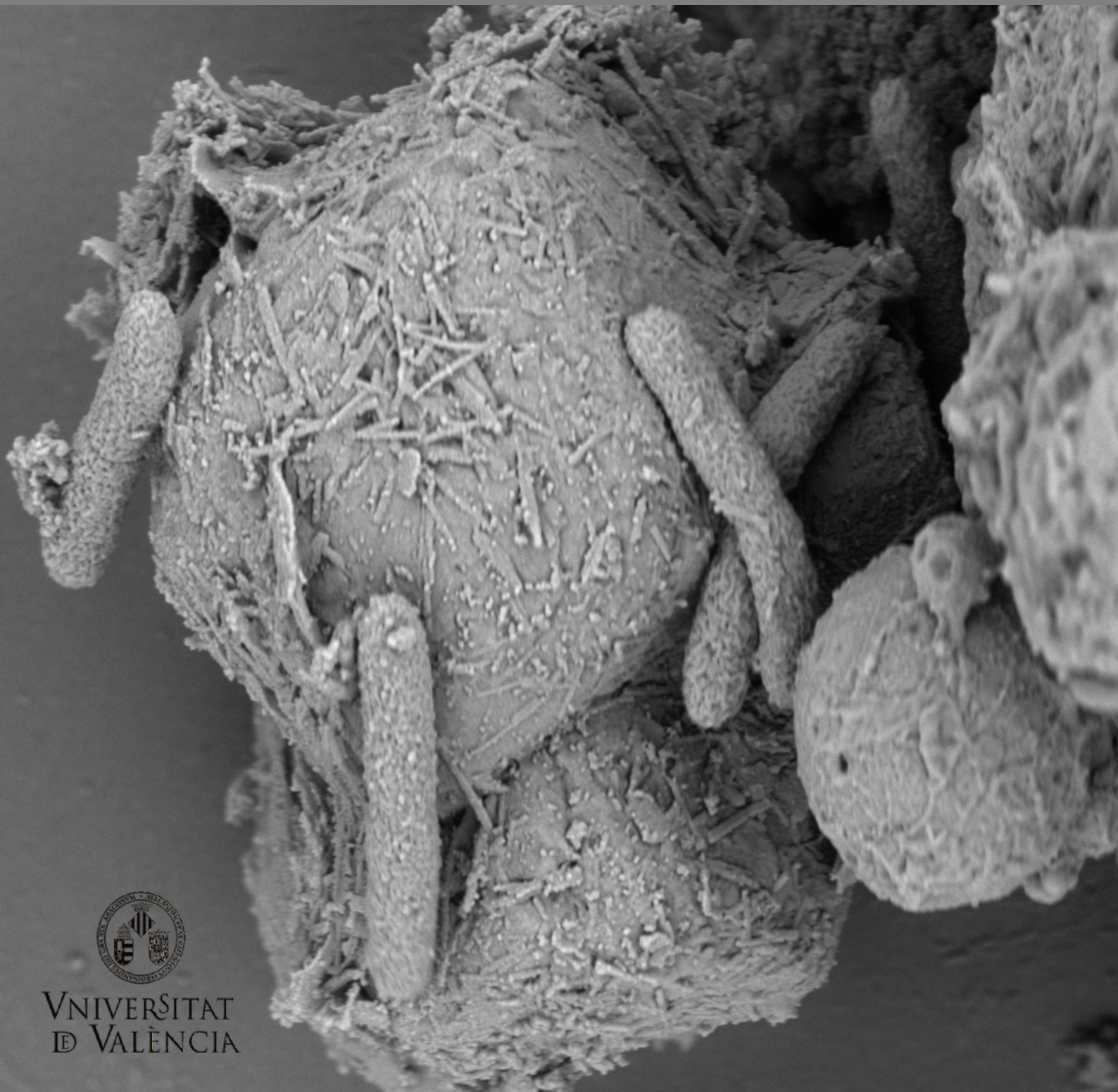


Doctoral Thesis
Immunotoxicity of metal nanoparticles
in *Eisenia andrei* earthworms



VNIVERSITAT
DE VALÈNCIA

Programa de doctorado en Contaminación, Toxicología y Sanidad Ambientales
PhD student: Natividad Isabel Navarro Pacheco

Supervisor: Andreu Rico Artero

Co-supervisors: Petra Prochazkova and Tomas Cajthaml

Tutor: Antonio Camacho González

September, 2022

Tesis Doctoral

Programa de doctorado 3108 en Contaminación, Toxicología y Sanidad

Ambientales



VNIVERSITAT
DE VALÈNCIA

Immunotoxicity of metal nanoparticles in *Eisenia andrei* earthworms

Immunotoxicidad de las nanopartículas metálicas en las lombrices terrestres

Eisenia andrei

Immunotoxicitat de les nanopartícules metàliques als cucs de terra *Eisenia andrei*

Memoria para optar al título de Doctora por

Natividad Isabel Navarro Pacheco

Director: Andreu Rico Artero

Cavanilles Institute of Biodiversity and Evolutionary Biology (ICBiBE), University of Valencia

Co-director: Petra Prochazkova

Institute of Microbiology of the Czech Academy of Sciences. Laboratory of Cellular and
Molecular Immunology

Co-director: Tomas Cajthaml

Institute of Microbiology of the Czech Academy of Sciences. Laboratory of Environmental
Biotechnology.

Institute for Environmental Studies, Faculty of Science, Charles University

Tutor: Antonio Camacho González

Cavanilles Institute of Biodiversity and Evolutionary Biology (ICBiBE), University of Valencia

Contents

	Pages
Contents	5-6
Figures and tables	7-10
Acknowledgements.....	11-14
List of abbreviations	15-18
Abstract.....	19-24
Resumen	25-32
Resum	33-40
Chapter 1: Introduction.....	41-64
Chapter 2. Research questions and hypothesis.....	65-68
Chapter 3. Material and methods.....	69-82
Chapter 4. Results.....	83-116
Chapter 5. Final discussion.....	117-140

Chapter 6. Conclusions.....141-144

Chapter 7. References145-158

Annex I.....159-164

Annex II. Chemicals and Instruments165-168

Curriculum vitae169-172

Figures and tables

	Pages
Figure 1. Zeta potential graph (mV).....	44
Figure 2. NPs fate.....	47
Figure 3. Earthworm anatomy.....	51
Figure 4. Immunology system evolution.....	52
Figure 5. Coelomocytes subsets.....	54
Figure 6. Recognition of PAMPs and DAMPs by PRRs.....	51
Figure 7. Summary of experimental set-up.....	71
Figure 8. TEM images of CuO, TiO ₂ , and Ag ₂ S NPs.....	86
Figure 9. SEM-EDS soil samples at the start.....	88
Figure 10. SEM-EDS soil samples after 14 days.....	89
Figure 11. Dissolution of CuO NPs in R-RPMI 1640 medium.....	90
Figure 12. Scanning electron microscopy of coelomocytes.....	92
Figure 13. EDS pictures and spectra.....	93
Figure 14. Scanning electron microscopy images of CuO NPs.....	94
Figure 15. EDS spectra of coelomocytes exposed to CuO NPs.....	95
Figure 16. Transmission electron microscopy and STEM/EDS microanalysis of coelomocytes exposed to CuO NPs.....	96
Figure 17. Coelomocytes subsets.....	98
Figure 18. Viability of coelomocytes.....	99
Figure 19. ROS production in HA and GA subpopulations.....	100
Figure 20. NO generation.....	101
Figure 21. Relative MDA production.....	102
Figure 22. MDA production.....	103

Figure 23. DNA Damage (%) 104

Figure 24. Phagocytic activity 105

Figure 25. Early apoptosis..... 106

Figure 26. Late apoptosis..... 107

Figure 27. Necrosis 108

Figure 28. Viability 109

Figure 29. Phenoloxidase activity (%) of coelomocytes 110

Figure 30. Weight loss of earthworms (mg)..... 115

Figure 31. Brown bodies formation 126

Figure 32. Illustrative comet 130

Figure 33. Trojan-horse effect 138

Figure 34. Illustrative image of FACS analyses..... 161

Figure 35. Illustrative image of ROS and phagocytosis..... 162

Figure 36. Illustrative image of apoptosis..... 163

Table 1. Summary of the recent studies of different species of earthworms and the biomarkers assessed..... 59-62

Table 2. Primer sequences..... 80

Table 3. UV/Vis spectra absorbance (nm), Hydrodynamic sized (Z-average; nm) and zeta potential 87

Table 4. The concentration of Ag⁺ ions in the soil and in the earthworms..... 91

Table 5. The mRNA levels of different molecules in coelomocytes exposed to 1 and 10 µg mL⁻¹ TiO₂ NPs 111

Table 6. The mRNA levels of different molecules in coelomocytes exposed to 1 and 10 µg mL⁻¹ CuO NPs 112-113

Table 7. The mRNA levels of different molecules in coelomocytes exposed to 1 and 10 µg mL⁻¹ CuSO₄ 114

Table 8. Chemicals and reagents 165-166

Table 9. Instruments 167-168

Acknowledgements

I believe that when you find what you like and what you do are the same, you feel motivated to do the best in your work. Of course, I also think that every effort, it has its own award. In this PhD thesis I have to thanks so many people who were involved in. They were part of the thesis or they supported me during that time. First of all, I would like to express my gratitude to Petra Prochazkova and the Laboratory of Cellular and Molecular Immunology in Prague (Czech Republic). Thanks to teach me what you knew about earthworms and how to work with them. I can't forget Jirka, Fanda and Radka, good colleagues that aided me during the PhD and the laughs we also shared in the meanwhile. Thanks for the teaching lessons and tips you gave me during the process of the PhD.

Oh! I almost forget the cytometry department and the electron microscopy department. Oldrich and Honza, thanks to teach me and show me how to work with your machines. Thanks for your patience with me. I know I was always asking but I wanted to learn a lot from both of you. Special thanks to Funda and Mila, you were my experts in resolving cytometry troubleshooting. I think between both of you and Honza, cytometry doesn't have any secrets for me.

Of course, Tomás and the Environmental biotechnology department in Prague. Thanks to welcome there and help me in so many steps I needed. I learned a lot in your laboratory and thanks to all the members of that laboratory. Special thanks to Jarda and Alena G. I couldn't choose the best colleagues to work with and discuss. Jarda for his experience in his PhD and Ala because she had always lovely words to cheer me on in my bad days. Ala, you are the next one to finish the PhD, it will be great.

I can't forget Andreu Rico, Amparo T., Antonio Camacho and the members of Andreu Rico laboratory. Gracias por la oportunidad que me habéis dado. Amparo por su gran trabajo y su gran apoyo, gracias por iluminarme en los días no tan claros y ayudarme en todo. Andreu, gracias por aceptarme y embarcarme en este doctorado conmigo. Creo que es de las pocas veces que no sabría cómo expresar la gratitud que os tengo por todo lo que habéis hecho por mí. También agradecer a Pablo, Conny y Ricardo porque sin saberlo, han hecho mucho por mí. Eso es algo que siempre llevaré conmigo.

However, I believe I must express my gratitude to Diana Boraschi, Paola and the rest of the members of the PANDORA project. Without this project, I would never be here writing this thesis and these words. Thanks to involve me in such an interesting project, to have such a great friends and colleagues to work with and all the experience that Marie Curie gave me. It has been a pleasure to be part of this project.

During my time abroad I met good friends and supporters. Anietie, you are a great friend with who I shared great time. Thanks also for smiling every day in the laboratory and welcoming me with a huge GOOD MORNING. I also feel I must say thanks to Zuzka S. You made me part of Prague, Czech Republic and your

family. We also shared a lot with our respective PhDs and we cheered each other up when we had a bad day. I can't forget to open the door of your office and see your big smile. Thanks to be always there. Then, Betul was such a good supporter. I know we talked a lot of several things including our PhDs. I feel really happy to meet you and share most of the PhD thesis and the common classes. Good luck in yours! Willing to see it!

Por supuesto, no me puedo olvidar de David, Esther, Carlos, Sofía ni Edel. David por estar desde el primer día ahí. Has sido amigo, mentor y me has ayudado y apoyado en muchos momentos durante el tiempo de Praga. Gracias, aún sigo recordando muchas de nuestras conversaciones y los consejos. Esther, he sufrido cuando tú sufrías en tu tesis pero también he celebrado cuando así ha sido. Fue cosa del destino encontrarnos y coincidir a la par con las tesis pero nos hemos dado gran apoyo para que lo acabáramos a tiempo ambas. Gracias por estar ahí y ser quién me escucha y da buenos consejos. Carlos y Sofía, por nuestros cafés y nuestras charlas sobre nuestros doctorados. Nos hemos apoyado y hemos hecho muchas lluvias de ideas para resolver dudas de nuestro trabajo. Gracias Carlos por esas horas para estudiar inmunología conmigo, te has convertido en un gran amigo, y a Sofía, gracias por enseñarme la fortaleza. Sé que os queda poco y que pronto podréis defender la tesis. ¡Mucha suerte!

También he de agradecer el apoyo de mis amigos en España, Edurne con quién comencé la tesis al mismo tiempo. Gracias por estar siempre ahí y esos grandes consejos por Skype, nuestro apoyo mutuo y muchas risas. Juan con los memes para hacerme reír y es que la risa es la mejor medicina. Amparo y Sandra por estar ahí desde que nos conocimos en la uni y hacerme parte de cada paso de vuestra vida. Gracias de todo corazón. Sin decirnos nada, sabíais cuando os necesitaba y me llamábais. Ana C. te dije que te mencionaría y así lo hago. Gracias porque al leerme los agradecimientos de tu tesis me enseñaste que cada gesto, por pequeño que sea, puede ser uno grande para quién recibe ese gesto. Ana L. gracias por estar ahí siempre. Hermana, fisio y bueno, que más puedo decir que siempre he sentido tu apoyo. Amaia, gracias por decir sí tan rápidamente y querer formar parte en este proyecto. Tus imágenes son increíbles y saber que con mis explicaciones has podido hacerlo, hace que aún sea mejor. Gracias por esas charlas y contactar para ver cómo me iba yendo todo. Desde el ERASMUS y aquí seguimos. About ERASMUS, Tina and Alby, we met in the ERASMUS but you were my great supporters. I can't be so lucky as I am to have all of you. Thanks to open your homes and welcoming me when I needed to be out. I can't choose best friends to be my strength when I lost mine.

M. Mayra y M. Ana, gracias por todo y por toda la ayuda de estar ahí y vuestros rezos. Dicen que quién tiene un amigo tiene un tesoro y yo tengo la suerte de tener a todos ellos. Mercedes, gracias por el apoyo que me has dado en los últimos meses. No sabes cuánto ha significado tenerte ahí igual que al resto de la familia, gracias.

Sin embargo, no puedo olvidar mencionar a mi familia. Mis padres y mi hermana que sé que han sufrido tanto como yo cuando algo pasaba pero también son los primeros en celebrar cuando así ha sido. Mi madre porque es mi fan #1 de quién he recibido un apoyo continuo en cada momento y ha estado ahí cuando la he necesitado. Mujer valiente y fuerte de quién aún me queda por aprender mucho. Mi padre con esa calma y paciencia, y además fuerte y con gran fuerza de voluntad. Sin lo que ellos me han enseñado y educado, no llegaría hasta aquí. Y no existen suficientes GRACIAS para lo que ellos han hecho por mí. Mi hermana por ser ese apoyo, a pesar de nuestras diferencias, has luchado conmigo y has sido la primera en salir para protegerme. Gracias de todo corazón y lanzarme la mano cuando más lo he necesitado. Si una es afortunada por los grandes amigos que ha encontrado durante su vida, aún es más afortunada por la familia que tiene. Sin él apoyo de ellos, jamás habría llegado hasta aquí.

Por último, GRACIAS a todos los luceros que iluminan mi camino. Que no os mencione, no significa que hayáis sido esa luz cuando la he necesitado. GRACIAS.

List of abbreviations

AMP	Antimicrobial peptide
ATP	Adenosin triphosphate
BME	Basal Medium Eagle
BPI	Bactericidal/permeability-increasing protein
CAT	Catalase
CuZnSOD	Copper-zinc-superoxidase dismutase
CCF	Coelomic cytolytic factor
DNA	Deoxyribonucleic acid
DAMP	Damage-associated molecular patter
DCF- DA	2', 7'-dichlorofluorescein diacetate
DOM	Dissolved organic matter
<i>E. andrei</i>	<i>Eisenia andrei</i>
ECs	Eleocytes
ENMs	Engineered Nanomaterials
EMAP II	Endothelial monocyte-activating polypeptide II
FBS	Fetal Bovine Serum
Fet/Lys	Fetidin/Lysenin
FSC	Forward-scattered light
GAs	Granular Amoebocytes subpopulation
HAs	Hyaline Amoebocytes subpopulation
H	hours
HPLC-FLD	High-performance liquid chromatography with fluorescence detection
ICP-OES	Inductively coupled plasma optic emission spectroscopy

ISO	International Organization for Standardization
LBP	Lipopolysaccharide binding protein
LMA	2-hydroxyethyl agarose
LPS	Lipopolysaccharide
MWCNTs	Multiwalled Carbon nanotubes
MDA	Malondialdehyde
MEKK 1	MEK Kinase 1
MnSOD	Manganese superoxide dismutase
mRNA	Messenger RNA
min	minutes
NEED	N-alpha-naphthyl-ethylenediamine
NMs	Nanomaterials
NO	Nitric oxide
NOM	Natural organic matter
NOS	Nitrogen Oxygen Species
NPs	Nanoparticles
OECD	Organisation for Economic Co-operation and Development
PAMPs	Pathogen-associated molecular pattern
PCR	Polymerase Chain Reaction
PKC 1	Protein Kinase C 1
PI	Propidium iodide
PO	Phenoloxidase
PRRs	Pattern Recognition Receptors
qPCR	Quantitative Polymerase Chain Reaction
RNA	Ribonucleic acid

ROS	Reactive Oxygen Species
RPL 13	Ribosomal protein L13
RPL 17	Ribosomal protein L17
RT-PCR	Reverse transcription-polymerase chain reaction
SEM	Scanning Electron Microscope
SOD	Superoxide dismutase
SSC	Side-scattered light
TEM	Transmission Electron Microscope
TLR	Toll-like receptor
UV/Vis	Ultraviolet-visible
WHC	Water holding capacity
WWTPs	WasteWater Treatment Plants

Abstract

Nanotechnology has been evolving during the past decades, becoming more present in different industries like cosmetics, mechanical devices, electronics, painting, ceramics, biomedicine, the food industry, etc. Although nanoparticles (NPs) are produced naturally (ash from volcanoes, smoke from forest fires, and rock erosion processes), manufactured nanoparticles are the most concerning NPs. To date we can confirm that the higher the production of NPs and nanomaterials is, the higher will be their release into the environment. The environmental release of NPs into aquatic and terrestrial ecosystems during their life cycle and disposal is becoming a global environmental concern, which has attracted the attention of researchers from a wide range of disciplines.

NPs can reach terrestrial environments by different pathways. For instance, they can be released in the form of nanopesticides, where they are used due to their antimicrobial activity. NPs can also reach agricultural soils through the disposal of WWTP sludge, which is used as fertilizer. Hence, monitoring of exposure levels and the assessment of their environmental risks for terrestrial organisms is required.

Eisenia andrei earthworms are terrestrial invertebrates typically used as model organisms in ecotoxicity studies. *E. andrei* possess an innate immune system that defends the animals against pollutants, bacteria, fungi, and viruses that can be found in the soil. In the coelomic cavity, *E. andrei* contain free-floating immune cells called coelomocytes. Coelomocytes are differentiated into eleocytes (ECs) and granular (GAs) or hyaline amoebocytes (HAs). The ECs are autofluorescent cells whose function is mainly nutritional, while HAs and GAs are the immune coelomocytes of *E. andrei*. Nowadays, several NPs toxicity studies have been carried out regarding acute mortality and reproduction with earthworms following the OECD guidelines. However, the special physicochemical characteristics of NPs differ from other chemical contaminants due to, among other things, their size, their high reactivity, and their big surface area. Therefore, toxicity testing protocols and guidelines need to be adapted to these NPs.

The overall aim of this PhD thesis was to assess the toxic effects of three types of NPs (two metal oxide NPs, TiO₂ NPs and CuO NPs, and a transformation product of Ag NPs, Ag₂S NPs) to *Eisenia andrei* and to assess their interaction with its coelomocytes by performing *in vitro* and *in vivo* toxicity tests. The thesis was developed within the project "Probing safety of nano-objects by defining immune responses of environmental organisms" (PANDORA), which formed part of the H2020 Marie Skłodowska-Curie Innovative Training Network programme, which focused on studying the potential impact of NPs on the immune system of different living organisms (human dendritic cells, hemocytes from *Porcellio scaber* and marine bivalve *Mytilus*, cells from sea urchin, and coelomocytes from *Eisenia andrei*).

The specific research objectives of this PhD thesis were: to optimize the cultivation medium for *in vitro* testing of NPs and the testing techniques using flow cytometry; to assess the possible differences in

sensitivity between HAs and GAs exposed to the same NPs and the same exposure times; to describe the protection mechanisms derived from the exposure to the metal oxide NPs and Ag₂S NPs; to describe the potential toxicity mechanisms of NPs; and to understand the potential risks of NPs for the earthworms' immune system.

TiO₂ and CuO NPs toxicity tests were performed *in vitro* with coelomocytes chemically extruded from *E. andrei* at different sublethal concentrations (1, 10 and 100 µg mL⁻¹) over 2, 6 and 24 h. In addition, an *in vivo* test with Ag₂S NPs was carried out with 180 *E. andrei* earthworms exposed to a sublethal concentration of Ag₂S NPs, 5 mg Ag Kg⁻¹ soil, for 14 days following the OECD 207 guideline. The earthworm endpoints assessed during this PhD thesis were associated with oxidative stress, genotoxicity, immune biomarkers and mRNA levels of assorted defence and signalling molecules. In the *in vitro* test, reactive oxygen (ROS) production, malondialdehyde (MDA) production, alkaline comet assay, apoptosis, phagocytic activity and the mRNA levels of relevant molecules in *E. andrei* were analysed. ROS production, apoptosis, and phagocytic activity were measured with a flow cytometer. As for the the *in vivo* test, mortality and weight were also analysed as well as other endpoints like cellular viability, nitric oxide (NO) production, phenoloxidase activity, and MDA production. Apart from the cellular and earthworm physiology analyses, NPs were also characterized by multiple-angle diffraction light scattering (MADLS), transmission electron microscope (TEM), and scanning electron microscope (SEM). The TEM and SEM were also used in the *in vitro* analyses to locate the TiO₂ and CuO NPs in the coelomocytes.

The results of the *in vitro* tests showed that the bioavailability of TiO₂ and CuO NPs differed among them. TiO₂ NPs were more stable and tended to precipitate at 24 h, while CuO NPs were more unstable. Moreover, it was observed that the lower concentrations of CuO NPs (1 and 10 µg Cu mL⁻¹) were almost dissolved at 6 h while 100 µg Cu mL⁻¹ was not at all dissolved after 48 h. Through SEM and the energy dispersive X-ray spectroscopy (EDS), we could localize TiO₂ and CuO NPs with the coelomocytes and over their membranes. TEM-EDS analysis revealed that CuO NPs were localised inside the cytoplasm of the coelomocytes exposed to 100 µg Cu mL⁻¹ after 2 and 6 h. The cellular studies also showed differences between TiO₂ NPs and CuO NPs exposure to coelomocytes in R-RPMI 1640 (cultivation medium). ROS production was shown neither by TiO₂ NPs exposure nor by CuO NPs at the different concentrations. However, greater MDA production was detected in cells treated with CuO NPs at 10 and 100 µg Cu mL⁻¹ at 6 h, while TiO₂ NPs did not produce stronger MDA production in comparison with the control coelomocytes. Similar to MDA production, alkaline comet assay showed no DNA damage at any concentration and time after TiO₂ NPs exposure while CuO NPs showed increasing DNA damage along time after the 100 µg Cu mL⁻¹ exposure. Concerning phagocytic activity, we could observe the same differences between TiO₂ and CuO NPs. TiO₂ NPs did not decrease or increase the phagocytic activity in comparison with the control coelomocytes. CuO NPs, meanwhile, decreased the phagocytic activity at 6

and 24 h, when coelomocytes were exposed to $100 \mu\text{g Cu mL}^{-1}$. Concerning apoptosis, the different concentrations of TiO_2 NPs did not produce necrosis, early apoptosis or late apoptosis at the different exposures and times in comparison with the control coelomocytes. Nevertheless, the greatest concentration of CuO NPs ($100 \mu\text{g Cu mL}^{-1}$) increased the number of necrotic coelomocytes and decreased the early and late apoptosis and the viability at 6 and 24 h.

The gene expression analyses revealed slight changes in mRNA levels of assorted molecules after the exposure to TiO_2 NPs. Metallothioneins (at 2, 6, and 24 h), fetidin/lysenins, lumbricin and MEK kinase 1 (at 6 h) were upregulated when coelomocytes were exposed to $10 \mu\text{g mL}^{-1}$, while the antioxidative molecules were neither upregulated nor downregulated after the exposure to TiO_2 NPs at 2, 6, and 24 h. Exposure to $1 \mu\text{g Cu mL}^{-1}$ of CuO NPs upregulated metallothioneins at 2, 6, and 24 h, while $10 \mu\text{g Cu mL}^{-1}$ upregulated metallothionein at 24 h. Manganese superoxidase dismutase (MnSOD) and copper-zinc superoxidase dismutase were downregulated when coelomocytes were exposed to $1 \mu\text{g Cu mL}^{-1}$ at 2 and 24 h, and 2 h, respectively. Catalase (CAT) was also downregulated when coelomocytes were exposed to $1 \mu\text{g Cu mL}^{-1}$ at 24 h. However, the immune molecules and signal transductional expression was not affected by the exposure to 1 and $10 \mu\text{g Cu mL}^{-1}$ CuO NPs at the different times assessed (2, 6, and 24 h).

The results of the *in vivo* test showed that NPs containing 5 mg Ag Kg^{-1} soil did not cause earthworms' mortality; however, changes in earthworms' weight were detected. After 14 days, the earthworms exposed to Ag_2S NPs decreased their weight in comparison to the control earthworms. The coelomocytes' viability was assessed and there was no decrease in viability in comparison with the control earthworms. MDA and NO productions were also assessed. The results showed that there was no significantly different MDA production in the NP treatments compared to the control. The NO production was similar in the different exposures, however, bigger variations were observed suggesting an imbalance in the NO metabolism. The phenoloxidase activity, a common immune biomarker among invertebrates, showed no changes between the exposure of Ag_2S NPs and the control after 14 days of exposure. SEM-EDS showed that Ag_2S NPs were found before and after 14 days of earthworms' exposure in the soil. Furthermore, the inductively coupled plasma optical emission spectrometry (ICP-OES) was carried out with the soil and earthworms. The values obtained in the soil showed that the quantity of 5 mg Ag Kg^{-1} soil was properly applied. Interestingly, the earthworm analyses showed that they were able to uptake Ag_2S NPs during the 14-day exposure period.

The ICP-OES technique was also used to measure the dissolution of CuO NPs in the R-RPMI 1640 medium. The results showed that the CuO NPs were quite unstable. The lower concentrations (1 and $10 \mu\text{g Cu mL}^{-1}$) were dissolved between 2 - 6 h, while the $100 \mu\text{g Cu mL}^{-1}$ concentration was partially dissolved at 24 h. Probably, the aggregation in the greatest concentration of CuO NPs slowed down the dissolution process, and there were Cu^{+2} ions detected in the cultivation medium after 48 h. The dissolution and aggregation

processes could occur due to the chemicals contained in the R-RPMI 1640. For example, fetal bovine serum (FBS) could stabilize the NPs, the HEPES could lead to precipitation. The number of salts contained in the medium could also enhance the aggregation. However, it would depend on the concentration that R-RPMI 1640 contained. The salts were reduced in the R-RPMI 1640 medium due to the sensitivity of coelomocytes to osmolarity because coelomocytes needed 176 mOsm in the R-RPMI 1640 medium. Higher osmolarity than 176 mOsm leads to the death of coelomocytes. Thus, it shows the importance of NPs characterization because the toxicity effects could vary if NPs change or if NPs are aggregated or dissolved. Differences in the protocols of NPs dispersion in the medium and the interaction of NPs with the culture medium can explain the different toxic effects observed in the literature. The dissolution process is important because it can explain whether the effects are caused by the ions or by the NPs themselves. In this PhD study, it was observed that TiO₂ NPs and Ag₂S NPs were not dissolved. Concerning NPs characterization, the ζ potential showed that CuO NPs tended to aggregate from 2 h to 24 h in the R-RPMI 1640 medium.

The PhD indicates that the coelomocytes exposed to TiO₂ NPs and CuO NPs were in contact with the NPs as was shown by the SEM-EDS images. The most surprising was the detection of CuO NPs in the cytoplasm of coelomocytes at 2 and at 6 h of exposure. It indicates that coelomocytes could uptake the NPs and keep them inside the cell before their dissolution, leading to a “Trojan horse effect” mechanism. This mechanism explains that the observed toxicity effects could be produced due to the engulfed NPs. The pH inside of the coelomocytes could be determinant for the CuO NPs dissolution in the cytoplasm. Moreover, the Fenton-like redox copper could have enhanced the production of oxygen free radicals such as Cu⁺² ions, which interact with H₂O₂ and release the free radicals. The free radicals interacted with membrane lipids leading to the production of MDA as it was observed in the experiments when MDA production was stronger after 100 $\mu\text{g Cu mL}^{-1}$ of exposure. Moreover, it was described that MDA interacts with DNA causing DNA damages which was seen in our experiments. This “Trojan horse effect” is seen as a toxicity mechanism of NPs and shows that immune cells are the NPs’ target as they have the ability to engulf NPs. Surprisingly, ROS production measurements showed there was different sensitivity between HAs and GAs. Such differences were explained by the different sizes of HAs and GAs.

Although coelomocytes were in contact with TiO₂ NPs, toxic effects were not detected. Former studies indicate that TiO₂ NPs toxicity is activated with UVA light. However, the toxicity test was performed in darkness, simulating earthworms’ natural conditions, which supports the absence of toxic effects. However, the mRNA analyses showed some genetic alterations. Metallothioneins are proteins which participate in metal detoxification and the elimination of metal stress. It was observed that both TiO₂ and CuO NPs were upregulating the levels of these proteins. In addition, it was observed that the antioxidative system was slightly activated with CuO NPs, where there was also high oxidative stress produced (MDA).

The TiO₂ NPs did not activate the antioxidative system as there was no oxidative stress produced but it activated MEK Kinase 1, which is a signal transducer associated with oxidative stress and homeostasis of the cells. Surprisingly, the immune molecules were activated, probably by the use of no-LPS free NPs. Potentially, the TiO₂ NPs could affect the immune system as enhancers.

In the case of the *in vivo* studies, oxidative stress was not observed. However, it was found that NO production required longer time and adding L-arginine to increase the levels of earthworms' NO. To improve NO production, tests with longer exposure periods are recommended. It was observed that the earthworms were able to ingest the NPs in the soil so internal, damages could be produced, but may require a longer time to be expressed in effective biomarkers. It is known that Ag₂S NPs are stable and need longer time to be dissolved in comparison with Ag NPs. Another tested parameter was phenoloxidase activity associated with the melanisation process with the final product melanin. In the presence of oxidative stress, melanin and lipofuscin were produced by earthworm coelomocytes. Phenoloxidase was not activated after the treatment of coelomocytes with NPs, in line with the measurement of oxidative stress. As there were no free radicals to be scavenged by melanin and lipofuscin, the phenoloxidase cascade was not activated. The coelomocytes' viability did not vary, which was in agreement with the measurements done for the previous parameters.

The conclusions of this thesis indicate that metal oxide NPs and their transformation products can affect earthworms. It is highlighted that HAs and GAs were key NPs' targets as they were able to engulf the NPs. The optimal conditions for coelomocytes cultivation were 20 °C, darkness and cells cultivation in R-RPMI 1640 medium. Among the different biomarkers studied here, ROS and MDA production, phagocytic activity, apoptosis, were found to be reliable and sensitive. Another main conclusion includes the differences in response between HAs and GAs, as HAs were more sensitive than GAs when they were exposed to NPs. Regarding the defence mechanism of coelomocytes, it was observed that HAs and GAs upregulated antioxidative enzymes to decrease the oxidative stress produced by NPs. Metallothioneins seem to be promising molecules as their expression was upregulated, increased after the TiO₂ and CuO NPs treatment of coelomocytes. Metallothioneins could help to decrease the oxidative stress produced by metals, and the high levels detected in earthworms may explain why these organisms have a high tolerance to metals.

The biomarkers used in the *in vitro* and *in vivo* tests showed how coelomocytes can protect earthworms. However, in the CuO NPs test, the "Trojan-horse" effect could have produced stronger damage in coelomocytes and consequently, in the animal itself. The common precursor observed in the mechanism is the free radicals produced after exposure to NPs. Another conclusion extracted from this PhD is that the earthworm immune system risk is associated with the phagocytic activity of the coelomocytes (HAs and

GAs). As a consequence of engulfing NPs, and the damage exerted to HAs and GAs, there was a suppression of the earthworms' immune system, leading to the death of the animals directly or indirectly.

Overall, this PhD thesis shows that new cellular, molecular and immunological techniques could reveal toxicity mechanisms of NPs in terrestrial organisms, and provides new endpoints to be used in the ecotoxicological risk assessment of NPs.

Resumen

La nanotecnología ha ido evolucionando durante las últimas décadas, haciéndose más presente en diferentes industrias como la cosmética, dispositivos mecánicos, electrónica, pintura, cerámica, biomedicina, industria alimentaria, etc. A pesar de que las nanopartículas (NPs) pueden producirse de forma natural (ceniza de volcanes, humo de incendios forestales, y procesos de erosión de rocas), es en las nanopartículas de diseño donde se observa el mayor incremento. Por lo que, cuanto mayor sea la producción de NPs y nanomateriales, mayor será su liberación al medio ambiente. La liberación ambiental de las NPs durante su ciclo de vida y su desecho se está convirtiendo en una preocupación emergente. Las NPs pueden alcanzar tanto los ecosistemas terrestres, como los agua dulce o los marinos, presentando problemas de toxicidad para los organismos vivos que habitan dichos ecosistemas. Por lo tanto, se requiere el seguimiento de los niveles de exposición y la evaluación de sus riesgos ambientales.

Las NPs se suelen encontrar comúnmente en ambientes terrestres, entre otros aspectos, por su utilización como nanopesticidas debido a su actividad antimicrobiana. Sin embargo, las NPs también podrían llegar a los suelos agrícolas a través de la eliminación de los lodos de las estaciones de depuración de aguas residuales (EDAR) aplicados como fertilizante, lo que podría afectar a los organismos que viven allí.

Las lombrices de tierra *Eisenia andrei* (*E. andrei*) son invertebrados terrestres típicamente utilizados como organismos modelo en estudios de ecotoxicidad. *E. andrei* posee un sistema inmunológico innato que protege a los animales contra contaminantes, bacterias, hongos y virus que se pueden encontrar en el suelo. En la cavidad celómica de *E. andrei*, hay células inmunitarias que flotan libremente llamadas celomocitos. Los celomocitos se subdividen en ECs, HAs y GAs. Las ECs se caracterizan principalmente por su autofluorescencia y su función nutricional mientras que las HAs y GAs son los celomocitos inmunes de *E. andrei*. En la actualidad se han realizado varios estudios de toxicidad de NPs en cuanto a mortalidad aguda y reproducción con lombrices siguiendo las directrices de la OCDE. Sin embargo, las peculiares características fisicoquímicas de las NPs difieren de otros contaminantes químicos debido, entre otras cosas, a su tamaño, su alta reactividad y su gran área de superficie. Por lo tanto, los protocolos y las guías para el ensayo de su toxicidad deben adaptarse a estas NPs.

El objetivo general de esta tesis doctoral fue evaluar los efectos tóxicos de tres tipos de NPs (dos NP de óxido metálico, las NPs de TiO_2 y las NPs de CuO y un producto de transformación de NPs de Ag , las NPs de Ag_2S) en *E. andrei* y su estudiar la interacción de las NPs con las células inmunocompetentes de *E. andrei* llamadas celomocitos mediante la realización de ensayos *in vitro* e *in vivo*. La tesis se enmarca en el proyecto "Probing safety of nano-objects by definition immune answers of Environmental organisms" (PANDORA), desarrollado como parte del programa H2020 Marie Skłodowska-Curie Innovative Training

Network, que se centró en estudiar el posible impacto de NPs en el sistema inmunológico de diferentes organismos vivos (células dendríticas humanas, hemocitos de *Porcellio scaber* y bivalvo marino *Mytilus*, células de erizo de mar y celomocitos de *Eisenia andrei*).

Los objetivos específicos de este proyecto fueron: la optimización del medio de cultivo para el ensayo *in vitro* y también la optimización de las técnicas *in vitro* mediante citómetro de flujo; evaluar las posibles diferencias de sensibilidad entre las HAs y GAs expuestos a las mismas NPs y a los mismos tiempos de exposición; comprender los posibles mecanismos de protección derivados de la exposición a las NPs de óxidos metálicos y NPs de Ag₂S; describir los posibles mecanismos de toxicidad derivados de la exposición a las NPs; y comprender los posibles riesgos para el sistema inmunológico de las lombrices.

La metodología ha sido optimizada y desarrollada para los ensayos de toxicidad de las NPs de TiO₂, las NPs de CuO y las NPs de Ag₂S. Para ello, los experimentos de toxicidad de las NPs de TiO₂ y las NPs de CuO fueron realizadas *in vitro* con celomocitos extruidos químicamente de *E. andrei* a diferentes concentraciones subletales (1, 10 y 100 µg mL⁻¹) y a las 2, 6 y 24 h de exposición. Los experimentos realizados con las NPs de Ag₂S se llevaron a cabo *in vivo*, para lo que 180 lombrices de tierra *E. andrei* fueron expuestas a una concentración subletal de las NPs de Ag₂S, 5 mg Ag Kg⁻¹ de suelo durante 14 días siguiendo la directriz OECD 207. En este caso, para la extrusión de los celomocitos se utilizó una suave estimulación eléctrica (9 V). Los puntos finales evaluados durante la tesis doctoral se asociaron con el estrés oxidativo, la genotoxicidad, los biomarcadores inmunitarios y los niveles de ARN mensajero (ARNm). En las pruebas *in vitro* se analizaron la producción de las especies reactivas de oxígeno (ROS), la producción de malondialdehído (MDA; también llamado peroxidación lipídica), el ensayo de cometa alcalino, la apoptosis, la actividad fagocítica y los niveles de ARNm de moléculas relevantes en *E. andrei*. La producción de ROS, la apoptosis y la actividad fagocítica se midieron mediante un citómetro de flujo. En el experimento *in vivo*, además de analizarse los puntos finales típicos como la mortalidad y el peso, se analizaron otros puntos finales como la viabilidad celular, la producción de óxido nítrico (NO), la actividad de la fenoloxidasas y la producción de MDA. Además de los análisis de fisiología celular y de lombrices de tierra, las NPs también se caracterizaron por dispersión de luz de difracción de múltiples ángulos (MADLS), microscopio electrónico de transmisión (TEM) y microscopio electrónico de barrido (SEM). Además, el TEM y SEM se utilizaron en los análisis *in vitro* para localizar las NPs de TiO₂ y las NPs de CuO en los celomocitos.

Los resultados de las pruebas *in vitro* mostraron que la disponibilidad de las NPs de TiO₂ y las NPs de CuO difería entre ellas. Las NPs de TiO₂ fueron más estables y tendieron a precipitar a las 24 h, mientras que las NPs de CuO fueron más inestables. Además, se observó que las concentraciones más bajas de las NPs de CuO (1 y 10 µg Cu mL⁻¹) casi se disolvieron a las 6 h, mientras que 100 µg Cu mL⁻¹ no se disolvieron en absoluto después de 48 h. A través del SEM y la espectroscopia de rayos X de energía dispersiva (EDS), pudimos localizar las NPs de TiO₂ y las NPs de CuO con los celomocitos y, también, sobre sus membranas

celulares. Mediante el el TEM, se estudiaron los celomocitos expuestos a las NPs de CuO, y luego, se observó a través de imágenes TEM-EDS que las NPs de CuO se encontraban dentro de los celomocitos, exactamente, estaban localizados en el citoplasma tanto a las 2 h como a las 6 h de exposición con $100 \mu\text{g Cu mL}^{-1}$. Los estudios celulares también mostraron diferencias entre la exposición de las NPs de TiO_2 y las NPs de CuO a celomocitos en R-RPMI 1640 (medio de cultivo celular). La producción de ROS no se afectó ni en las NPs de TiO_2 ni en las NPs de CuO en los diferentes tiempos de exposición (2, 6 y 24 h), sin embargo, se detectó una mayor producción de MDA para las NPs de CuO a 10 y $100 \mu\text{g Cu mL}^{-1}$ a las 6 h, mientras que las NPs de TiO_2 no produjeron una elevada producción de MDA en comparación con los celomocitos de control. Similar a la producción de MDA, el ensayo cometa alcalino no mostró daño en el ADN en ninguna de las concentraciones utilizadas ni tampoco en ninguno de los tiempos de exposición con las NPs de TiO_2 . Mientras que las NPs de CuO mostraron un aumento del daño en el ADN a lo largo de los diferentes tiempos de exposición para la concentración subletal de $100 \mu\text{g Cu mL}^{-1}$. Para la actividad fagocítica pudimos observar las mismas diferencias entre las NPs de TiO_2 y las NPs de CuO. En ninguna de las diferentes concentraciones de las NPs de TiO_2 , no hubo ni disminución ni aumento de la actividad fagocítica en comparación con los celomocitos del control. Las NPs de CuO, por su parte, disminuyeron la actividad fagocítica a las 6 y 24 h de exposición cuando los celomocitos fueron expuestos a $100 \mu\text{g Cu mL}^{-1}$. Respecto a la apoptosis, las concentraciones de las NPs de TiO_2 usadas no difirieron de los celomocitos de control. Por lo tanto no hubo un aumento en la necrosis ni en la apoptosis temprana o la apoptosis tardía en las diferentes concentraciones y en los diferentes tiempos. Sin embargo, la mayor concentración de las NPs de CuO ($100 \mu\text{g Cu mL}^{-1}$) se detectó un aumento de los celomocitos necróticos y una disminución en la apoptosis tardía, en la apoptosis temprana y en la viabilidad desde las 6 h hasta las 24 h de exposición.

En los análisis de expresión génica o los niveles de ARNm, se detectaron ligeros cambios en la exposición con las NPs de TiO_2 . Las metalotioneínas (a las 2, 6 y 24 h), fetidina/lisenina, lumbricina y MEK quinasa 1 (a las 6 h) aumentaron cuando los celomocitos se expusieron a $10 \mu\text{g mL}^{-1}$ de las NPs de TiO_2 , mientras que las moléculas antioxidantes no aumentaron ni disminuyeron con la exposición a las NPs de TiO_2 a lo largo de los diferentes tiempos de exposición. Asimismo, MEK quinasa 1 mostró un aumento cuando los celomocitos estaban expuestos a $1 \mu\text{g mL}^{-1}$ de las NPs de TiO_2 a las 24 h. Sin embargo, la exposición de los celomocitos a las NPs de CuO produjo un incremento de los niveles de ARNm de las metalotioneínas (2, 6 y 24 h) a la concentración de $1 \mu\text{g Cu mL}^{-1}$ y a las 24 h para la concentración de $10 \mu\text{g Cu mL}^{-1}$. También se observó una disminución de la superoxidasa dismutasa de manganeso (MnSOD; a las 2 y a las 24 h para $1 \mu\text{g Cu mL}^{-1}$), la superoxidasa dismutasa de cobre-zinc (CuZnSOD; a las 2 h para $1 \mu\text{g Cu mL}^{-1}$) y la de catalasa (CAT; a las 24 h para $10 \mu\text{g Cu mL}^{-1}$). Por otro lado, las moléculas inmunes y la expresión transduccional de la señal no se vieron afectadas por la exposición a 1 y $10 \mu\text{g Cu mL}^{-1}$ de las NPs de CuO en los diferentes tiempos evaluados (2, 6 y 24 h).

En el caso de los resultados de los experimentos *in vivo*, la concentración de 5 mg Ag Kg⁻¹ de suelo no produjo mortalidad de lombrices; sin embargo, se detectaron cambios en el peso de las lombrices después de 14 días. Las lombrices expuestas a las NPs de Ag₂S, disminuyeron su peso en comparación con las lombrices control mientras que el peso de las lombrices del control de iones (AgNO₃) no mostró ningún tipo de variación. Además, los celomocitos fueron extraídos de *E. andrei* mediante estimulación eléctrica suave. Se evaluó la viabilidad de los celomocitos y no hubo ni disminución ni aumento de la viabilidad en comparación con las lombrices de tierra control. También se evaluaron la producción de óxido nítrico (NO) y la producción de MDA. En los resultados se mostró que hubo producción de MDA pero que no era significativamente diferente en comparación con el control. La producción del NO fue similar entre las diferentes exposiciones, sin embargo, se observaron mayores variaciones, lo que significó que hubo un posible desequilibrio en el metabolismo del NO. La actividad de la fenoloxidasa, que también es un biomarcador inmunológico común entre los invertebrados, no mostró cambios entre la exposición de las NPs de Ag₂S y el control después de 14 días. También se realizaron análisis mediante el SEM-EDS y mostraron que se encontraron las NPs Ag₂S antes y después de 14 días en el suelo. Además, los análisis realizados mediante la espectroscopia de emisión óptica con plasma acoplado inductivamente (ICP-OES) con las lombrices y con el suelo detectaron la concentración de las NPs de Ag₂S. Los resultados de las muestras del suelo confirmaron que se había dispersado 5 mg Ag Kg⁻¹ de suelo. Curiosamente, los datos obtenidos a partir de las muestras de las lombrices de tierra expuestas en las NPs de Ag₂S, mostraron que las lombrices de tierra pudieron haber ingerido las NPs de Ag₂S durante ese período de exposición de 14 días.

El ICP-OES también se utilizó para analizar la concentración de las NPs de CuO en el medio de cultivo celular (R-RPMI 1640). Por lo tanto, los resultados obtenidos de estos análisis mostraron los procesos de disolución de las NPs de CuO. Las concentraciones más bajas (1 y 10 µg Cu mL⁻¹) se diluyeron entre las 2 y las 6 h mientras que la concentración de 100 µg Cu mL⁻¹ necesitó más de 24 h para diluirse completamente. Probablemente, la agregación de las NPs en la concentración más elevada (100 µg Cu mL⁻¹) ralentizó el proceso de disolución de las NPs de CuO y aún a las 48 h, había NPs de CuO en el medio de cultivo. Los procesos de agregación de las NPs se observaron a través del potencial zeta y el tamaño hidrodinámico. Los procesos pudieron suceder debido a los productos químicos contenidos en el R-RPMI 1640. Por ejemplo, el suero bovino fetal (FBS) estabiliza las NPs, el HEPES puede provocar la precipitación de las mismas. El número de sales contenidas en el medio también afecta a la agregación. Sin embargo, estos procesos de disolución y agregación tendrían lugar según la concentración de cada uno de los reactivos que contuviera R-RPMI 1640. Las sales, por ejemplo, se redujeron debido a la osmolaridad celular. Los celomocitos necesitaron 176 mOSM en el medio R-RPMI 1640 para su supervivencia. Una osmolaridad más alta produciría la muerte de los celomocitos. Por lo tanto, se mostró la importancia de la caracterización ya que los efectos de toxicidad pueden variar si las NPs cambian o si las NPs se agregan o

disuelven en los medios de dispersión respectivos. Los correctos protocolos de dispersión de las NPs en el medio y la interacción de las NPs con el medio de cultivo explicarían los diferentes efectos tóxicos observados. El proceso de disolución es importante porque podría explicar si los efectos detectados provienen de los iones o provienen de las propias NPs. Durante el trabajo de doctorado, se observó que las NPs de TiO_2 y las NPs de Ag_2S , siendo las últimas las más estables, no se disolvían en el medio de cultivo ni en el suelo, respectivamente. Sin embargo, las NPs de CuO eran bastante inestables. El potencial zeta medido para las NPs de CuO mostraban una agregación de las NPs desde las 2 h hasta las 24 h en el medio R-RPMI 1640, y la agregación comenzaba a partir de las 24 h cuando las NPs de CuO estaban dispersas en agua destilada. Además, se detectó una tendencia a la agregación por parte de las NPs de TiO_2 ($100 \mu\text{g mL}^{-1}$) a partir de las 6 h en R-RPMI 1640.

Curiosamente, los celomocitos expuestos a las NPs de TiO_2 y a las NPs de CuO estaban en contacto directo con las NPs que mostraban las imágenes SEM-EDS. Por tanto, los celomocitos podrían interactuar directamente con las NPs. Sorprendentemente, se observaron las NPs de CuO en el citoplasma de los celomocitos a las 2 y a las 6 h. Ésto significaba que los celomocitos podrían engullir las NPs y mantenerlas dentro antes de que se pudieran disolver. Por lo que los resultados obtenidos conducen al mecanismo del "efecto caballo de Troya". Este mecanismo explicaría que los efectos de toxicidad observados pudieron producirse debido a las NPs engullidas y situadas en el citoplasma de la célula. El pH en el interior de los celomocitos podría ser un posible factor que iniciara la disolución de las NPs de CuO en el citoplasma. Por un lado, la exposición produciría un aumento de los ROS en la célula. Por otro lado, el cobre redox similar a Fenton daría lugar, a su vez, a un aumento de la producción de radicales libres de oxígeno (ROS), ya que el Cu^{+2} interactúa con el H_2O_2 , generado durante el metabolismo celular, y, por ello, la liberación de los radicales libres. Los ROS interactuarían con los lípidos de la membrana, lo que conduciría a la producción de MDA, ya que se observó que la MDA era más elevada para la concentración de $100 \mu\text{g Cu mL}^{-1}$. Además, se describió que la MDA es capaz de interactuar con el ADN provocando daños en el ADN que también se detectaron en los resultados a través del ensayo cometa alcalino. Este "efecto de caballo de Troya" podría ser un posible mecanismo de toxicidad de las NPs. Asimismo, este mecanismo también realizó el hecho de que las células inmunitarias son el objetivo de las NPs, ya que éstas tienen la capacidad de engullir las NPs. Sorprendentemente, la producción de ROS mostró que había diferente sensibilidad entre las células HAs y las células GAs indistintamente de las NPs evaluadas. Podría ser que los diferentes tamaños que tuvieran los HAs y los GAs pudieran ejercer diferentes niveles de ROS o podría ser que los HAs fueran más sensibles que los GAs.

Aunque los celomocitos estuvieron en contacto con las NPs de TiO_2 , no se detectaron los efectos de toxicidad que si se observaron en las NPs de CuO . Debe entenderse que las NPs de TiO_2 podrían ejercer un daño mayor si se activaran con luz UVA ya que se volverían más reactivas. Sin embargo, las condiciones

de trabajo fueron en oscuridad y simulando las condiciones de las lombrices de tierra, por lo que la razón más probable de la ausencia de efectos tóxicos en los celomocitos se debió a la no irradiación de las NPs de TiO_2 con luz UVA. Sin embargo, los análisis de ARNm mostraron algunas variaciones. Las metalotioneínas son proteínas con función de desintoxicación de metales y estrés producido por exposición a metales. Se observó que los celomocitos expuestos tanto a las NPs de TiO_2 como a las NPs de CuO se regulaban al alza durante los diferentes tiempos de exposición. También se detectó que el sistema antioxidante se activaba levemente con las NPs de CuO donde también se producía un alto estrés oxidativo (MDA) a las 6 h. Las NPs de TiO_2 no activaron el sistema antioxidante ya que no se produjo estrés oxidativo, pero activaron la MEK quinasa 1, que es un transductor de señales asociado con el estrés oxidativo y la homeostasis de las células. Sorprendentemente, las moléculas inmunitarias (fetidin/lysenin y lumbricin) se activaron cuando los celomocitos estaban expuestos a las NPs de TiO_2 . Esta activación podría deberse al hecho de que las NPs no estaban libres de LPS (lipopolisacárido) o también podría ser que las NPs de TiO_2 pudieran actuar como potenciadores del sistema inmunitario.

En el caso de los estudios *in vivo* con las NPs de Ag_2S no se observó ningún tipo de estrés oxidativo. Sin embargo, se detectó que los análisis de la producción del NO requerían de más tiempo, además de la adición de L-arginina para aumentar los niveles de NO de las lombrices de tierra (*E. andrei*). Este hecho supuso que la utilización de los análisis de la producción del NO en *E. andrei* como biomarcador, no era suficientemente fiable para su uso con *E. andrei*. Además, se debería prolongar los períodos de exposición con las NPs ya que en periodos cortos no se atisbaba daños ni a nivel celular ni a nivel de organismo cuando *E. andrei* estaba expuesto a las NPs de Ag_2S . Sin embargo, sí que se detectó que las lombrices de tierra fueron capaces de ingerir las NPs del suelo por lo que internamente se podrían producir daños pero que se requeriría de un mayor tiempo para que estos biomarcadores detectaran efectos tóxicos derivados de la exposición. Por ejemplo, las plantas requirieron tiempos más prolongados para mostrar los efectos tóxicos de las NPs de Ag_2S , aunque pudieron incorporar las NPs de Ag_2S dentro de la planta. Se sabe que las NPs de Ag_2S son estables y tardan más tiempo en disolverse en comparación con las NPs de Ag , por lo que los potenciales efectos tóxicos derivados de su exposición, no serían fácilmente detectables en un corto plazo de tiempo. Otro parámetro probado fue la actividad de la fenoloxidasa, que está asociada al proceso de melanización porque el producto final es la melanina. La actividad feneloxidasa es, por tanto, un parámetro inmunológico en *E. andrei*. La melanina y la lipofusceína son sustancias producidas por los celomocitos de las lombrices de tierra cuando hay estrés oxidativo y están asociados con el proceso de encapsulación. En la exposición *in vivo* con las NPs de Ag_2S , la actividad de la fenoloxidasa no se activó. Por lo que se correlacionó con los resultados obtenidos del estrés oxidativo. Por lo tanto, al no haber radicales libres, la cascada feneloxidasa no se activó y por tanto, ni la melanina ni la lipofusceína se produjeron para eliminar los radicales libres. Por último, la viabilidad de los celomocitos analizados con un hemocitómetro, no produjo ninguna variación, es decir, no hubo mortalidad. Estos resultados, por

tanto, estuvieron en concordancia con los parámetros analizados anteriores en la exposición *in vivo* con las NPs de Ag₂S.

En conclusión, se demostró que las NPs de óxidos metálicos (NPs de TiO₂ y NPs de CuO) y sus productos transformados (NPs de Ag₂S) pueden afectar a las lombrices de tierra. Se destacó que las células HAs y las células GAs fueron objetivos clave de las NPs, ya que pudieron engullir a las NPs. Las condiciones óptimas establecidas fueron 20 °C, en oscuridad y las células fueron cultivadas en un medio de cultivo R-RPMI 1640.

Entre los diferentes biomarcadores, la producción de ROS, la producción de MDA, actividad fagocítica, apoptosis y la actividad fenoloxidasa se observaron como biomarcadores fiables y sensibles. Otra conclusión principal fueron las diferencias en sensibilidad detectadas entre los HAs y los GAs, ya que los HAs fueron más sensibles que los GAs cuando estaban expuestos a las NPs. En cuanto al mecanismo de defensa de los celomocitos, se observó que los HAs y los GAs fueron capaces de aumentar las enzimas antioxidantes para disminuir el estrés oxidativo producido por la exposición con las NPs. Además, las metalotioneínas parecen ser unas moléculas prometedoras, ya que fue regulada positivamente para las NPs de TiO₂ y las NPs de CuO. Por tanto, las metalotioneínas podrían ayudar a disminuir el estrés oxidativo producido por los metales. Esto también podría explicar la razón por la cual las lombrices de tierra tengan una alta tolerancia a los metales.

Los biomarcadores utilizados tanto en los experimentos *in vitro* como en los experimentos *in vivo* mostraron cómo los celomocitos pueden ser capaces de proteger a las lombrices de tierra. Sin embargo, en los experimentos donde se utilizaron las NPs de CuO, el efecto “caballo de Troya” podría haber dado lugar a un daño mayor en los celomocitos y, en consecuencia, en el propio animal. Como resultado de los diferentes análisis realizados, el precursor común observado en el efecto “caballo de Troya” son los radicales libres producidos durante el estrés oxidativo tras la exposición a las NPs. Otra de las conclusiones extraídas de esta tesis doctoral es que el riesgo del sistema inmunitario de las lombrices de tierra está asociado a la propia actividad fagocítica de los celomocitos (HAs y GAs). Como consecuencia de la ingestión de las NPs, las células HAs y las células GAs pueden potencialmente sufrir daños durante la exposición. Entonces, se podría producir una supresión del sistema inmunológico de las lombrices de tierra, lo que indirecta o directamente podría dar lugar a la muerte de los animales ya que las células inmunitarias no serían capaces de proteger a la lombriz frente a patógenos oportunistas.

En general, esta tesis doctoral muestra como las diferentes técnicas celulares, moleculares e inmunológicas pueden ayudar a entender los posibles mecanismos de toxicidad derivados de las NPs en los organismos terrestres, y, por consiguiente, proporciona nuevos criterios de valoración para su uso en la evaluación del riesgo ecotoxicológico de las NPs en los organismos terrestres.

Resum

La nanotecnologia ha anat evolucionant durant les últimes dècades, fent-se més present en diferents indústries com la cosmètica, dispositius mecànics, electrònica, pintura, ceràmica, biomedicina, indústria alimentària, etc. A pesar que les nanopartícules (NPs) poden produir-se de manera natural (cendra de volcans, fum d'incendis forestals, i processos d'erosió de roques), és en les nanopartícules dissenyades (ENPs) on s'observa el major increments. Pel que, com més gran siga la producció de nanopartícules (NPs) i nanomaterials (NMs), major serà el seu alliberament al medi ambient. L'alliberament ambiental de les NPs durant el seu cicle de vida i la seua deixalla s'està convertint en una gran preocupació. Les NPs poden arribar tant als ecosistemes terrestres, com als d'aigua dolça o als marins, presentant problemes de toxicitat per als organismes vius que habiten aquests ecosistemes. Per tant, es requereix el seguiment dels nivells d'exposició i l'avaluació dels seus riscos ambientals.

Les NPs se solen trobar comunament en ambients terrestres, entre altres aspectes, per la seua utilització com nanopesticides a causa de la seua activitat antimicrobiana. No obstant això, les NPs també podrien arribar als sòls agrícoles a través de l'eliminació dels llots de les estacions de depuració d'aigües residuals (EDAR) aplicats com a fertilitzant, la qual cosa podria afectar els organismes que viuen allí.

Els cucs de terra *Eisenia andrei* (*E. andrei*) són invertebrats terrestres típicament utilitzats com a organismes model en estudis d'ecotoxicitat. *E. andrei* posseeix un sistema immunològic innat que protegeix els animals contra contaminants, bacteris, fongs i virus que es poden trobar en el sòl. En la cavitat celòmica de *E. andrei*, hi ha cèl·lules immunitàries que suren lliurement dites celomocitos. Els celomocitos se subdivideixen en ECs, HAs i GAs. Les ECs es caracteritzen principalment per la seua autofluorescència i la seua funció nutricional mentre que les HAs i GAs són els celomocitos immunes de *E. andrei*. En l'actualitat s'han realitzat diversos estudis de toxicitat de NPs quant a mortalitat aguda i reproducció amb cucs seguint les directrius de l'OCDE. No obstant això, les peculiars característiques fisicoquímiques de les NPs difereixen d'altres contaminants químics degut, entre altres coses, a la seua grandària, la seua alta reactivitat i la seua gran àrea de superfície. Per tant, els protocols i les guies han d'adaptar-se a aquestes NPs.

L'objectiu general d'aquesta tesi doctoral va ser avaluar els efectes tòxics de tres tipus de NPs (dos NP d'òxid metàl·lic, les NPs de TiO₂ i les NPs de CuO i un producte transformat de NPs de Ag, les NPs de Ag₂S) en *Eisenia andrei* i la seua interacció amb les cèl·lules immunocompetents de *E. andrei* anomenades celomocitos mitjançant la realització d'assajos *in vitro* i *in vivo*. La tesi s'emmarca en el projecte "Probing safety of nano-objects by definition immune answers of Environmental organisms" (PANDORA), desenvolupat com a part del programa H2020 Marie Skłodowska-Curie Innovative Training Network, que es va centrar en estudiar el possible impacte de NPs en el sistema immunològic de diferents organismes

vius (cèl·lules dendrítiques humanes, hemocitos de *Porcellio scaber* i bivalve marí *Mytilus*, cèl·lules d'eriçó de mar i celomocitos de *Eisenia andrei*).

Els objectius específics d'aquest projecte van ser: l'optimització del mitjà de cultiu per a l'assaig *in vitro* i també l'optimització de les tècniques *in vitro* mitjançant citòmetre de flux; avaluar les possibles diferències entre HAs i GAs exposats a les mateixes NPs i als mateixos temps d'exposició; comprendre els possibles mecanismes de protecció derivats de l'exposició a les NPs d'òxids metàl·lics i NPs de Ag₂S; descriure els possibles mecanismes de toxicitat derivats de l'exposició a les NPs i comprendre els possibles riscos per al sistema immunològic dels cucs.

La metodologia ha sigut optimitzada i desenvolupada per als assajos de toxicitat de les NPs de TiO₂, les NPs de CuO i les NPs d'Ag₂S. Per a això, els experiments de toxicitat de les NPs de TiO₂ i les NPs de CuO van ser realitzades *in vitro* amb celomocitos extrets químicament de *E. andrei* a diferents concentracions subletals (1, 10 i 100 µg mL⁻¹) i a les 2, 6 i 24 h. Els experiments realitzats amb les NPs d'Ag₂S es va dur a terme *in vivo* pel que 180 cucs de terra *E. andrei* van ser exposades a una concentració subletal de les NPs d'Ag₂S, 5 mg Ag Kg⁻¹ de sòl durant 14 dies seguint la directriu OECD 207. En aquest cas, per a l'extrusió dels celomocitos es va utilitzar una suau estimulació elèctrica (9 V). Els punts finals avaluats durant la tesi doctoral es van associar amb l'estrés oxidatiu, la genotoxicitat, els biomarcadors immunitaris i els nivells d'ARN missatger (ARNm). En les proves *in vitro* es van analitzar la producció de les espècies reactives d'oxigen (ROS), la producció de malondialdehído (MDA; també dit peroxidació lipídica), l'assaig de cometa alcalí, l'apoptosi, l'activitat fagocítica i els nivells de ARNm de molècules rellevants en *E. andrei*. La producció de ROS, l'apoptosi i l'activitat fagocítica es van mesurar mitjançant un citòmetre de flux. En l'experiment *in vivo*, a més d'analitzar-se els punts finals típics com la mortalitat i el pes, es van analitzar altres punts finals com la viabilitat cel·lular, la producció d'òxid nítric (NO), l'activitat de la fenoloxidasa i la producció de MDA. A més de les anàlisis de fisiologia cel·lular i de cucs de terra, les NPs també es van caracteritzar per dispersió de llum de difracció de múltiples angles (MADLS), microscopi electrònic de transmissió (TEM) i microscopi electrònic d'escombratge (SEM). A més, el TEM i SEM es van utilitzar en les anàlisis *in vitro* per a localitzar les NPs de TiO₂ i les NPs de CuO en els celomocitos.

Els resultats de les proves *in vitro* van mostrar que la disponibilitat de les NPs de TiO₂ i les NPs de CuO diferia entre elles. Les NPs de TiO₂ van ser més estables i van tendir a precipitar a les 24 h, mentre que les NPs de CuO van ser més inestables. A més, es va observar que les concentracions més baixes de les NPs de CuO (1 i 10 µg Cu mL⁻¹) quasi es van dissoldre a les 6 h, mentre que 100 µg Cu mL⁻¹ no es van dissoldre en absolut després de 48 h. A través del SEM i l'espectroscòpia de raigs X d'energia dispersiva (EDS), vam poder localitzar les NPs de TiO₂ i les NPs de CuO amb els celomocitos i, també, sobre les seues membranes cel·lulars. Mitjançant el TEM, es van estudiar els celomocitos exposats a les NPs de CuO, i després, es va observar a través d'imatges TEM-EDS que les NPs de CuO es trobaven dins dels celomocitos, exactament,

estaven localitzats en el citoplasma tant a les 2 h com a les 6 h d'exposició amb $100 \mu\text{g Cu mL}^{-1}$. Els estudis cel·lulars també van mostrar diferències entre l'exposició de les NPs de TiO_2 i les NPs de CuO amb els celomocitos en R-RPMI 1640 (mitjà de cultiu cel·lular). La producció de ROS no es va mostrar ni en les NPs de TiO_2 ni en les NPs de CuO en els diferents temps d'exposició (2, 6 i 24 h), no obstant això, es va detectar una major producció de MDA per a les NPs de CuO a 10 i $100 \mu\text{g Cu mL}^{-1}$ a les 6 h, mentre que les NPs de TiO_2 no van produir una elevada producció de MDA en comparació amb els celomocitos de control. Similar a la peroxidació lipídica (MDA), l'assaig cometa alcalí no va mostrar mal en l'ADN en cap de les concentracions utilitzades ni tampoc en cap dels temps d'exposició amb les NPs de TiO_2 . Mentre que les NPs de CuO van mostrar un augment del mal en l'ADN al llarg dels diferents temps d'exposició per a la concentració subletal de $100 \mu\text{g Cu mL}^{-1}$. Per a l'activitat fagocítica vam poder observar les mateixes diferències entre les NPs de TiO_2 i les NPs de CuO . En cap de les diferents concentracions de les NPs de TiO_2 , no va haver-hi ni disminució ni augment de l'activitat fagocítica en comparació amb els celomocitos de control. Les NPs de CuO , per part seua, van disminuir l'activitat fagocítica a les 6 i 24 h d'exposició quan els celomocitos van ser exposats a $100 \mu\text{g Cu mL}^{-1}$. Per a l'apoptosi, les concentracions de les NPs de TiO_2 usades no van diferir dels celomocitos de control. Per tant no va haver-hi un augment en la necrosi ni en l'apoptosi primerenca o l'apoptosi tardana en les diferents concentracions i en els diferents temps. No obstant això, la major concentració de les NPs de CuO ($100 \mu\text{g Cu mL}^{-1}$) es va detectar un augment els celomocitos necròtics i una disminució en l'apoptosi tardana, en l'apoptosi primerenca i en la viabilitat des de les 6 h fins a les 24 h d'exposició.

En les anàlisis d'expressió gènica o els nivells de ARNm, es van detectar lleugers canvis en l'exposició amb les NPs de TiO_2 . Les metalotioneïnes (a les 2, 6 i 24 h), fetidina/lisenina, lumbricina i MEK cinasa 1 (a les 6 h) van augmentar quan els celomocitos es van exposar a $10 \mu\text{g mL}^{-1}$ de les NPs de TiO_2 , mentre que les molècules antioxidants no van augmentar ni van disminuir amb l'exposició a les NPs de TiO_2 al llarg dels diferents temps d'exposició. Així mateix, MEK cinasa 1 va mostrar un augment quan els celomocitos estaven exposats a $1 \mu\text{g mL}^{-1}$ de les NPs de TiO_2 a les 24 h. No obstant això, l'exposició dels celomocitos a les NPs de CuO va produir un increment dels nivells de ARNm de les metalotioneïnes (2, 6 i 24 h) a la concentració d' $1 \mu\text{g Cu mL}^{-1}$ i a les 24 h per a la concentració de $100 \mu\text{g Cu mL}^{-1}$. També es va observar una disminució de la superoxidasa dismutasa de manganés (MnSOD; a les 2 i a les 24 h per a $1 \mu\text{g Cu mL}^{-1}$), la superoxidasa dismutasa de coure-zinc (CuZnSOD; a les 2 h per a $1 \mu\text{g Cu mL}^{-1}$) i la de catalasa (CAT; a les 24 h per a $10 \mu\text{g Cu mL}^{-1}$). D'altra banda, les molècules immunes i l'expressió transduccional del senyal no es van veure afectades per l'exposició a les diferents concentracions de les NPs de CuO en els diferents temps avaluats (2, 6 i 24 h).

En el cas dels resultats dels experiments *in vivo*, la concentració de 5 mg Ag Kg^{-1} de sòl no va produir mortalitat de cucs; no obstant això, es van detectar canvis en el pes dels cucs després de 14 dies. Els cucs

exposats a les NPs d'Ag₂S, van disminuir el seu pes en comparació amb els cucs control mentre que el pes dels cucs del control d'ions (AgNO₃) no va mostrar cap mena de variació. A més, els celomocitos van ser extrets de *E. andrei* mitjançant estimulació elèctrica suau. Es va avaluar la viabilitat dels celomocitos i no va haver-hi ni disminució ni augment de la viabilitat en comparació amb els cucs de terra control. També es van avaluar la producció de l'òxid nítric (NO) i la producció de MDA. En els resultats es va mostrar que va haver-hi producció de MDA però que no era significativament diferent en comparació amb el control. La producció del NO va ser similar entre les diferents exposicions, no obstant això, es van observar majors variacions, cosa que va significar que va haver-hi un possible desequilibri en el metabolisme del NO. L'activitat de la fenoloxidasa, que també és un biomarcador immunològic comú entre els invertebrats, no va mostrar canvis entre l'exposició de les NPs d'Ag₂S i el control després de 14 dies. També es van realitzar anàlisi mitjançant el SEM-EDS i van mostrar que es van trobar les NPs d'Ag₂S abans i després de 14 dies en el sòl. A més, les anàlisis realitzades mitjançant l'espectroscòpia d'emissió òptica amb plasma acoblat inductivament (ICP-OES) amb els cucs i amb el sòl van detectar la concentració de les NPs d'Ag₂S. Els resultats de les mostres del sòl van confirmar que s'havia dispersat 5 mg Ag Kg⁻¹ de sòl. Curiosament, les dades obtingudes a partir de les mostres dels cucs de terra exposades en les NPs d'Ag₂S, van mostrar que els cucs de terra podien haver ingerit les NPs d'Ag₂S durant aqueix període d'exposició de 14 dies.

El ICP-OES també es va utilitzar per a analitzar la concentració de les NPs de CuO en el mitjà de cultiu cel·lular (R-RPMI 1640). Per tant, els resultats obtinguts d'aquestes anàlisis van mostrar els processos de dissolució de les NPs de CuO. Les concentracions més baixes (1 i 10 µg Cu mL⁻¹) es van diluir entre les 2 i les 6 h mentre que la concentració de 100 µg Cu mL⁻¹ va necessitar més de 24 h per a diluir-se completament. Probablement, l'agregació de les NPs en la concentració més elevada (100 µg Cu mL⁻¹) va alentir el procés de dissolució de les NPs de CuO i encara a les 48 h, hi havia NPs de CuO en el mitjà de cultiu. Els processos d'agregació de les NPs es van observar a través del potencial zeta i la grandària hidrodinàmica. Els processos van poder succeir a causa dels productes químics continguts en el R-RPMI 1640. Per exemple, el sèrum boví fetal (FBS) estabilitza les NPs, el HEPES pot provocar la precipitació d'aquestes. El nombre de sals contingudes en el mitjà també afecta a l'agregació. No obstant això, aquests processos de dissolució i agregació tindrien lloc segons la concentració de cadascun dels reactius que continguera R-RPMI 1640. Les sals, per exemple, es van reduir a causa de l'osmolaritat cel·lular. Els celomocitos van necessitar 176 mOSM en el mitjà R-RPMI 1640 per a la seua supervivència. Una osmolaritat més alta produiria la mort dels celomocitos. Per tant, es va mostrar la importància de la caracterització ja que els efectes de toxicitat poden variar si les NPs canvien o si les NPs s'agreguen o dissolen en els mitjans de dispersió respectius. Els correctes protocols de dispersió de les NPs en el mitjà i la interacció de les NPs amb el mitjà de cultiu explicarien els diferents efectes tòxics observats. El procés de dissolució és important perquè podria explicar si els efectes detectats provenen dels ions o provenen de les pròpies NPs. Durant el treball de doctorat, es va observar que les NPs de TiO₂ i les NPs d'Ag₂S, sent

les últimes les més estables, no es dissolien en el mitjà de cultiu ni en el sòl, respectivament. No obstant això, les NPs de CuO eren bastant inestables. El zeta potencial mesurat per a les NPs de CuO mostraven una agregació de les NPs des de les 2 h fins a les 24 h en el mitjà R-RPMI 1640, i, l'agregació començava a partir de les 24 h quan les NPs de CuO estaven disperses en aigua destil·lada. A més, es va detectar una tendència a l'agregació per part de les NPs de TiO₂ (100 µg mL⁻¹) a partir de les 6 h en R-RPMI 1640.

Curiosament, els celomocitos exposats a les NPs de TiO₂ i a les NPs de CuO estaven en contacte directe amb les NPs que mostraven les imatges SEM-EDS. Per tant, els celomocitos podrien interactuar directament amb les NPs. Sorprenentment, es van observar les NPs de CuO en el citoplasma dels celomocitos a les 2 i a les 6 h. Això significava que els celomocitos podrien engolir les NPs i mantindre-les dins abans que es pogueren dissoldre. Pel que els resultats obtinguts condueixen al mecanisme del "efecte cavall de Troia". Aquest mecanisme explicaria que els efectes de toxicitat observats van poder produir-se a causa de les NPs engolides i situades en el citoplasma de la cèl·lula. El pH a l'interior dels celomocitos podria ser un possible precursor de la dissolució de les NPs de CuO en el citoplasma. D'una banda, l'exposició produiria un augment dels ROS en la cèl·lula. D'altra banda, el coure redox similar a Fenton donaria lloc, al seu torn, a un augment de la producció de radicals lliures d'oxigen (ROS), ja que el Cu⁺² interactua amb el H₂O₂, generat durant el metabolisme cel·lular, i, per això, l'alliberament dels radicals lliures. Els ROS interactuarien amb els lípids de la membrana, la qual cosa conduiria a la producció de MDA, ja que es va observar que la MDA era més elevat per a la concentració de 100 µg Cu mL⁻¹. A més, es va descriure que la MDA és capaç d'interactuar amb l'ADN provocant danys en l'ADN que també es van detectar en els resultats a través de l'assaig cometa alcalí. Aquest "efecte de cavall de Troia" podria ser un possible mecanisme de toxicitat de les NPs. Així mateix, aquest mecanisme també va realçar el fet que les cèl·lules immunitàries són l'objectiu de les NPs, ja que aquestes tenen la capacitat d'engolir les NPs. Sorprenentment, la producció de ROS va mostrar que hi havia diferent sensibilitat entre les cèl·lules HAs i les cèl·lules GAs indistintament de les NPs avaluades. Podria ser que les diferents grandàries que tingueren els HAs i els GAs pogueren exercir diferents nivells de ROS o podria ser que els HAs anaren més sensibles que els GAs.

Encara que els celomocitos van estar en contacte amb les NPs de TiO₂, no es van detectar els efectes de toxicitat que si es van observar en les NPs de CuO. Ha d'entendre's que les NPs de TiO₂ podrien exercir un mal major si s'activaren amb llum UVA ja que es tornarien més reactives. No obstant això, les condicions de treball van ser en foscor i simulant les condicions dels cucs de terra, per la qual cosa la raó més probable de l'absència d'efectes tòxics en els celomocitos es va deure a la no irradiació de les NPs de TiO₂ amb llum UVA. No obstant això, les anàlisis de ARNm van mostrar algunes variacions. Les metalotioneïnes són proteïnes amb funció de desintoxicació de metalls i estrès produït per exposició a metalls. Es va observar que els celomocitos exposats tant a les NPs de TiO₂ com a les NPs de CuO es regulaven a l'alça durant els

diferents temps d'exposició. També es va detectar que el sistema antioxidant s'activava lleument amb les NPs de CuO on també es produïa un alt estrès oxidatiu (MDA) a les 6 h. Les NPs de TiO₂ no van activar el sistema antioxidant ja que no es va produir estrès oxidatiu, però van activar la MEK cinasa 1, que és un transductor de senyals associat amb l'estrès oxidatiu i l'homeòstasi de les cèl·lules. Sorprenentment, les molècules immunitàries (fetidina/lisenina i lumbricina) es van activar quan els cel·locitos estaven exposats a les NPs de TiO₂. Aquesta activació podria haver-se del fet que les NPs no estaven lliures de LPS (lipopolisacàrid) o també podria ser que les NPs de TiO₂ pogueren actuar com a potenciadors del sistema immunitari.

En el cas dels estudis *in vivo* amb les NPs d'Ag₂S no es va observar cap mena d'estrès oxidatiu. No obstant això, detectà que els anàlisis de la producció del NO requeria de més temps, a més de l'addició de L-arginina per a augmentar els nivells de NO dels cucs de terra (*E. andrei*). Aquest fet va suposar que la utilització dels anàlisis de la producció del NO en *E. andrei* com biomarcador, no era prou fiable per al seu ús amb *E. andrei*. A més, s'hauria de prolongar els períodes d'exposició amb les NPs ja que en períodes curts no s'entrellucava danys ni a nivell cel·lular ni a nivell d'organisme quan *E. andrei* estava exposat a les NPs d'Ag₂S. No obstant això, sí que es va detectar que els cucs de terra van ser capaces d'ingerir les NPs del sòl pel que internament es podrien produir danys però que es requeriria d'un major temps perquè aquests biomarcadors detectaren efectes tòxics derivats de l'exposició. Per exemple, les plantes van requerir temps més prolongats per a mostrar els efectes tòxics de les NPs d'Ag₂S, encara que van poder incorporar les NPs d'Ag₂S dins de la planta. Se sap que les NPs d'Ag₂S són estables i tarden més temps a dissoldre's en comparació amb les NPs d'Ag, per la qual cosa els potencials efectes tòxics derivats de la seua exposició, no serien fàcilment detectables en un curt termini de temps. Altre paràmetre provat va ser l'activitat de la fenoloxidasa, que està associada al procés de melanització perquè el producte final és la melanina. L'activitat fenoloxidasa és, per tant, un paràmetre immunològic en *E. andrei*. La melanina i la lipofusceïna són substàncies produïdes pels cel·locitos dels cucs de terra quan hi ha estrès oxidatiu i estan associats amb el procés d'encapsulació. En l'exposició *in vivo* amb les NPs d'Ag₂S, l'activitat de la fenoloxidasa no es va activar. Pel que es va correlacionar amb els resultats obtinguts de l'estrès oxidatiu. Per tant, al no haver-hi radicals lliures, la cascada fenoloxidasa no es va activar i per tant, ni la melanina ni la lipofusceïna es van produir per a eliminar els radicals lliures. Finalment, la viabilitat dels cel·locitos analitzats amb un hemocítometre, no va produir cap variació, és a dir, no va haver-hi mortalitat. Aquests resultats, per tant, van estar en concordança amb els paràmetres analitzats anteriors en l'exposició *in vivo* amb les NPs d'Ag₂S.

En conclusió, es va demostrar que les NPs d'òxids metàl·lics (NPs de TiO₂ i NPs de CuO) i els seus productes transformats (NPs d'Ag₂S) poden afectar els cucs de terra. Es va destacar que les cèl·lules HAs i les cèl·lules

GAs van ser objectius clau de les NPs, ja que van poder engolir a les NPs. Les condicions òptimes establides van ser 20 °C, en foscor i les cèl·lules van ser cultivades en un mitjà de cultiu R-RPMI 1640.

Entre els diferents biomarcadors, activitat la producció de ROS, la producció de MDA, activitat fagocítica, apoptosi i l'activitat fenoloxidasa es van observar com biomarcadors fiables i sensibles. Una altra conclusió principal van ser les diferències detectes entre els HAs i els GAs, ja que els HAs van ser més sensibles que els GAs quan estaven exposats a les NPs. Quant al mecanisme de defensa dels cel·locitos, es va observar que els HAs i els GAs van ser capaços d'augmentar els enzims antioxidants per a disminuir l'estrès oxidatiu produït per l'exposició amb les NPs. A més, les metalotioneïnes semblen ser unes molècules prometedores, ja que va ser regulada positivament per a les NPs de TiO₂ i les NPs de CuO. Per tant, les metalotioneïnes podrien ajudar a disminuir l'estrès oxidatiu produït pels metalls. Això també podria explicar la raó que els cucs de terra tinguen una alta tolerància als metalls.

Els biomarcadors utilitzats tant en els experiments *in vitro* com en els experiments *in vivo* van mostrar com els cel·locitos poden ser capaços de protegir els cucs de terra. No obstant això, en els experiments on es van utilitzar les NPs de CuO, "l'efecte cavall de Troia" podria haver donat lloc a un mal major en els cel·locitos i, en conseqüència, en el propi animal. Com a resultat de les diferents anàlisis realitzats, el precursor comú observat en "l'efecte cavall de Troia" són els radicals lliures produïts durant l'estrès oxidatiu després de l'exposició a les NPs. Una altra de les conclusions extretes d'aquesta tesi doctoral és que el risc del sistema immunitari dels cucs de terra està associat a la pròpia activitat fagocítica dels cel·locitos (HAs i GAs). A conseqüència de la ingestió de les NPs, les cèl·lules HAs i les cèl·lules GAs poden potencialment patir danys durant l'exposició. Llavors, es podria produir una supressió del sistema immunològic dels cucs de terra, la qual cosa indirecta o directament podria donar lloc a la mort dels animals ja que les cèl·lules immunitàries no serien capaces de protegir el cuc enfront de patògens oportunistes.

En general, aquesta tesi doctoral mostra com les diferents tècniques cel·lulars, moleculars i immunològiques poden ajudar a entendre els possibles mecanismes de toxicitat derivats de les NPs en els organismes terrestres, i, per consegüent, proporciona nous criteris de valoració per al seu ús en l'avaluació del risc ecotoxicològic de les NPs en els organismes invertebrats terrestres.

Chapter 1



Introduction

1. Introduction

1.1 Nanoparticles

1.1.1. Definition

Over the past decades, the industry has increased exponentially in manufacturing NPs for their use in different sectors (e.g. drugs, electronics, cosmetics, etc.). The NPs became necessary due to their unique properties compared to their bulks. Furthermore, their particular physicochemical properties made them appropriate for some uses that their common bulks would not be so useful. Therefore, the Organisation for Economic Co-operation and Development (OECD) and European Commission (EC) present them as any particles whose size is smaller than 100 nm at any of their dimensions. They also included the differences between NPs and nanomaterials. Thus, nanomaterials are particles at any state (either agglomerate or aggregate), with a size distribution of 50% or more between 1 and 100 nm (CE, 2012).

1.1.2. Types of nanoparticles

The NPs could be subdivided depending on their dimensionality and composition. In composition, there are organic, composites, and inorganic NPs. E.g. Fullerenes are organic, while golden NPs (Au NPs) are inorganic. Among the inorganic, several have been studied during the past years as they were the most manufactured ones (Ag NPs, Au NPs, TiO₂ NPs, etc).

Regarding the dimensions, we could find 0, 1, 2, and 3 dimensions. 0 dimensions are NPs, and graphene quantum dots, and their properties in optical stability make them essential for their use in biomedicine and optoelectronic devices (Barhoum et al., 2022 and papers there in). 1 dimension of nanomaterial is the nanowires, nanotubes, or nanofibers. Due to their characteristics, they could be used as catalyzers, filters, etc. (Barhoum et al., 2022 and papers there in). The 2 dimensions are flat shape NMs with thin layers, e.g. graphene, silicate clays, etc., providing a high surface area (Barhoum et al., 2022 and papers there in). Finally, 3 dimension NMs are complex structures with different shapes apart from the box one. Thus, their use is widely spread in micro-electromechanical, solar, biomedical, or robotic devices (Barhoum et al., 2022 and papers there in).

1.1.3 Physicochemical properties

According to the OECD, some endpoints of physicochemical properties must be included in each research study of NPs (OECD, 2010). Among the majority of NPs studies, the principal analyses performed are focused on providing the hydrodynamic size and zeta potential, which can be measured through zeta sizer Ultra (Malvern Panalytical), UV/Vis wavelength (TECAN 200 Pro plate reader), NPs primary size (TEM) and surface area.

Chapter 1. Introduction

Noteworthy, the zeta potential indicates the stability of nanoparticles in the dispersed medium (i.e. cultivation medium, citrate, Milli-Q water). Then, every nanoparticle measured with a result over 30 mV or lower than -30 mV indicates stable NPs (Figure 1). On the other hand, if the zeta potential values belong between -30 mV to 30 mV, there is no stability, and NPs are prone to aggregate (Figure 1). Then, the values obtained would reveal the aggregation and agglomeration state of NPs.

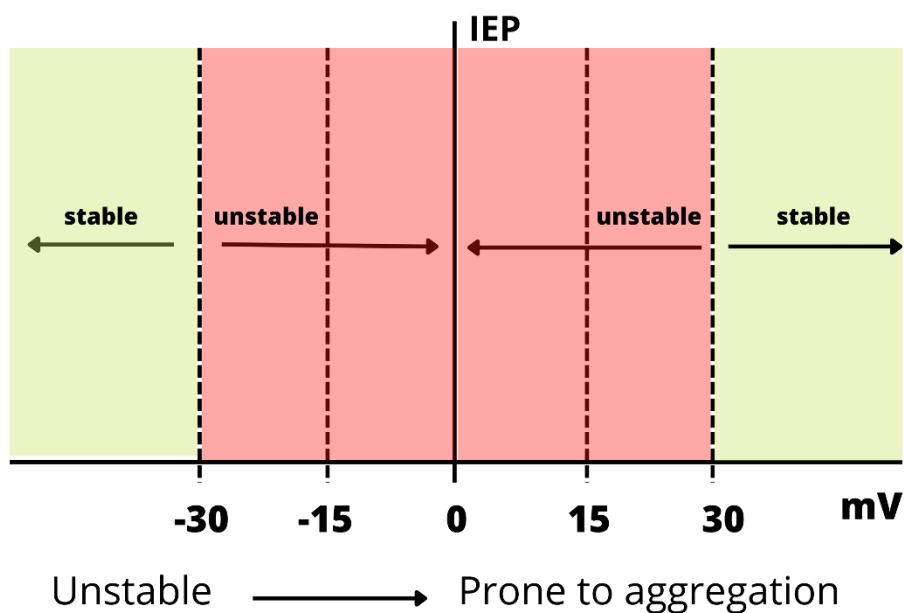


Figure 1. Zeta Potential graph (mV). IEP: Isoelectric point.

Sometimes the instability is enhanced due to the chemicals they are dissolved with. Thus, the importance of the zeta potential is necessary. Zeta potential is usually measured by Diffraction Light Scattering (DLS).

Hydrodynamic size would provide information on how NPs behave inside the liquid they are dispersed. Then, the hydrodynamic and primary sizes do not have to be the same. The information on zeta potential and hydrodynamic size would aid in the characterization because it provides information on how NPs behave when they are dispersed in any fluid (Milli-Q water, culture medium).

The TEM provides two characteristics: the shape and primary size of the NPs. Likewise, NPs could have a primary size of 30 nm, although 3 h later, they agglomerate, so the distribution size varies, but the primary measure of each NPs remains the same. Thus, NPs still have a 30 nm primary size, but their hydrodynamic size after 3 h showed a bigger size because they have agglomerated. Knowing the size is also crucial in toxicity because there are some sizes (30-50 nm) that cells can ingest, while sizes smaller than 5 nm would enter the cells via translocation (Sukhanova et al., 2018 and papers there in). TEM also provides information about the shape because depending on the type of the shape, the NPs will be prone to be ingested by cells (Sukhanova et al., 2018 and papers there in).

Chapter 1. Introduction

Surface charge is another characteristic of NPs. The surface charge has a key role in toxicity because positive charged NPs are able to enter the cells through the membranes compared to negative charge NPs (Sukhanova et al., 2018 and papers there in). However, zeta potential and surface charge can not be associated with the same function. Therefore, NPs could have negative or positive zeta potential independently of the surface charge.

Then, the surface area is associated with the NPs' primary size. If the NPs are smaller, the surface area increases, leading to higher interaction with the surroundings. Then, the toxic effects derived from the interaction will be higher as well (OECD, 2010).

Therefore, the fate of NPs would affect the physicochemical properties we have explained. Different parameters like pH, solubility, ionic strength or in the case of soil, the NOM or DOM would vary the properties allowing the mobility and bioavailability of NPs with the consequence of toxic effects on living organisms (Cornelis et al., 2014 and papers there in; Sukhanova et al., 2018 and papers there in). In nanosafety regulations, the proper characterisation of the NPs and the tools used for the analyses must be considered (OECD, 2010).

1.2 Origin and fate of nanoparticles

NPs could be naturally produced or manufactured in the industry called engineered nanomaterials (ENMs) and engineered nanoparticles (ENPs; Figure 2), and they could be released into the environment unintentionally.

The origin of NPs from nature could be found in the ash released in vulcanos, fire forest foam, and some erosion processes that affect the metals that rocks contain (Figure 2). Then, the manufactured NPs are produced in the laboratories or industry for specific purposes, so their characteristics are explicitly designed for that use (Barhoum et al., 2022 and papers there in). The beneficial effects of NPs are extended from drug delivery (nano-carriers) to the technology industry to develop solar panels for others uses. They can also be found in ceramic, cosmetics (e.g. sun creams), the food industry (e.g. TiO₂ NPs, also called E171 additive), and the paint industry (TiO₂ NPs with their white characteristic colour; CE, 2012).

During the life cycle of NMs, their design and processing to their end of life could be unintentionally released into the marine, freshwater and terrestrial ecosystem (Figure 2). The availability and mobility of NPs depend on the ecosystem. For example, in marine ecosystems is known the quickly sedimentation of NPs due to the high content of salts. In freshwater, the NOM is the functional group (humic and fulvic acids) that lead to aggregation of NPs (Wang and Liu, 2022 and papers there in). Moreover, the different processes vary from one to another ecosystem being similar parameters to all of them, the ionic strength and the pH. The ionic strength can accelerate the NPs aggregation and the pH is related to the surface

Chapter 1. Introduction

charge NPs, so high pH may lead to higher NPs mobility (Cornelis et al., 2014 and papers there in). According to this fact, the fate of NPs vary and their toxicity effect differ between the ecosystems. Thus, the typical parameter of each ecosystem and the common ones must be studied as it could aid to predict if NPs may be uptaken by living organisms of that ecosystem and produce ecotoxicological effects. This PhD thesis is focused on the terrestrial organism *Eisenia andrei earthworm* and the interaction between the *E. andrei* and some of the most common NPs (TiO_2 , CuO and Ag_2S NPs).

Some studies show CuO NPs are commonly found in soil ecosystems through direct applications like nanopesticides. The nanopesticides use Cu's antimicrobial effects to eliminate the crops' plagues. It was suggested that only well-formulated nanopesticides would target the pest and not affect the ecosystem (Kah et al., 2018). Nanofertilizers are other direct applications of CuO NPs in the soil (Kah et al., 2018). Nanofertilizers are designed to release slowly the fertilizer that the plant would use (Liu and Lal, 2015). Then, these based Cu fertilizers are available for the plants as they are important oligo-elements. (Liu and Lal, 2015). Therefore, there is also an indirect application of these NPs in the soil as sludge from wastewater treatment plants applied in the agricultural fields (Keller et al., 2017). Keller and Lazareva predicted that 73% of CuO NPs would be in the landfills, which is the indirect arrival of NPs to the soil (Keller and Lazareva, 2014). It was also corroborated by Keller et al. (2017), suggesting that during the life cycle, the NPs would reach mainly soil and sediments.

TiO_2 NPs are commonly found in different industries like cosmetics, painting, ceramic etc. They can get into landfills and the soil through the environmental release of sludge produced in WWTPs. However, recently, the use of TiO_2 NPs has been developed as nanopesticides and nanofertilizers (Thiagarajan and Ramasubbu, 2021). Therefore, the terrestrial organisms are a new target, because, similarly to CuO NPs, the terrestrial organisms will be in permanent contact with TiO_2 NPs. The bioavailability and mobility of TiO_2 NPs in the soil would depend on the NOM in the soil, the pH and ionic strength (basically, the salinity in the soil) and then the concentration of clay in the soil. For example, soils with a high concentration of clay would retain Ti leading to low toxicity for plants. However, the retention of Ti could be harmful to soil

Chapter 1. Introduction

invertebrates because they will be in continued contact with these NPs (Cornelis et al., 2014 and papers there in; Thiagarajan and Ramasubbu, 2021).

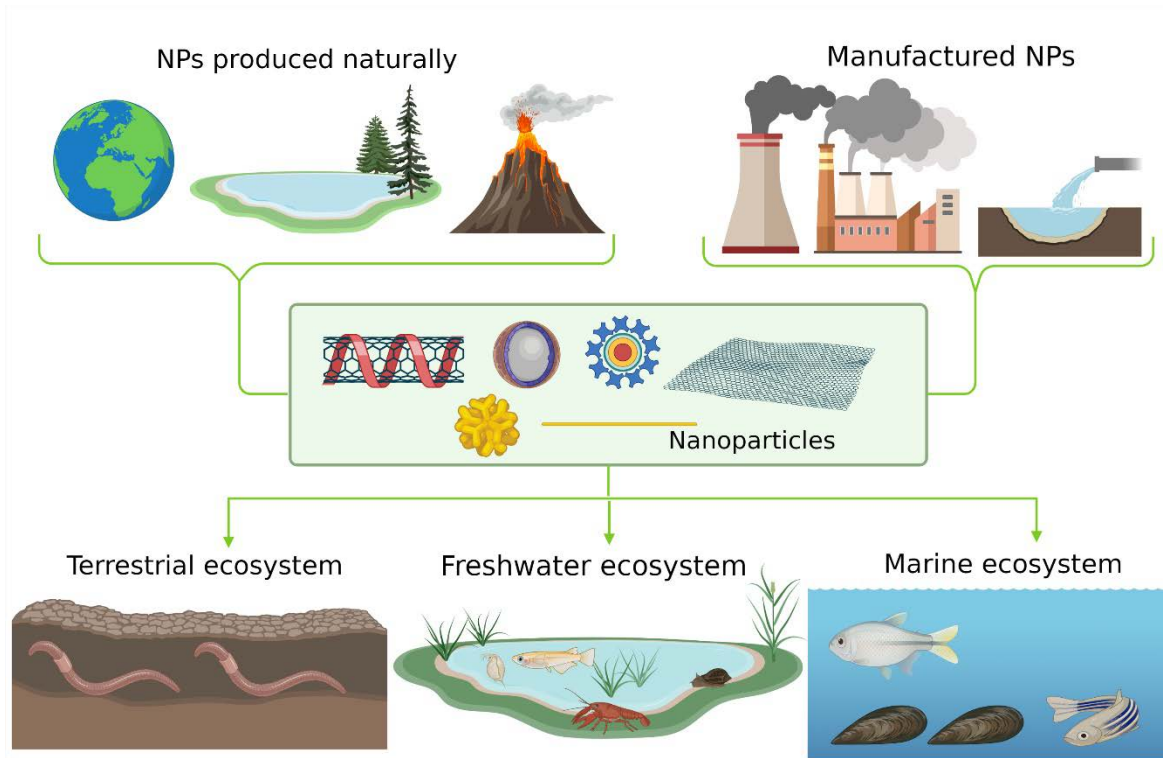


Figure 2. NPs fate. Different types of NPs which are naturally produced or manufactured could end in the terrestrial, freshwater and marine ecosystem. Created with BioRender.com

Ag₂S NPs are a transformation product of Ag NPs. Ag NPs are quite widely spread in different areas of industry. Their antibiotic protection made them essential in biomedicine. It has been demonstrated that between the different products derived from Ag NPs (AgNO₃, AgCl, Ag₂S NPs), Ag₂S NPs have the highest persistence and stability in the soil (Sekine et al., 2015). Therefore, the most significant quantity of Ag released to the environment would arrive in the soil as Ag₂S NPs (Sekine et al., 2015). It was reported that Ag NPs would become Ag₂S NPs in the WWTPs. It happens in the anaerobic tanks, where the anaerobic bacteria would produce sulfides that then they would interact with Ag⁺ ions from Ag NPs and form Ag₂S NPs (Courtois et al., 2019 and papers there in; Kaegi et al., 2013). The sulfidation would depend mainly on the size and residence time in the sewer (Kaegi et al., 2013). Thus, the sludge would contain sulphidized Ag NPs introduced in agricultural soils.

1.3 Common effects exerted by NPs

According to their fate, the metal oxide NPs and their transformed products could trigger different adverse toxic effects. It was observed that Ag NP have a strong oxidative activity (Tortella et al., 2020). They also

Chapter 1. Introduction

showed that different species of terrestrial organisms (earthworms) were sensitive to Ag NPs but, differently to AgNO₃, the damages were elongated during the time due to the slow release of Ag⁺ ions (Tortella et al., 2020). Therefore, Tortella and colleagues suggested that there is a lack of information regarding the internalization, bioaccumulation and transformation of NPs in aquatic and terrestrial organisms (Figure 2; Tortella et al., 2020). Moreover, one of the main characteristics is that if NPs are ingested, they could slowly release their ions and trigger ROS production (Tortella et al., 2020). The ions released would depend on solubility and characteristics of NPs, including the coating. NMs are considered "foreign particles" that disturb the defence mechanism of the organisms (Boraschi et al., 2020 and papers there in). Boraschi and colleagues suggested that NMs could affect the innate immune system provoking weakness and suppression of the immune system of the organism or develop a chronic inflammatory response (Boraschi et al., 2020 and papers there in). Among the specific endpoints measured in organisms exposed to NMs like mortality or weight loss, there are sublethal effects that, at prolonged exposure, could result in the organism's death. It has been suggested that oxidative activity is one of the main precursors of observed damage in the cells (Boraschi et al., 2020 and papers there in; Keller et al., 2017; Sukhanova et al., 2018 and papers there in; Thiagarajan and Ramasubbu, 2021; Tortella et al., 2020). In the case of the cellular effects, which is the main study in this PhD thesis, the NPs effects vary. The susceptibility or sensitivity of the cells depend on their physiology, function, cellular membrane properties, signalling pathways, mechanisms of repairing/defending, antioxidative system, genome, and shape (Azhdarzadeh et al., 2015).

Hence, most of the assessed endpoints are associated with sooner mortality, but some studies demonstrated that the oxidative stress could be a precursor for greater damages triggered at the cellular level, which may produce the death of the organism.

The future of NPs is related to their manufacture and their use. According to this and their unique characteristics, there will be an increased production of these NPs. Due to the life cycle of NPs, their release to the environment will also increase. Therefore, it is necessary to implement guidelines for testing nanoparticles and to generate relevant toxicity data for their risk assessment (Azhdarzadeh et al., 2015; Bondarenko et al., 2013; Boraschi et al., 2020 and papers there in; Tortella et al., 2020).

1.4 Earthworms *Eisenia andrei* (*E. andrei*)

1.4.1 Role in soil ecosystem

In general, earthworms are detritivore organisms located at the base of the food chain in the ecosystem. The function of detritivores is to digest the dead organic material like leaves falling from the trees. Then,

Chapter 1. Introduction

the detritivores would transform that organic material into smaller molecules to allow the roots of plants and trees to uptake them. Earthworms live everywhere, including dry areas but they preferably populate areas with high vegetation and humidity.

Another role is related to their movement. Earthworms have their burrows underground, and thus, they break the compact soil through the created tunnels. Hence, the earthworms are allowed to avoid compacted soil and create more porous and aerated soil needed for the plants' livelihood.

Among the different earthworm species, *E. andrei* was chosen as a model organism due to the availability of standard OECD toxicity testing guidelines and also because they are widespread. Earthworms are divided into three ecotypes: epigeic, endogeic, and anecic earthworms. Epigeic earthworms (*E. andrei*, *E. fetida* within others) live in the top layer of the soil, where they find a great variety of microorganisms and a lower quantity of mineral soil (Dvořák et al., 2013). The endogeic earthworms (*Aporrectodea caliginosa*) are located in the layer under the topsoil containing a lower quantity of organic material and a higher quantity of mineral soil (Bouché, 1977; Dvořák et al., 2013). The microbiota population in that layer of the soil is also much lower. The anecic earthworms (*Lumbricus terrestris*) is located under the layer of endogeic earthworms. The anecic earthworms dwell in soil depth and construct long vertical tunnels. Endogeic and anecic earthworms are out of the soil rarely. They only come out to bring some organic material like leaves and bring them to their burrows. For the studies presented in this PhD thesis, *E. andrei* earthworm was chosen due to its constant contact with the pollutants and microbiota in the topsoil.

1.4.2. Earthworm's anatomy

Eisenia andrei earthworms are protostomian invertebrates belonging to the Lumbricidae family and Annelida phylum. These animals are hermaphrodites, so they can reproduce sexually and asexually and have female and male reproductive organs. They consist of a segmented body that seems to fuse with several rings (approximately 100-150). Each circular ring is separated by a septum but whole body is passable. The anatomy of earthworms is described in Figure 3.

The first layer is the cuticle found on the outer side of the body. Next, it is the epidermis followed by circular and longitudinal muscles. The coelomic cavity is filled with coelomic fluid containing freely floating coelomocytes. The coelomocytes originated from the mesenchymal lining of the cavity (**1.4.3.1 Cellular response**, Bilej et al., 2010). A fold of the wall projecting into the cavity of the intestine is called typhlosole. It is a tube inside a tube in the intestine. The role of typhlosole is to enhance the adsorption and digestion of the nutrients by increasing the surface area (Figure 3 B). The whole intestine is a long tube that starts after the clitellum and ends in the anus. Before the clitellum, earthworms have the hearts (5), the brain, seminal vesicles and receptacles, and parts of the digestive tract, esophagus, pharynx, crop, and gizzard.

Chapter 1. Introduction

The circulatory system consists of aortic vessels that work similarly to the aortic vessel in humans and connect to the dorsal and ventral vessels. The dorsal and ventral vessels are located at the top and bottom of the body, and they go from the mouth to the anus of the earthworm (Figure 3).

Each earthworm segment is connected to the outer space through the nephridia pores and the dorsal pores (Figure 3 B). The nephridia are the excretory organ of earthworms, consisting of 3 loops where the first loop is connected to the previous ring through the septa forming the nephridiosome. Then, the third loop is connected to the outer space through the nephridia pores in the same ring where nephridia are. Thus, earthworms have two nephridia located on both lateral sides of earthworms (Figure 3; Lund et al., 2014 and papers there in). Curiously, the symbiont bacteria located in the ampulla of the nephridia can be transferred to the cocoons from the adults during the reproduction (Davidson and Stahl, 2006).

Interestingly, earthworms do not have lungs, so they breathe through the skin. In addition, they breathe through diffusion, which means that oxygen and carbon dioxide diffuse to the earthworms through the skin.

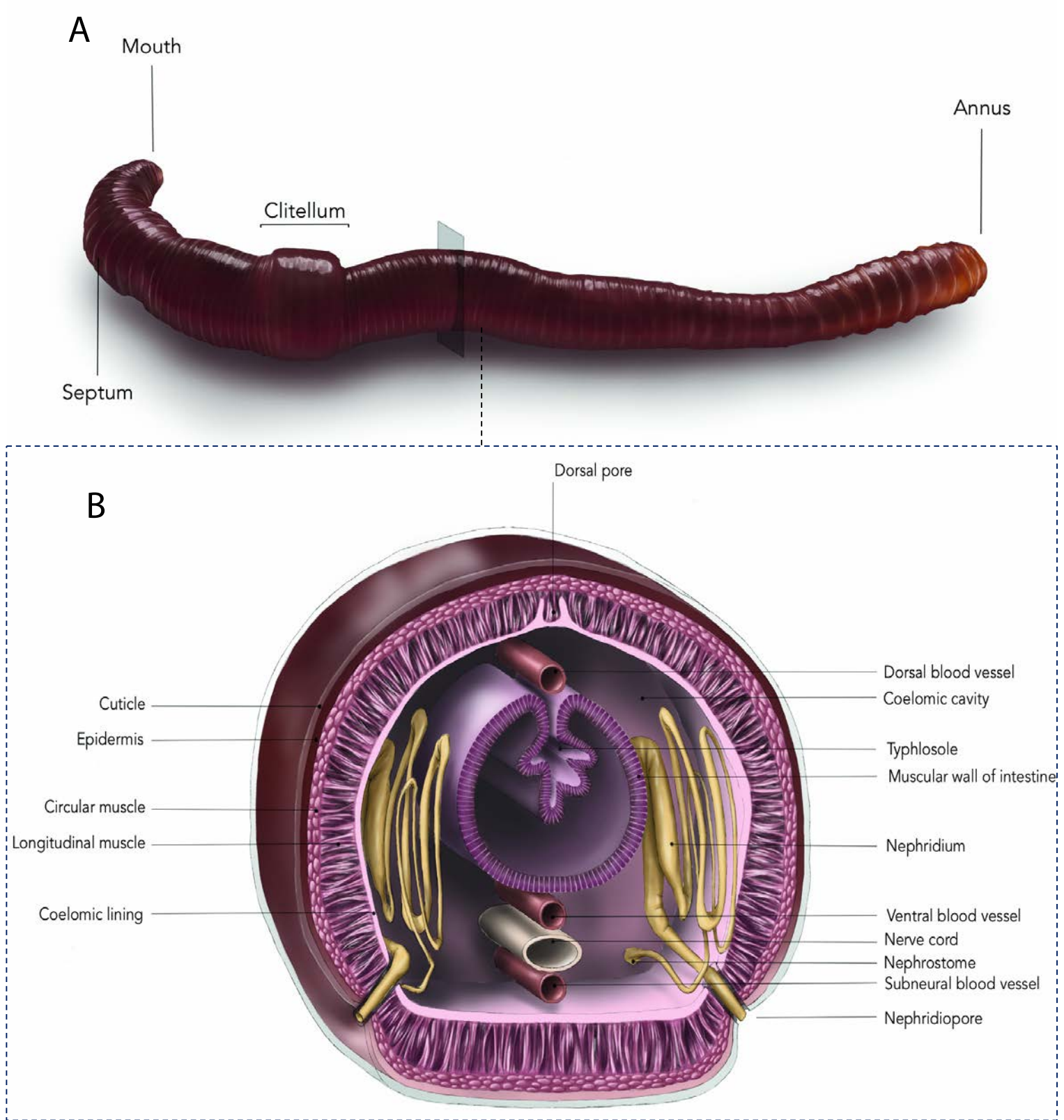


Figure 3. Earthworm’s anatomy. A) Earthworm image. The black square indicates where the cross-section was performed. B) Cross-section with all components of earthworm’s body. Illustrative image idea, design and draw are from Natividad Isabel Navarro Pacheco and Amaia Torres Piñeiro (estudio AMABI).

Chapter 1. Introduction

1.4.3. Immune system

The immune system has evolved from bacteria to mammals, including human beings. The immune system works coordinated between innate or native and adaptive or acquired immune system. In the evolution of the immune system, adaptive immune responses started to be developed from jawless fish (Figure 4). So then, invertebrates and other organisms below the jawless fish only possess an innate immune system (Figure 4).

The innate immune response instantly works to eliminate the microorganisms (fungi, bacteria, viruses) that injure the cells (Abbas et al., 2021). In the case of invertebrates like earthworms, the innate immune system is the unique immune response against any pathogen would harm the organism. Then, earthworms develop some barriers to be protected.

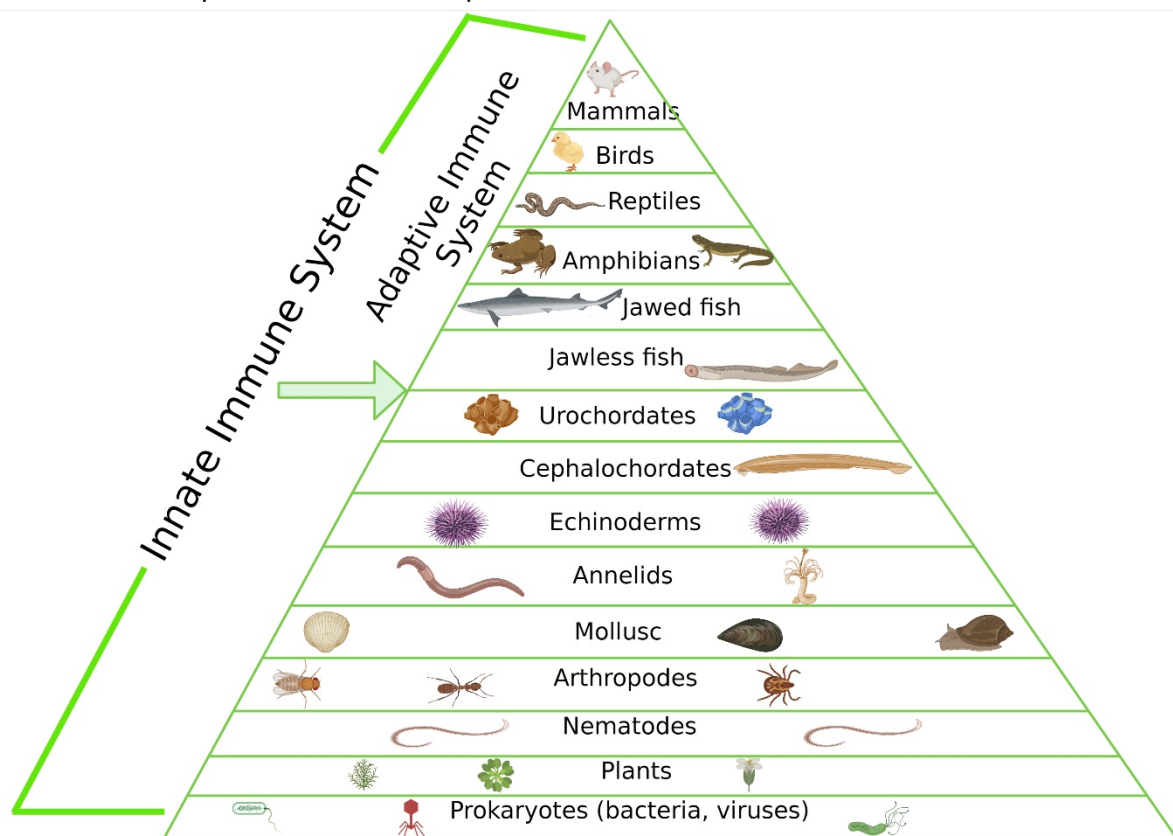


Figure 4. Immunology system evolution. Evolution of the immunology between different species. From jawless fish, adaptive immune system started to develop. Created with BioRender.com

The first barrier of their defence is the cuticle (Figure 3). The cuticle is a mucus membrane containing antibacterial proteins (Bilej et al., 2010). If foreign material, bacteria, viruses, and fungi can survive in this barrier, they can enter the coelomic cavity through the dorsal pores (Figure 3). Then, the immune response would be triggered.

Chapter 1. Introduction

1.4.3.1 Cellular response

The coelomocytes, which are the earthworm immune effector cells, are divided into eleocytes (chloragocytes) and amoebocytes (Figure 5). The eleocytes (ECs) represent a homogeneous group of coelomocytes that are derived from chloragogenous tissue (Figure 3; Homa et al., 2013)). They are characterized by their high autofluorescence. ECs are granular cells with autofluorescence that can be observed through a confocal microscope and flow cytometer. The fluorescence is detectable in each wavelength (green, blue, orange, yellow, and red) which can interfere with the fluorescence used in different analyses. ECs are described as being round in shape and having chloragosomes intracellularly (Engelmann et al., 2016). Riboflavin is one of the main compounds of ECs, with an excitation fluorescence peak of 370 and 420 nm peak and an emission peak at 525 nm, which is shared between flavins (Koziol et al., 2006). It is suggested that ECs contain lipofuscin, which may endow the autofluorescence of ECs (Koziol et al., 2006). However, their function is not clearly known. This type of coelomocytes is considered a source of nutrients for the rest of the cells (Šíma, 1994), but they are not immune effector coelomocytes (Engelmann et al., 2016). Then, the amoebocytes population is divided into hyaline (HAs) and granular (GAs), sometimes called amoebocytes and granulocytes (Engelmann et al., 2016). HAs are flattened cells with long filopodia, which could be seen as fried-egg shapes, while GAs are granular shapes cells with small filopodia or pseudopodia (Engelmann et al., 2016). Amoebocyte populations' functions are related to immune functions like phagocytosis of foreign material and removal of injured tissues/cells.

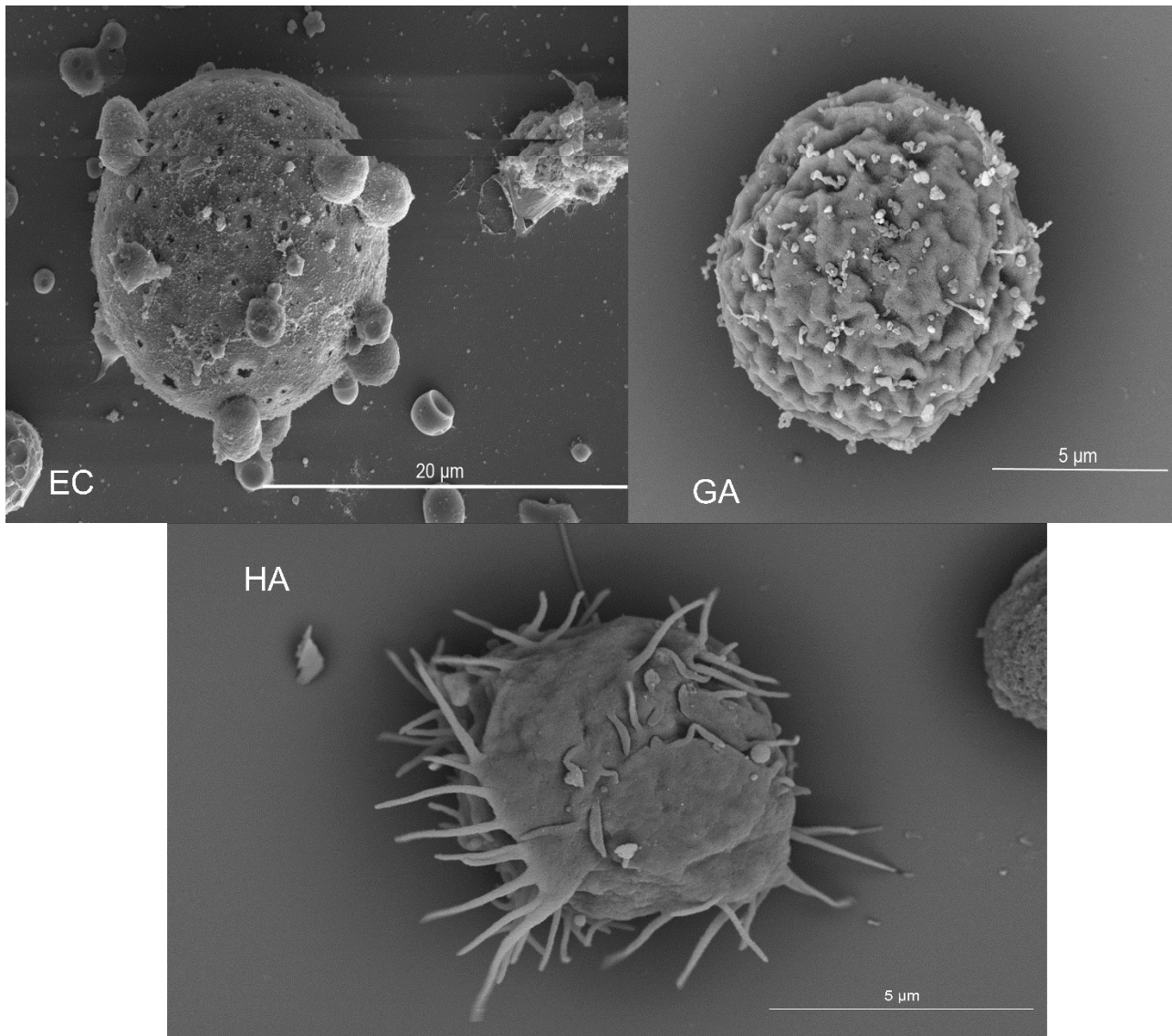


Figure 5. Coelomocytes subsets. EC) Eleocytes population. GA) Granular amoebocytes and HA) Hyaline amoebocytes.

Similar to human's innate immunity, the recognition of pathogen-associated molecular patterns (PAMPs) or damage-associated molecular patterns (DAMPs) is mediated by the pattern recognition receptors (PRRs).

Coelomocytes floating in the coelomic fluid inside the coelomic cavity recognise the foreign material introduced through dorsal pores by the pattern recognition receptors (PRRs; Figures 3 and 6). Earthworms have three identified PRRs to detect self and non-self structures:

Coelomic cytolytic factor (CCF) was described as protein with cytotoxic activity. This PRR shares a similar function with tumour necrosis factors in mammals (TNF; Beschin et al., 2004; Prochazkova et al., 2020 and papers there in). Moreover, CCF is also secreted by the phagocytic amoebocytes after incubating with

Chapter 1. Introduction

lipopolysaccharides (LPS; Aggarwal et al., 1985; Bilej et al., 1998; Bodó et al., 2018). It also has lytic and opsonisation properties (Procházková et al., 2020 and papers there in). It was demonstrated that it is expressed strongly in chloragogenous tissue and exclusively in the amoebocytes subset (Beschlin et al., 1998; Bodó et al., 2018).

Lipopolysaccharide (LPS) binding protein and bacterial permeability proteins (LBP/BPI) is the second PRR described. Both molecules are antagonists, but they act against Gram-negative bacteria. LPS modulates the inflammatory response, while the BPI molecule is anti-inflammatory and antimicrobial. In earthworms, the LBP/BPI is described as an antibacterial molecule expressed in the earthworm tissue except for the intestine. This PRR is exclusively found in the amoebocytes subset and seminal vesicles (Bodó et al., 2018; Procházková et al., 2020 and papers there in; Škanta et al., 2016). Probably, LBP/BPI plays a defensive role against pathogens during the development of gametes and offspring (Procházková et al., 2020 and papers there in).

Toll-like receptor (TLR) is a transmembrane protein that has been identified in *E. andrei* (Škanta et al., 2013). There are two subtypes of TLRs, the single cysteine cluster TLR (scCTLR) and the multiple cysteine cluster (mccTLR). Both probably share a common origin due to their existence in different invertebrates and mammals and also the well-conserved downstream signalling pathway (Procházková et al., 2020 and papers there in). The scCTLR is highly expressed in the digestive tract and in amoebocytes (Bodó et al., 2018; Škanta et al., 2013).

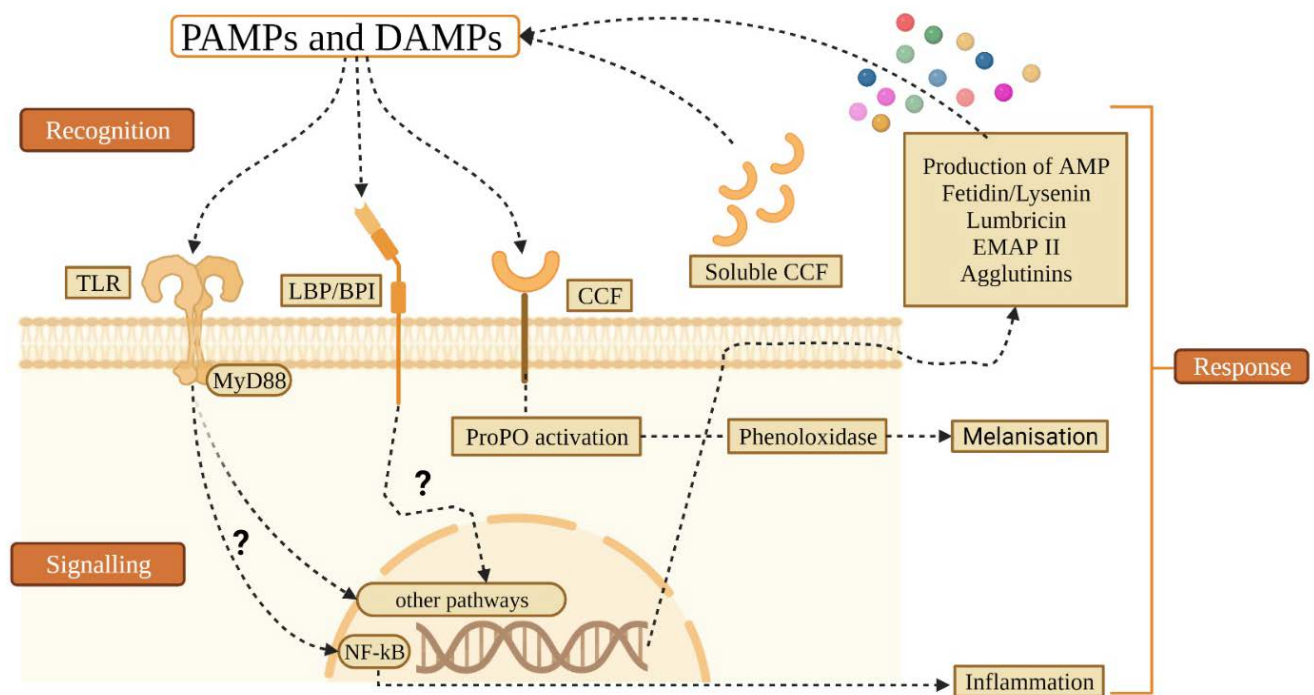


Figure 6. Recognition of PAMPs and DAMPs by PRRs, the possible signalling pathways and the response in coelomocytes. Created with BioRender.com

Chapter 1. Introduction

The difference between sccTLR and mccTLR is related to the age of earthworms. sccTLR is expressed in adult earthworms while mccTLR is expressed mainly in cocoons and offsprings (Prochazkova et al., 2019). The function of mccTLR is more associated with the development of earthworms in the first stages than with the immune response (Prochazkova et al., 2019).

After the recognition of PAMPs/DAMPs by PRRs (Figure 6), the signal transduction is developed; however, the earthworms' downstream signalling pathways are still not well known. TLR may initiate the NF- κ B pathway (Procházková et al., 2020 and papers there in), leading to the production of antimicrobial peptides or EMAP II (Figure 6; **1.4.3.2 Humoral response**). In the case of CCF, the prophenoloxidase cascade (PO) with the production of melanin as the end product can be triggered (Figure 6). The combination of melanin and lipofuscein aids in eliminating the foreign material that is encapsulated by coelomocytes and secreted through nephridia pores (Figure 3; Bilej et al., 2010). There are other signalling molecules like MEKK1 and PKC 1. MEKK 1 belongs to the mitogen-activated protein kinases (MAPK), and it coordinates the activation or production of some proteins like metallothioneins (Hayashi et al., 2012). Hayashi et al., (2012) observed a low expression of MEKK 1 and failure in metallothioneins induction when coelomocytes were exposed to Ag NPs compared to THP-1 cells, which could corroborate the suggested signalling pathway. MEKK 1 also participates in cellular homeostasis. Bodó et al. showed that MEKK 1 was exclusively expressed by HAs and GAs, although there was a weak signal in ECs (Bodó et al., 2018). Another studied signal transduction molecule is PKC 1, which is associated with cellular homeostasis and immune response. The expression of PKC 1 was exclusively detected in HAs and GAs. In humans, PKC is an enzyme that phosphorylates proteins downstream leading to the activation of the NF- κ B pathway, which may trigger the inflammatory response (Abbas et al., 2021).

Moreover, there are other ways how amoebocytes defend the organism against foreign material like ability of phagocytosis or encapsulation. Phagocytosis is the process when amoebocytes or, in the case of humans, the antigen-presenting cells (APC; macrophages, dendritic cells) engulf the foreign material to phagolysosomes (Abbas et al., 2021). Then, amoebocytes can throw the foreign material engulfed through the dorsal pores (Abbas et al., 2021; Bilej et al., 2010). The encapsulation is a process when amoebocytes form a capsule and inside, the agglutinated PAMPs are enclosed (Roubalová et al., 2015 and papers there in; Šíma, 1994). Then, the encapsulated PAMPs will be expelled (Figure 3).

1.4.3.2 Humoral response

The humoral response is maintained by the different molecules participating in the innate response. These are antimicrobial peptides (AMP), lysozyme, agglutinins, cytolytic molecules, and soluble PRRs (Figure 6).

Chapter 1. Introduction

Among the antimicrobial peptides, the most known are lumbricin, fetidin, and lysenin. Lumbricin was initially described in *Lumbricus terrestris* (Cho et al., 1998). Lumbricin is not expressed in ECs, while is weakly expressed in HAs and GAs. Its high expression was found in the foregut (Bodó et al., 2018). Lumbricin reacts with Gram-positive and harmful bacteria and fungi without hemolytic activity (Bodó et al., 2019; Cho et al., 1998).

The *Eisenia fetida andrei* factors (EFAFs) are other compounds found in the coelomic fluid. EFAFs are two glycoproteins secreted by HAs, GAs and ECs with strong hemolytic activity and antibacterial properties that protect earthworms against pathogenic soil bacteria (Bilej et al., 2010; Roch, 1979; Vaillier et al., 1985). Fetidins and lysenins belong to this group.

Fetidins are, antimicrobial peptides with lytic properties and peroxidase activity (Bilej et al., 2010). Lysenins are another antimicrobial peptides with haemolytic activity (Bruhn et al., 2006). Bodó et al showed that both ECs and HAs and GAs expressed lysenins (Bodó et al., 2018).

Fetidin and lysenin display a certain level of homology, suggesting a close relationship between both molecules, although it is known that both molecules are encoded by two different genes (Bilej et al., 2010; Procházková et al., 2006a). A universal primers combining all fetidin and lysenin molecules with hemolytic activity was designed (Dvořák et al., 2013). The use of these primers revealed that *E. andrei* expressed a higher quantity of these genes than *E. fetida*, suggesting a possible duplication of these genes in the genome of *E. andrei* (Dvořák et al., 2013).

EMAP II is a cytokine associated with the proinflammatory response and also a chemoattractancy of monocytes (Prochazkova et al., 2019). The relation between apoptotic cells and EMAP II production has been observed (Knies et al., 1998). It was also shown how TLR regulates downstream EMAP II production after the stimulation with bacteria (Zhang et al., 2005). However, it was not observed in earthworms exposed to bacteria (Prochazkova et al., 2019). Procházková et al., (2019) showed EMAP II was more highly expressed in seminal vesicles tissues than in colomocytes.

Lysozyme is an enzyme protecting against Gram-positive and Gram-negative bacteria. This enzyme is highly preserved in evolution, from plants to humans (Bodó et al., 2018). Josková et al. described the lysozyme similar to other invertebrate lysozymes (Josková et al., 2009). Although ECs, HAs and GAs expressed this AMP, the expression was slightly higher in HAs and GAs (Bodó et al., 2018).

1.4.4 Antioxidative system

The different exposures to immunostimulants or chemicals affect the earthworms by the increased oxidative stress. Therefore, several biomarkers used as antioxidants have been used in different studies (Table 1). Within these biomarkers, ROS and NO production, and SOD and CAT activity are commonly used (Table 1).

Chapter 1. Introduction

ROS are free radicals of oxygen species that are strong oxidising agents (Abbas et al., 2021). Coelomocytes can produce ROS when they are exposed to irritant substances that damage the cells. ROS should be used as a substance to destroy microbes, but it can damage the coelomocytes in higher concentrations. Thus, the ROS could be considered DAMPs recognised by other coelomocytes so the infected or damaged cell is eliminated. NO behave similarly to ROS. However, some other studies introduced respiratory burst consisting of the oxygen consumed in order to produce ROS (Abbas et al., 2021).

Metallothioneins are cysteine proteins. These proteins are associated with metal sequestering, usually exerted upon metal stress exposure. Therefore, they are highly expressed in HAs and GAs while are weakly expressed in ECs (Bodó et al., 2018).

CAT and SOD are molecules that reduce oxidative stress production. They decrease the excess of ROS exerted by coelomocytes. Then, the coelomocytes would not be damaged by ROS. CAT and SOD have different modes of action. While catalase efficiently removes the H_2O_2 , MnSOD or CuZnSOD is less specific and triggers different responses after metal exposure (Mincarelli et al., 2019; Qi et al., 2018; Roubalová et al., 2018). In earthworms, catalase is expressed in ECs, HAs, and GAs. The MnSOD and CuZnSOD are weakly expressed in ECs, HAs, and GA. After the phagocytosis, the engulfed material may be “killed” by ROS and NO. Therefore, CAT, MnSOD and CuZnSOD are needed to re-establish the homeostasis of coelomocytes and stop the NO and ROS production.

Chapter 1. Introduction

Tested substance	Concentration (mg/Kg)	Exposure media	Time exposure	Species	Biomarkers	Main findings	Reference	Year
nZVI	0, 100, 500, 1000	Soil and filter paper	7, 14, 21 and 28 days	<i>Eisenia fetida</i>	ROS	Inhibition of SOD and CAT at 100 and 1000 mg Kg ⁻¹ at 28 day. Inhibition respiratory to 500 and 1000 mg Kg ⁻¹ at 28 day. Increasing of ROS, CAT and MDA at 1000 mg Kg ⁻¹ at 28 day and 21 day for CAT.	Liang et al.	2017
					Respiratory test			
					MDA			
					SOD and CAT activities			
<i>Bacillus megaterium</i> and <i>Arthrobacter globiformis</i> (Gram +). <i>Pseudomonas stutzeri</i> and <i>Azotobacter chroococcum</i> (Gram -)	MOIs ranged 4:1 to 500:1.	Culture medium	16-18 h	<i>Eisenia hortensis</i>	NO generation	Increase of NO production after exposure to <i>B. megaterium</i> and <i>A.globiformis</i> . Dose-response in NO production.	Cook et al.	2015
					NOS			

Chapter 1. Introduction

Immunostimulants (LPS, PMA, ConA)	0.01, 0.05, 0.1, 0.5, 1.5, 10 $\mu\text{g mL}^{-1}$	Filter paper	3 days	<i>Eisenia andrei</i>	NO generation	Increase of NO, ROS and apoptosis with PMA exposure.	Homa et al.	2012
					ROS			
CuO NPs	100, 500, 1000	Soil	7 and 14 days	<i>Metaphire posthuma</i>	NO generation	At 1000 mg Kg-1 soil was observed adverse effects: Inhibition of phenoloxidase and catalase and SOD, at 7 and 14 day, respectively. Depletion of alkaline phosphatase, nitric oxide and total protein at 14 day. High generation of superoxide anion and depletion of phagocytic activity at 14 day.	Gautam et al.	2018
					Phagocytic response			
					SOD activity			
					Alkaline phosphatase activity			
					Catalase			
					Phenoloxidase			
					Superoxide anion generation			
					Total protein			
					Acid phosphatase			
NM-300K	2 $\mu\text{g mL}^{-1}$	Cultivation medium (CCM)	2,4,8, 24 h	<i>Eisenia fetida</i>	ROS generation	EC ₁₀ MTT and Neutral red assay of NM-300K: 2 $\mu\text{g mL}^{-1}$. No induction of ROS and no changes in calcium levels after 24 h. Induction of MEKK 1, TLR, LBP/BPI, metallothionein and lysenin at 24 h.	Hayashi et al.	2015
					MTT			
					Neutral Red Assay			
					Basal calcium levels			
					Gene Expression profiling			
PCDD/Fs		Soil	14 days		ROS			2018

Chapter 1. Introduction

PAHs	PCDDs (2.85, 50.2, 368, 5870, 627, 40900, 79300 ng Kg ⁻¹). PCDFs (65.7, 231, 254, 2360, 1130, 325, 2660, 373000, 4520, 239000 ng Kg ⁻¹). PAHs (167 mg Kg ⁻¹).			<i>Eisenia andrei</i>	Superoxidase dismutase activity	Increased of ROS in PCDD/F-polluted soil.intestinal villi and intestinal wall qas reduced in PCDD/F- polluted soil. Decrease of SOD in PCDD/F-. Reduction of CuZnSOD and increase of MnSOD in PCDD/F-polluted soil.	Roubalova et al.	
					Gene analyses			
					Histology			
n-HAP	0.007-70 g L ⁻¹	Filter paper	48 h	<i>Eisenia fetida</i>	POD activity	The highest peak of CAT and POD was at 0.7 g L ⁻¹ for all NPs. Depletion of CAT and POD at 70 g L ⁻¹ for n-HAP and n-Fe ₃ O ₄ . Depletion of SOD of 7 g L ⁻¹ for n-Fe ₃ O ₄ and increase the activity for 0.7 g L ⁻¹ . MDA increase for all of them from 0.7 to 70 g L ⁻¹ .	Liu et al.	2019
n-Fe ₃ O ₄		Soil			MDA			
n-zeolite					CAT activity			
ZnO NPs	10, 50, 250 mg Kg ⁻¹	Soil	7,14,21,28 days	<i>Eisenia fetida</i>	ROS	Highest ROS and LDH content in 50 µg mL ⁻¹ . Decreased of SOD at 250 mg Kg ⁻¹ at 14 day.	Li et al.	2019
					SOD activity			
					MDA			

Chapter 1. Introduction

					LDH	MDA increase in all concentrations of ZnO NPs.		
ZnO NPs	20, 250, 500 and 1000 mg Kg ⁻¹	Soil	29 days	<i>Eisenia andrei</i>	MDA	ROS and neutral red decrease in all the concentrations and >250 mg Kg ⁻¹ soil concentrations. No changes in CAT, GST and MTT exposed to ZnO NPs.	Garcia-Gómez et al.	2020
					CAT			
					Glutathione S-transferase (GST)			
					ROS			
					Neutral Red			
					MTT			

Table 1. Summary of the recent studies of different species of earthworms and the biomarkers assessed

Chapter 1. Introduction

1.4.5 Relevance of *E. andrei* for toxicity testing with NPs

In vitro approach has brought a new perspective into understanding the toxicity mechanisms of NPs with *E. andrei*. The typical acute and long-term toxicity testing are not enough regarding NPs toxicity because NPs are able to interact at molecular and cellular level affecting afterwards whole organism. The cellular and molecular approaches imply new toxicity testing for the risk assessment. Although commonly it is determined the NPs toxicity risk due to the mortality in *E. andrei*, the immune system of *E. andrei* plays a vital role into the earthworms protection.

The cellular and humoral responses explain how the immune system protects earthworms against non-self substances or living organisms like bacteria or viruses. Thus, the immune system opens a new broad field to understanding how NPs would interact with earthworms.

For example, *E. andrei* produces CAT or metallothioneins when they are under oxidative stress produced due to the interaction of NPs and metal NPs with earthworm coelomocytes. Then, risk assessment should include the molecular and cellular studies to understand the NPs realistic risk in the environment. Moreover, the risk assessment should also include combination of *in vivo/in vitro* exposure. Thus, it can be analysed the potential NPs dose at which could cause greater harm in *E. andrei*.

Although further studies would be needed to understand their immune system, the current resources and knowledge of earthworms' immune systems show the harm damages derived from NPs exposure.

Chapter 2



Research questions and hypotheses

2. Research questions and hypotheses

According to the evolution of nanoparticle manufacturing and how it reaches the environment, the soil ecosystems are one of the most significant sinks of NPs. Thus, NPs could affect invertebrates and other organisms inhabiting soil ecosystems. The starting hypothesis of this thesis is that earthworms may be toxicologically affected by NPs, and their immune cells could detect them and trigger their elimination.

The main research question of this work was: Can metal oxide NPs and their transformation products affect earthworms and their immune system through interaction with their immune-competent cells called coelomocytes?

Subsequently, the following research objectives were developed:

1. To optimize the cultivation medium for performing *in vitro* studies with coelomocytes.
2. To optimize the *in vitro* technique for their study through flow cytometry.
3. To understand the possible different sensitiveness between the subpopulation of coelomocytes.
4. To understand the protection mechanisms of *E. andrei* earthworms against metal oxide NPs (TiO₂ NPs and CuO NPs) and transformation products (Ag₂S NPs).
5. To describe the potential mechanism of toxicity of metal oxide NPs on coelomocytes and the subpopulation of amoebocytes.
6. To understand the possible risks for the immune system of earthworms.
7. To assess if environmentally predicted concentrations can affect earthworms.

The proposed research question and specific objectives are tackled in the chapters that form this thesis. This thesis was partially carried out as a part of the project PANDORA in the European Union's Horizon 2020 (PANDORA, <https://www.pandora-h2020.eu/>). Pandora is a European Training Network (ETN) in the framework of Marie Curie Skłodowska-Curie ITN programme and grant agreement No.67188. The Pandora project focused on the assessment of engineered nanoparticles (EMNPs) on the immune and defensive reaction of different organisms, from marine environments (sea urchins, mussels), to terrestrial environments (earthworms, plants and isopods), and humans. The focus was the immune-nanosafety by finding common techniques and mechanisms between the different species. This thesis has contributed to the characterization of NPs effect on the immune system of the model earthworm species *Eisenia andrei*, and to the optimisation of cellular and molecular techniques for their assessment.

Chapter 3



Material and methods

3. Material and methods

This thesis includes three different experiments, whose methodology is summarized in Figure 7. Two of the experiments were assessed *in vitro* using a coelomocyte culture and CuO NPs and TiO₂ NPs. The third experiment was based on an *in vivo* exposure following the OECD guideline for toxicity assessment with earthworms and including different lethal and sub-lethal endpoints (Figure 7).

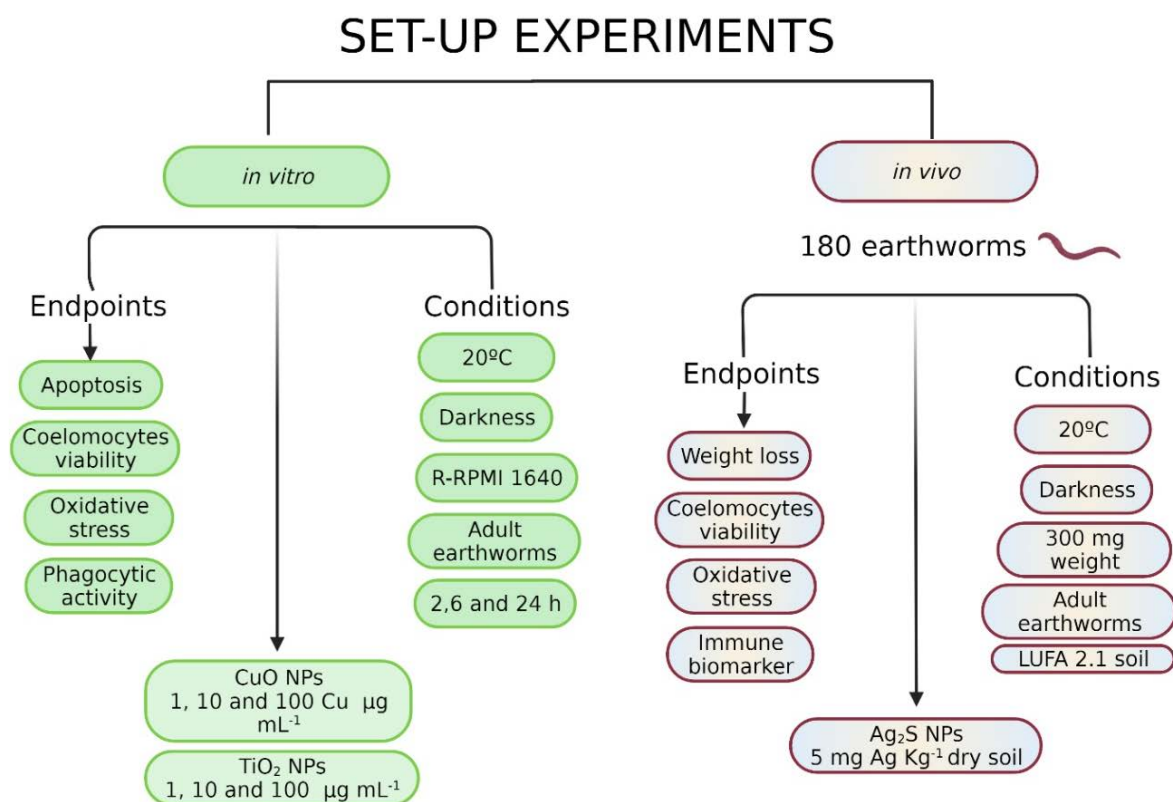


Figure 7. Summary of experimental set-up. Illustrative image of the three experiments performed for the PhD thesis. Endpoints and conditions are described in the figure and the methodology. Created with Biorender.com

3.1 NPs characterization

The metal oxide NPs were characterized in the cultivation medium (R-RPMI 1640) and Milli-Q water. The concentration for TiO₂ NPs was 1, 10 and 100 µg mL⁻¹. CuO NPs and CuSO₄ concentrations were 1, 10 and 100 µg Cu mL⁻¹. Every assay was carried out with the respective negative control (medium or Milli-Q water without NPs). Aeroxide TiO₂ P25 NPs were purchased from Evonik Degussa (Essen, Germany). According to the manufacturer, aeroxide TiO₂ P25 NPs were irregular, semi-spherical shape, mesoporous NPs; anatase and rutile (4:1). TiO₂ manufacturer primary size was 10-65 nm (**Annex II. Table 8. Chemicals and**

Chapter 3. Material and methods

reagents). CuO NPs were purchased from the Promethean Particles LTd (rod shape and 15-50 nm size; **Annex II. Table 8. Chemicals and reagents**). The *in vivo* experiment was carried out with Ag₂S NPs, which were purchased from Applied Nanoparticles S.L (20.4 ± 11.9 nm size distribution of Ag₂S NPs colloids stabilized in 1 mg mL⁻¹ 55 kDa Polyvinylpyrrolidone (PVP) aqueous media; **Annex II. Table 8. Chemicals and reagents**).

3.1.1 UV/Vis, Hydrodynamic size and zeta potential

For the UV/Vis characterization, NPs were diluted in R-RPMI 1640 medium and Milli-Q water. Aliquots of TiO₂ and CuO NPs were then pipetted into a 96-well U bottom plate (**Annex II. Table 8. Chemicals and reagents**) for UV/Vis analyses. The plates with the samples in triplicates were laid into TECAN 200 Pro plate reader (**Annex II. Table 9. Instruments**), and the analyses were performed.

The ζ-potential and hydrodynamic size of the metal NPs were performed by Multi-angle Dynamic Light Scattering (MADLS) using a Zetasizer Ultra (**Annex II. Table 9. Instruments**). Therefore, samples diluted in the different tested concentrations were analysed.

3.1.2 Primary size by TEM

5 µL of TiO₂ NPs (500 µg mL⁻¹) and CuO NPs (100 µg mL⁻¹), respectively, were laid onto glow-discharge activated 400 mesh Cu-grids (**Annex II. Table 8. Chemicals and reagents**) with a carbon coating film. Then, NPs were settled for 1 minute, and later the left solution was dried with paper, and the grids were air-dried.

The grids were checked by a Philips CM100 electron microscope (**Annex II. Table 9. Instruments**) with a Veleta slow-scan CCD camera (**Annex II. Table 9. Instruments**). Then, the TEM images were handled with iTEM software (**Annex II. Table 9. Instruments**) using standard modules. Finally, the primary size was analysed by manual measurement (64) and particle analyses from iTEM software (**Annex II. Table 9. Instruments**).

Ag₂S NPs were characterized by the manufacturer Applied Nanoparticles S.L. Fresh NPs were acquired by JEOL 1010 transmission electron microscope (**Annex II. Table 9. Instruments**) at 80 keV. Later, aliquots of stock solution of Ag₂S NPs (1:10 in Milli-Q water) were submerged in carbon-stabilized 200-mesh Cu-grids with a formvar coating (**Annex II. Table 9. Instruments**). After, samples were air-dried for 12 hours. The mean size and size distribution from TEM images were analyzed by ImageJ (**Annex II. Table 9. Instruments**).

Chapter 3. Material and methods

3.1.3 NPs-soil interaction

The NP spiking procedure was performed as follows. The WHC of LUFA 2.1 soil (**Annex II. Table 8. Chemicals and reagents**) was determined prior to the experiment. Later, dried LUFA 2.1 soil was placed in 1.5 L containers and moistened up to 50% with Ag₂S NPs or AgNO₃ (5 mg Ag Kg⁻¹ soil). According to OECD guideline 207 (OECD, 1984), 75 g of soil per earthworm (300 mg) was used for the *in vivo* experiment. The earthworms were kept for 24 h in a container with LUFA 2.1 soil (50% moistened) for their acclimatisation before the start of the experiment. Subsequently, the different exposure treatments (control soil, Ag₂S NPs or AgNO₃) were kept in darkness at 20 °C for 14 days. Soil samples from the start and end of the experiment were collected and processed by field-emission scanning electron microscope (FE-SEM) Hitachi SU6600 with an ultrahigh point-to-point resolution (1-2 nm) with elemental mapping using integrated energy-dispersive X-Ray (EDX) spectroscopy (**Annex II. Table 9. Instruments**).

3.1.4 ICP-OES

The quantification of Cu in CuO NPs was performed with ICP-OES (**Annex II. Table 9. Instruments**). The samples of the CuO NPs concentrations (1, 10, and 100 µg Cu mL⁻¹) were assessed at different time exposures (2, 6 and 24 h). After each exposures times, the samples were centrifuged four times (18400xg, 4 °C, 10 min) for the precipitation of NPs. The supernatant was analyzed by ICP-OES to determine the Cu concentration. The Cu concentration was as well quantified in parallel with CuSO₄.

Moreover, after the experiment, the extraction and quantification of silver in both earthworms and soils (0 and 14 days) were performed. First, earthworms and soil were lyophilized and homogenized. Then, according to Baccaro et al. (2018) protocol, 300 mg of soil or earthworm were supplemented by 8 mL of an acid mixture of HNO₃ and HCl (ratio 3:1; **Annex II. Table 8. Chemical and reagents**) in polytetrafluoroethylene vessel. Then, the samples were digested in a microwave MARS 5 (**Annex II. Table 9. Instruments**) by increasing the temperature from 160 °C for 20 min to 200 °C for 40 min. Later, the samples were centrifuged 4 times (18400xg, 4 °C, 10 min) to sediment the non-dissolved impurities. After, the supernatant was evaluated by ICP-OES to determine the silver concentration. The soluble silver concentration was determined in parallel for a solution of AgNO₃ (1, 10, and 100 µg Ag mL⁻¹) in 3% HNO₃. The instrumental quantification errors for Ag and Cu were lesser than 3%.

3.2 Animal handling and culture medium preparation

For every experiment and assay performed during the thesis, adult *Eisenia andrei* earthworms with clitellum were used. In the case of the *in vivo* experiment, 180 adult clitellated earthworms with 300 mg weight were handled.

Chapter 3. Material and methods

The culture of coelomocytes extruded from *E.andrei* was done with RPMI 1640 medium. First, the RPMI 1640 was supplemented with 5% FBS, 1 M HEPES, 100 mM Na-pyruvate, 100 mg mL⁻¹ gentamycin, and antibiotic-antimycotic solution (**Annex II. Table 8. Chemical and reagents**). Then, 60 % (v/v) dilution with Milli-Q water was done to obtain R-RPMI 1640 (Hayashi et al., 2013) for the *in vitro* experiments (ROS production, phagocytic activity, apoptosis, alkaline comet assay) with NPs (TiO₂ and CuO NPs; **Annex II. Table 8. Chemical and reagents**) at 2, 6 and 24 h.

3.3 Electron microscopy

3.3.1 Fixation

After the cultivation with CuO NPs and TiO₂ NPs, the coelomocytes were collected from 48 well-plate flat bottom. The viability of the coelomocytes was assessed by PI (**Annex II. Table 8. Chemical and reagents**) and measured with a flow cytometer (**Annex II. Table 9. Instruments**). The fixation was performed in a 1:1 (v:v) ratio by the mixture of 2.5% fixation solution with the coelomocytes suspension. The fixation solution contained 1 mL 5X PBS (3:2), 1 mL glutaraldehyde (25%), and 3 mL distilled water. Later, the cells with the fixation solution were mixed gently for 15 min and then, they were kept overnight at 4 °C.

3.3.2 SEM samples

Fixed coelomocytes were washed three times with PBS (3:2) at room temperature for 20 min. Then, they were spun down at 150×g and allowed to adhere to coverslips with poly-L-lysine coating in the refrigerator overnight. Subsequently, the coverslips were washed with distilled water and fixed with 1% OsO₄ for 1 h and at room temperature. Later, the coverslips were washed 3 times and 20 min each and dehydrated in alcohol series (25, 50, 75, 90, 96, and 100%). Later, they were critical point dried from liquid CO₂ in a K850 critical point dryer (**Annex II. Table 9. Instruments**). After the dried process, the coverslips were sputter-coated with a high-resolution turbo-pumped sputter coater Q150T (**Annex II. Table 9. Instruments**) with 3 nm platinum. Lastly, the samples were evaluated in an FEI Nova NanoSEM scanning electron microscope (**Annex II. Table 9. Instruments**) at 5 kV using CBS and TLD detectors. The high-resolution imaging used an electron beam deceleration (Müllerová, 2001) mode of the Nova NanoSEM scanning electron microscope performed at a StageBias of 883.845 V and an accelerating voltage of 5 kV. The EDS microanalysis was performed at 15 kV using an Ametek® EDAX Octane Plus SDD detector and TEAM™ EDS analysis systems (**Annex II. Table 9. Instruments**).

Chapter 3. Material and methods

3.3.3 TEM samples

The fixed coelomocytes were thoroughly washed and post-fixed with 1% OsO₄ in PBS (3:2) overnight at 4 °C. Then, the coelomocytes were washed with PBS at 4 °C and later with distilled water. After the washing steps, fixed coelomocytes suspension was warmed up to room temperature and embedded in 4% low-melting agarose. Later, the solidified agarose was cut into small cubes and dehydrated in alcohol series. Lastly, the cubes were embedded in an epoxy resin (**Annex II. Table 8. Chemicals and reagents**). Subsequently, the ultrathin sections were contrasted with uranyl acetate and lead citrate (Reynolds, 1963), and evaluated with a Philips CM100 electron microscope (**Annex II. Table 9. Instruments**). The digital images were acquired with a Veleta slow-scan camera (**Annex II. Table 9. Instruments**) and processed by the iTEM software package (**Annex II. Table 9. Instruments**).

3.3.4 STEM and X-ray microanalysis

For the CuO NPs samples, the ultrathin section was mounted over Ti-grids (**Annex II. Table 8. Chemical and reagents**) to avoid spurious X-rays from Cu-grids. Hence, the processing of the grids was similar to the ones described in **3.1.2 Primary size by TEM**. STEM images and EDS spectra were obtained on the JEOL F200 instrument with cold FEG operated at 200 kV and equipped with a HAADF detector and JED-2300 X-ray spectrometer with a windowless SDD detector (**Annex II. Table 9. Instruments**). Point spectra were recorded with a total live time of 60 s, and maps with a 256x256 points resolution were acquired with a total live time of 600 s at electron beam intensity setting, so then the X-ray detector accumulated a minimum of 1000 cps on the empty resin.

3.3.5 Data processing from Electron microscopy

The primary data was assessed by the proprietary software of electron microscopes and X-ray analyzers. The original pictures (16bit greyscale) were exported to TIFFs images (8bit greyscale). The spectra obtained from the JED-2300 X-ray spectrometer (**Annex II. Table 9. Instruments**) were exported into an industry-standard format for the following processing. The processing of every spectrum was performed in the NIST DTSA-II software (Ritchie et al., 2008; **Annex II. Table 9. Instruments**). The image plates were elaborated with the open-source Inkscape (<https://inkscape.org>; (**Annex II. Table 9. Instruments**)).

3.4 Cellular studies

3.4.1 In vitro experiments

2 mL of irritative substance (6.8 mM EDTA, 50.4 mM guaiacol glyceryl ether in diluted PBS (3 : 2), pH 7.3; **Annex II. Table 8. Chemical and reagents**) per earthworm was used for 2 min. Then, the earthworm was removed from the 15 mL falcon tube. Subsequently, the cells were centrifuged at (150xg, 4 °C, and 10 min). Next, the supernatant was removed, and the cells were washed two times with PBS (3:2; 150xg, 4 °C,

Chapter 3. Material and methods

10 min; (**Annex II. Table 8. Chemical and reagents**). After, the cells were counted with Brand™ Bürker Counting Chamber (**Annex II. Table 9. Instruments**). The exposure conditions were 2, 6 and 24 h at 20 °C and in darkness. The different experimental designs were performed with triplicates and their respective controls. The concentration of cells used in each assay was 10^5 cells/well, 2×10^5 cells/well, 3×10^5 cells/well, and 10^6 cells/well for ROS production, apoptosis, phagocytosis, scanning electron microscope, and lipid peroxidation, respectively.

The concentration chosen in TiO₂ NPs and CuO NPs were 1, 10, and 100 µg mL⁻¹. In the case of CuO NPs, there could be a tendency for ions released, so control of ions (CuSO₄) was chosen.

For *in vitro* experiments (TiO₂ NPs, CuO NPs or CuSO₄), the ROS production, apoptosis, and phagocytic activity were analyzed by laser scanning flow cytometer. The flow cytometer measurement is based on FSC, SSC, and fluorescence emission (green, orange, and blue wavelength). Different dyes such as PI (**Annex II. Table 8. Chemical and reagents**) and the fluorescences used in the assays were applied simultaneously because they were emitted in different ways wavelengths. Through a flow cytometer, the coelomocyte subsets were subdivided into eleocytes (ECs), hyaline (HAs), and granular amoebocytes (GAs). Due to the interference between the eleocytes fluorescences and the dyes used in the different assays, ECs were discarded from the analyses. The coelomocyte subsets detection was based on the cell size (FSC) and the cell inner complexity/granularity (SSC). The HAs gate and 10000 events were the thresholds for stopping the flow cytometer analyses. The minimum events collected were 1000 events per population. The events counts collected in each gate were calculated with Flowjo (**Annex II. Table 9. Instruments**). Finally, every assay was performed by three independent experiments with three technical replicates per treatment and time interval. Further, positive controls and control with and without PI and NPs (background noises) were included in each assay. Cells were washed after each exposure time to remove the R-RPMI 1640 (150xg, 4 °C, and 10 min).

3.4.2 *In vivo* experiment

Differently to the *in vitro* experiments, the extrusion of coelomocytes was performed by mild electrical stimulation (9 V battery) after 14 days of exposure to 5 mg Ag Kg⁻¹ soil as Ag₂S NPs or AgNO₃. Prior to the stimulation, *E. andrei* earthworms were kept in sparkling water and carefully dried with tissue paper. Then, earthworms were placed in a Petri dish and stimulated electrically to obtain the coelomic fluid. The collection of coelomic fluid was done by 5 µL capillary Brand™ Blaubrand® micropipettes (**Annex II. Table 8. Chemical and reagents**) and later, coelomic fluid was transferred into a 1.5 mL Eppendorf tube and kept on ice before the subsequent analyses (coelomocytes viability, nitric oxide and phenoloxidase activity).

Coelomocyte viability was assessed from 15 animals of each exposure (control soil, Ag₂S NPs or AgNO₃). Coelomocytes were stained 1:1 (v:v) by 0.4% trypan blue solution (**Annex II. Table 8. Chemical and**

Chapter 3. Material and methods

reagents). Stained coelomocytes were considered dead. Then, coelomocytes were counted by hemocytometer (**Annex II. Table 9. Instruments**). Every sample had two technical replicates. The viability of coelomocytes (%) was determined by the following equation:

$$\text{Viability (\%)} = [1 - ((\text{Dead cells}) / (\text{Total number of cells}))] \times 100$$

3.5 Oxidative stress

3.5.1 ROS and NO production

ROS production analyses were performed by adding 20.6 μM DCF-DA (**Annex II. Table 8. Chemical and reagents**) to the washed cell suspension (PBS 3:2; 200 \times g, 4 $^{\circ}\text{C}$, 10 min) for 15 min in darkness. Subsequently, the cell suspension was washed twice with PBS (3:2; 150 \times g, 4 $^{\circ}\text{C}$, 10 min) and stained with PI (1 mg L^{-1}). Then, the cell suspension was carried out through a flow cytometer. The positive control was 1 mM H_2O_2 (**Annex II. Table 7. Chemical and reagents**).

NO production was carried out after the collection of coelomic fluid. 60 μL coelomic fluid was mixed with a 28 μL solution composed of 1% sulphanilamide, 5% phosphoric acid, and 1 mM L-Arginine (**Annex II. Table 8. Chemical and reagents**). Similarly, the calibration curve with nitrate standards (0-200 μM NaNO_2 ; **Annex II. Table 8. Chemical and reagents**) was prepared with the same ratio. Then, samples were centrifuged (14,000 \times g; 10 min, 4 $^{\circ}\text{C}$), and the supernatant was transferred to a 384-well plate. Later, 20 μL 1% NED (**Annex II. Table 8. Chemical and reagents**) was added to the samples. Finally, the plate was shaken for 5 min before measuring the absorbances at 540 nm by TECAN Infinite 200 Pro (**Annex II. Table 8. Chemical and reagents**). The analyses consist of 10 samples per treatment (control, Ag_2S NPs or AgNO_3), a blank (distilled water), and standard duplicates.

3.5.2 MDA production

The MDA production was measured in coelomocytes as well as in earthworm tissue. For the earthworm tissue, MP FastPrep-24MP (**Annex II. Table 9. Instruments**) was used to homogenize the earthworm in 1 mL PBS with 0.5 g glass beads at 5.5 m s^{-1} for 1 min. Then, 1 mL of the tissue was taken for MDA extraction. MDA production was then assessed by HPLC-FLD (**Annex II. Table 9. Instruments**) using a derivatized complex with thiobarbituric acid as it was explained by Semerad et al. 2018. Similarly, the assessment of MDA was performed with coelomocytes exposed to TiO_2 NPs, CuO NPs, or CuSO_4 (10 and 100 $\mu\text{g mL}^{-1}$) after the cultivation times (2, 6 and 24 h).

Chapter 3. Material and methods

3.6 Genotoxicity and immune biomarkers

Genotoxicity was based on the protocol of the alkaline comet assay (Ciğerci et al., 2016; Olive and Banáth, 2006), and modifications were done to optimize the alkaline comet assay. First, 1.5×10^4 cells were exposed to 1, 10, and 100 $\mu\text{g mL}^{-1}$ (TiO_2 NPs, CuO NPs or CuSO_4) after 2, 6, and 24 h. Then, cells were mixed smoothly with 2% LMA (**Annex II. Table 8. Chemical and reagents**) at 37°C. Later, the LMA with cells over the glass slides was maintained at 4 °C for 10 min. After, the slides were immersed for 2 h in lysis buffer (2.5 M NaCl, 10 mM Tris-HCl, 100 mM EDTA, and 1% Triton X-100; **Annex II. Table 8. Chemical and reagents**). Subsequently, the slides were transferred into an unwinding buffer (0.03 M NaOH, 2 mM EDTA; **Annex II. Table 8. Chemical and reagents**) for 20 min. Next, the gel electrophoresis was performed at 24 V, 300 mA for 25 min. Carefully, the slides were rinsed 3 times in neutralizing buffer (0.4 M Tris; **Annex II. Table 8. Chemical and reagents**) at room temperature for 5 min and then stained for 20 min with PI (3 $\mu\text{g mL}^{-1}$). Last, the glass slides were washed with distilled water to remove the excess PI staining for 5 min and stored in humid chambers for a short time. The glass slides were analyzed by fluorescence microscope and LUCIA Comet Assay software (**Annex II. Table 9. Instruments**). 100 coelomocytes per replicate, treatment, and time were used, and the median of the DNA content in their 100 comet tails (%) was taken as a parameter of DNA damage.

Regarding the immune biomarkers, phagocytosis and apoptosis were chosen for *in vitro* tests, and phenoloxidase was used for *in vivo* experiments. After the incubation, phagocytic activity was carried out by applying latex beads Fluoresbrite® Plain YG (**Annex II. Table 8. Chemical and reagents**) in the culture cells in 1:100 (cell: beads) for 18 h at 17 °C in the dark. Later, the cells were washed twice with PBS (3:2; 150×g, 4 °C, 10 min) and stained with PI. Lastly, samples were brought for analysing by flow cytometer, and kept the cells on ice. It was considered phagocytic activity (%) when alive cells could engulf at least one bead from each subpopulation (HAs and GAs). Samples also included controls with beads and no beads to prepare the gates by FlowJo software (**Annex II. Table 9. Instruments**). Moreover, the confocal microscope Olympus FV1000 TIRF (**Annex II. Table 9. Instruments**) was used to check the samples after the analyses with the flow cytometer. Positive control (10 mM H_2O_2 ; **Annex II. Table 8. Chemical and reagents**) for 30 min, and the room temperature was included.

The apoptotic activity was measured for the *in vitro* experiments. After the incubation times (2, 6, and 24 h) with TiO_2 NPs, CuO NPs or CuSO_4 , the cell suspension was centrifuged (150×g, 10 °C, 10 min) and washed twice (150×g, 10 °C, 10 min) with Annexin V binding buffer (0.01 M HEPES, 0.14 M NaCl, 2.5 mM CaCl_2 , pH 7.4; **Annex II. Table 8. Chemical and reagents**). Later, the cells were stained with 5 μL Alexa Fluor 647-Annexin V solution (500 μL Annexin binding buffer and one drop from the stock solution; **Annex II. Table 8. Chemical and reagents**) for 15 min and in darkness. Subsequently, PI was added into the cell Annexin V-stained suspension and measured in the flow cytometer. The % of apoptotic activity and

Chapter 3. Material and methods

necrosis was represented as apoptotic/necrotic cell number out of each subpopulation (HAs and GAs). In addition, positive control (10 mM H₂O₂) was incubated with coelomocytes for 30 min at room temperature.

Phenoloxidase activity was assessed for the *in vivo* experiment after the extraction of coelomic fluid with mild electrical stimulation (**3.5.1 ROS and NO production**). First, 200 µL of a solution with 2 mM SDS and 4 mM dopamine hydrochloride (**Annex II. Table 8. Chemical and reagents**) diluted in PBS was added to 10 µL of coelomic fluid. Next, 40 µL of the suspension was transferred to a 384-well plate and shaken for 10 seconds. Then, the absorbance at 490 nm was evaluated every 2 min for 8 h by TECAN Infinite 200 Pro (**Annex II. Table 9. Instruments**). The samples collected (15 per treatment; control, Ag₂S NPs or AgNO₃) were analysed quadruplicated.

3.7 mRNA analyses

After the cultivation of TiO₂, CuO NPs or CuSO₄ (1 and 10 µg mL⁻¹) at 2, 6 and 24 h, coelomocytes were kept on ice prior to RNA extraction. RNA isolation was performed according to the RNAqueous®-Micro Kit (**Annex II. Table 8. Chemical and reagents**). 500 ng total RNA and treated with DNase I was reverse transcribed with Oligo (dT) 12-18 primer and Superscript IV Reverse Transcriptase (**Annex II. Table 8. Chemical and reagents**). Then, a PCR reaction was performed. Non-RT controls were run in parallel to ensure that gDNA contamination was eliminated.

Several qPCR (CFX96 Touch TM; **Annex II. Table 9. Instruments**) were carried out to detect the changes in the mRNA levels of the genes presented in Table 2. The qPCR reaction was performed as follows: a total of 25 µL within 4 µL cDNA (1/10 dilution for the genes except for 1/5 dilution for both SODs). Then, the cycling parameter was established as 94 °C and 4 min; 35 cycles at 94 °C for 10 s, 60 °C for 25 s (except for MEKK 1, CAT, PKC 1 at 58 °C), at 72 °C for 35 s. The final extension was 72 °C for 7 min. Melt curves and standard curves were also performed to check the specificity and the efficiency of the primer pairs. Last, the gene expression changes were calculated as the 2^{-ΔΔCT} (Livak) method. Moreover, RPL17 and RPL13 were selected as reference genes (internal controls) to normalize the other gene expression. The mRNA level fold change was related to the difference in the settled controls. The non-template controls were also analyzed in each experiment.

Chapter 3. Material and methods

Gene	Direction	Sequence	Size (bp)	GenBank No.
Metallothionein	Forward	5'-AAA AAG CTT TGC TGT GCT GAT GCT-3'	154	KP770991
	Reverse	5'-CGT ATT TCA ATG CCT TGG CTC TCA-3'		
Phytochelatin	Forward	5'-CTG GAA GGG ACC GTG GAG ATG-3'	202	KP770990
	Reverse	5'-ACC CTT CGA CAC CCG TTT CAC AA-3'		
MnSOD	Forward	5'-GAA GCT CAG ACC AAA GGA GAC-3'	91	KU057379
	Reverse	5'-TGA TTG ATA TGT CCT CCG CC-3'		
CuZnSOD	Forward	5'-ATG AGT TTA GCA AGA CCA CTG-3'	103	KR106132
	Reverse	5'-GTC CAA GCC AAC CAT ATC AC-3'		
CAT	Forward	5'-TAC AAA CTG GTG AAC GCC GA-3'	139	DQ286713
	Reverse	5'-AAA GGT CAC GGG TCG CAT AG-3'		
EMAP II	Forward	5'-CAT CCC GAT GCG GAC AGT CTG TA-3'	244	AEB92227
	Reverse	5'-TCC CCA ATG GCA GCA CCA ATT-3'		
Fet/Lys	Forward	5'-TGG CCA GCT GCA ACT CTT-3'	176	U02710 D85846 D85848 D85847 DQ144453
	Reverse	5'-CCA GCG CTG TTT CGG ATT AT-3'		
Lumbricin	Forward	5'-AGG CCA TAC TCG GAA CGC AAG AA-3'	213	KX816866
	Reverse	5'-CAC ACG CTC CAT CGA AAT CAA CTC-3'		
MEKK 1	Forward	5'-CAA GGA ACG ATC CCA TTC AT-3'	147	EH672240
	Reverse	5'-GTA TCA TGG TGC AAC CAA CG-3'		
PKC 1	Forward	5'-TTT TAT GCG GCC GAA GTC A-3'	120	DQ286716
	Reverse	5'-GTC GGC GAT TTT GCA GTG A-3'		
RPL 17	Forward	5'-CAT CAC ACC CTA CAT GAG CA-3'	179	BB998250
	Reverse	5'-TAA CGG AAG AAG GGG TTA GC-3'		
RPL 13	Forward	5'-CAC AAT TGG AAT TGC TGT CG-3'	144	BB998075
	Reverse	5'-GTG GCA TCA CCC TTG TTA GG-3'		

Table 2. Primer sequences used for RT-PCR.

3.8 Weight loss and mortality

The *in vivo* experiment was performed by the OECD guidelines (OECD 207; OECD 1984). The endpoints used were weight loss and mortality. For the *in vivo* experiment, 180 earthworms were used. Before starting the experiment, earthworms were weighed, and they were approximately 300 mg. Mortality was also assessed. According to OECD 207 guidelines (OECD, 1984), mortality was considered when it was found immobilized or dead earthworm body in the container after the 14 days of exposure.

Chapter 3. Material and methods

3.9 Statistical analyses

Results from the *in vitro* experiments (ROS and MDA production, alkaline comet assay, phagocytic activity, apoptosis, mRNA levels) were analysed by a two-way ANOVA and Bonferroni post-hoc test. The *in vivo* exposure analyses changed according to Gauss distribution of values and varied according to whether the data met the assumptions or not for parametric tests. Coelomocytes viability, NO production, phenoloxidase activity and weight loss were analysed by one-way ANOVA with Bonferroni's post-hoc test. The MDA production was analysed by the non-parametric Kruskal-Wallis test, followed by a Dunn's multiple comparison test. The statistical analyses were performed by GraphPad Prism software (8.4.3 version, **Annex II. Table 9. Instruments**) and Origin Lab software 2019b (**Annex II. Table 9. Instruments**). Statistically significant differences were assumed when the calculated p-value was below 0.05, and were generally represented with different stars according to the calculated p-value: *** $p < 0.001$, ** $p < 0.01$ and * $p < 0.05$

Chapter 4



Results

4. Results

The results of this thesis have been (partially) published in the *Nanomaterials Journal*, *Environmental Science Nano Journal*, and *Comparative Biochemistry and Physiology, Part C*. The article titles were: “*In vitro* interactions of TiO₂ nanoparticles with earthworm coelomocytes: Immunotoxicity assessment.”, “Understanding the toxicity mechanism of CuO nanoparticles: the intracellular view of exposed earthworm cells”, and “Effects of silver sulfide nanoparticles on the earthworm *Eisenia andrei*”.

4.1 NPs characterization

4.1.1 UV/Vis, Hydrodynamic size and zeta potential

The suspension of TiO₂ NPs and CuO NPs dispersed in distilled water, and R-RPMI 1640 medium were characterized (Table 3 A and B). The characterization was assessed at the different time exposures chosen for the *in vitro* analyses. We could observe that the values from zeta potential and hydrodynamic size were correlated in TiO₂ NPs (Table 3 A). The results showed that TiO₂ NPs remained stable in the distilled water (-30 mV approximately) so that their hydrodynamic size remained similar during the different time exposures (500-580 nm; Table 3 A). Unfortunately, the instability appeared when TiO₂ NPs were dispersed in R-RPMI 1640 medium. The values of zeta potential ranged from 0 to -15 mV approximately (Table 3 A). Then, the hydrodynamic size tended to increase along with the time exposures and the greatest size (597 nm) was at 24 h (Table 3 A).

At CuO NPs, the zeta potential was approximately 30 mV up to 6 h, then it decreased at 24 h (-15 mV) in distilled water (Table 3 B). In R-RPMI 1640 medium, the zeta potential values were -15,9, -20.7 and -15.7 mV at 2, 6 and 24 h, respectively (Table 3 B). Similarly to the TiO₂ NPs hydrodynamic size values, it could observe that the size of CuO NPs increased along the time exposures in R-RPMI 1640 medium (Table 3 A and B). However, in the case of distilled water, this increase was not observed; it remained similar in both exposure times.

The UV/Vis spectra measurements showed differences between both metal oxide NPs. While TiO₂ NPs were between 300-370 nm (Table 3 A), the CuO NPs were located at higher wavelengths (400-500 nm; Table 3 B). However, the wavelengths of both NPs were not in the same wavelengths of the reagents used in the different assays.

Chapter 4. Results

4.1.2 Primary size by TEM

The NPs' primary size was measured by TEM images and iTEM software. TiO₂ NPs and CuO NPs shapes were described as spherical or rod NPs. Their sizes varied between them. TiO₂ NPs were ranged between 20-100 nm while CuO NPs were between 5-15 nm sizes (Figure 8 A and B). The Ag₂S NPs were characterized by the manufacturer, Applied Nanoparticles (Barcelona, Spain). Ag₂S NPs shape was described as crystal rods, the Ag₂S NPs colloids had some degree of agglomeration (Figure 8 C). The size distribution of Ag₂S NPs was 20.4 ± 11.9 nm size after analysing 613 NPs (Figure 8 C). These NPs were provided from the same batch of Ag₂S NPs characterized by Baccaro et al (2018).

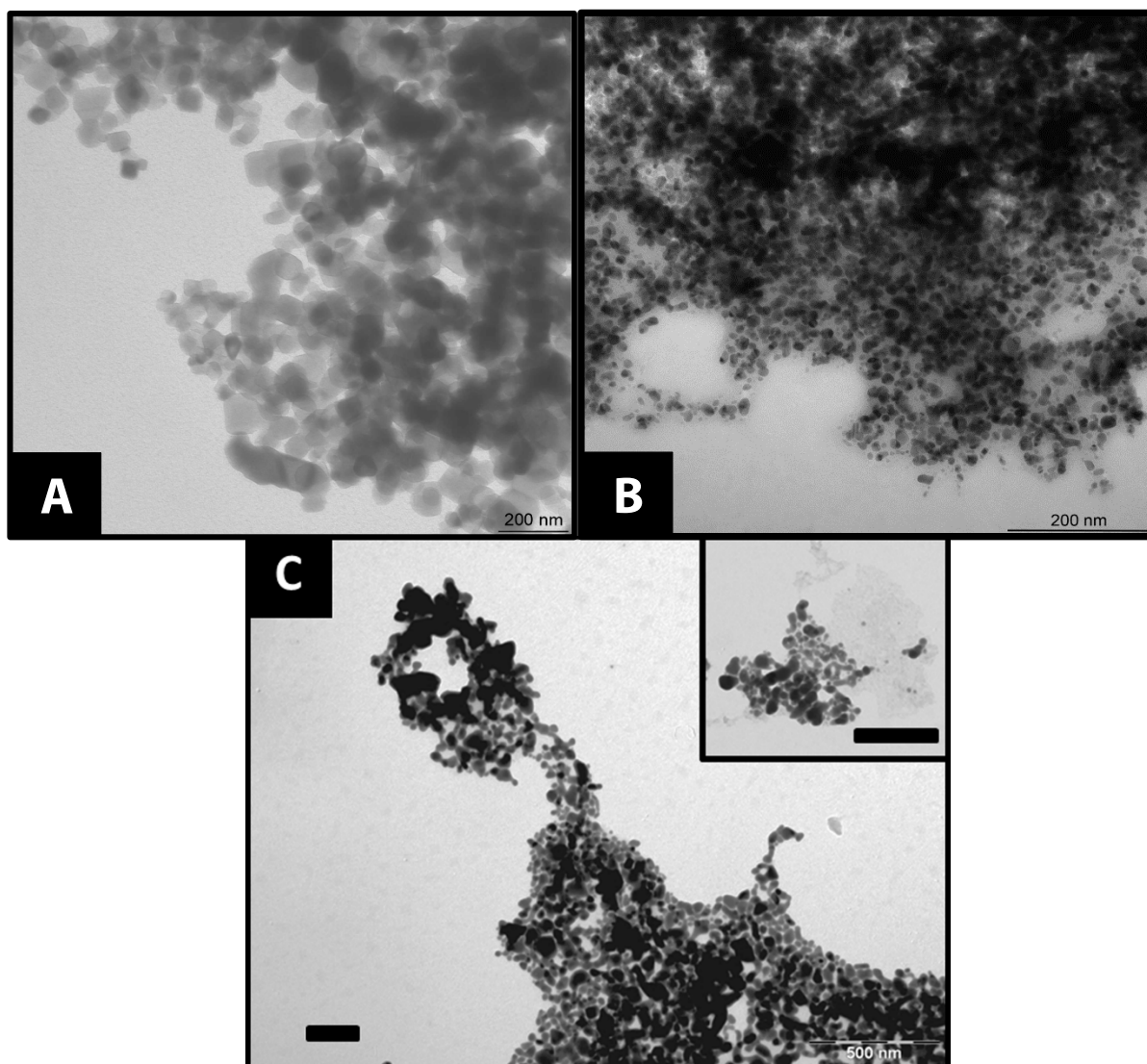


Figure 8. TEM images of TiO₂ NPs, CuO and Ag₂S NPs. A) 500 µg mL⁻¹ TiO₂ NPs aggregated in distilled water. The scale bar is 200 nm. B) 100 µg Cu mL⁻¹ CuO NPs in distilled water. The scale bar is 200 nm C) Low-magnification TEM image with a higher-magnification top-right inset with Ag₂S NPs. The scale bar is 500 nm.

	UV/Vis (nm)			Hydrodynamic size (nm)			ζ (mV)		
	2 h	6 h	24 h	2 h	6 h	24 h	2 h	6 h	24 h
A	TiO ₂ NPs	TiO ₂ NPs	TiO ₂ NPs	TiO ₂ NPs	TiO ₂ NPs	TiO ₂ NPs	TiO ₂ NPs	TiO ₂ NPs	TiO ₂ NPs
Distilled water	300-370	300-370	300-370	581±23.30	570±2.75	480±64.3	-26.8±2.99	-31.7±0.921	-32.9±2.59
R-RPMI 1640 medium	320-380	320-380	320-380	31.34±1.55	35.5±3.94	597±447	-16.9±0.60	-7.87±0.631	-5.94±0.94

	UV/Vis (nm)			Hydrodynamic size (nm)			ζ (mV)		
	2 h	6 h	24 h	2 h	6 h	24 h	2 h	6 h	24 h
B	CuO NPs	CuO NPs	CuO NPs	CuO NPs	CuO NPs	CuO NPs	CuO NPs	CuO NPs	CuO NPs
Distilled water	400-500	400-500	400-500	1050±74.9	808±303	934±343	26.1±1.92	37.1±2.81	-15.7±1.82
R-RPMI 1640 medium	<230	<230	<230	316±8.08	1920±765	351±51.7	-15.9±0.581	-20.7±1.05	-15.7±0.581

Table 3. UV/Vis spectra absorbance (nm), Hydrodynamic sized (Z-average; nm) measured by MADLS and zeta potential (ζ; mV). The values are expressed as a mean of three independent experiments ± SD. A) Characterization of 100 µg mL⁻¹ TiO₂ NPs and B) Characterization of 100 µg Cu mL⁻¹ CuO NPs.

Chapter 4. Results

4.1.3 NPs-soil interaction

The soil samples were collected to understand the possible ways NPs interact with the soil and the effects observed afterwards. Random samples from different Ag_2S NPs containers were collected after the spiking procedure, and, similarly it was done with samples after 14 days of exposure. Finally, according to **3.1.3 NPs-soil interaction**, samples were processed by SEM-EDS spectra. The SEM images taken at the start showed that NPs were found in the soil (Figure 9 A). Moreover, the EDS spectra analysed and confirmed the elemental detection of S and Ag from Ag_2S NPs (Figure 9 B and 9 C; spot 1 and 2). Moreover, gate 3 (Figure 9 A) was another point selected, and the EDS spectra showed that it did not contain either Ag or S. So it was not the Ag_2S NPs; maybe, it could be part of the soil as it contained C, O and Si (spot 3; Figure 9 D).

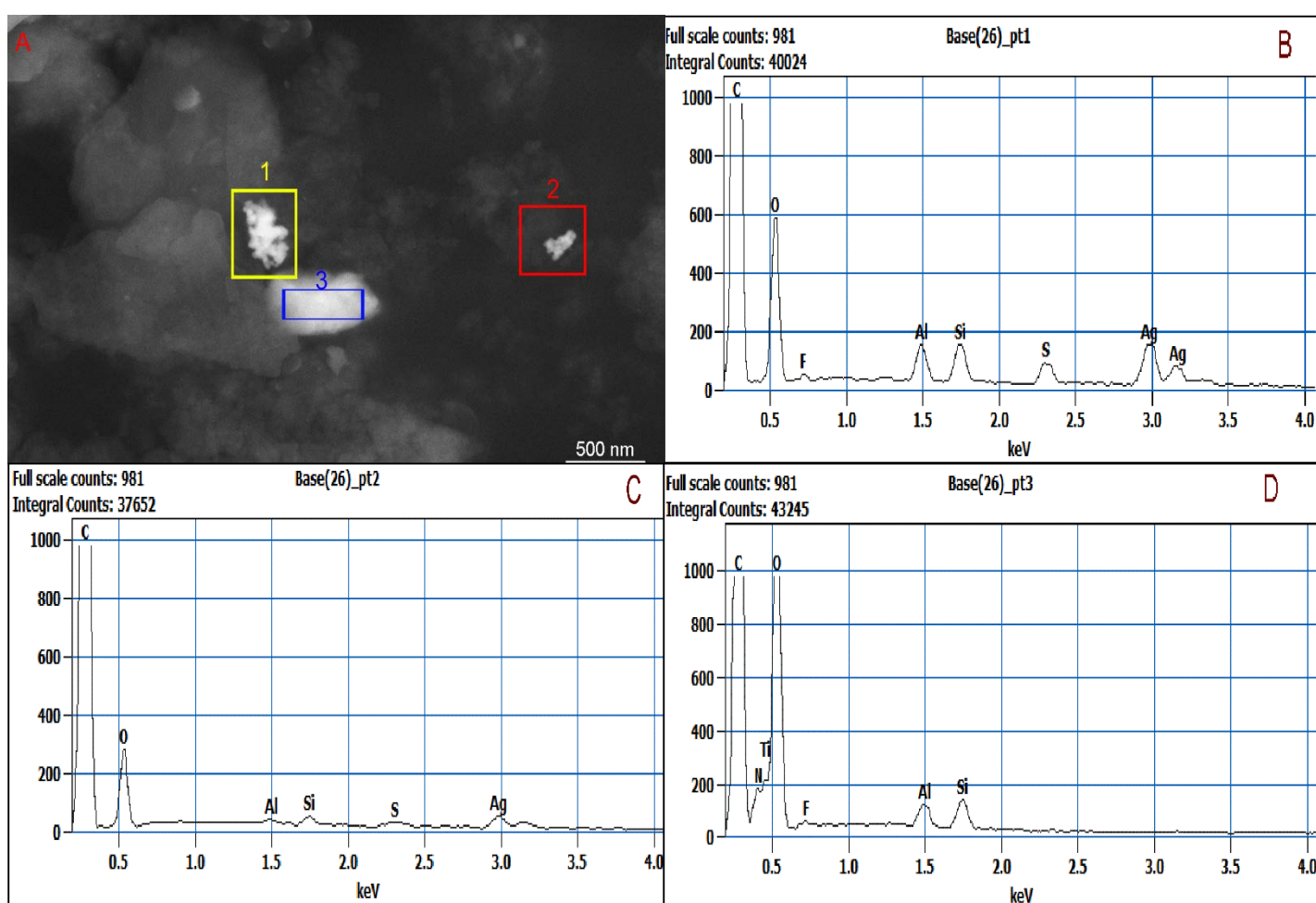


Figure 9. SEM-EDS soil samples at the start of exposure with Ag_2S NPs. Picture from SEM and EDS spectra from soil samples at the start. A) SEM image and the gates for EDS. B) EDS spectra from gate 1. C) EDS spectra from gate 2 and D) EDS spectra from gate 3. The scale bar is 500 nm. Acc. Voltage is 10000 kV and the magnification is 100000x.

Chapter 4. Results

The samples after 14 days of exposure were also processed. The picture (Figure 10 A) showed that we could observe NPs within the soil collected from the Ag₂S NPs. Furthermore, the elemental analyses performed (EDS) confirmed that the particles contained elemental Ag and S, which confirmed that they were the Ag₂S NPs we introduced (Figure 10 B).

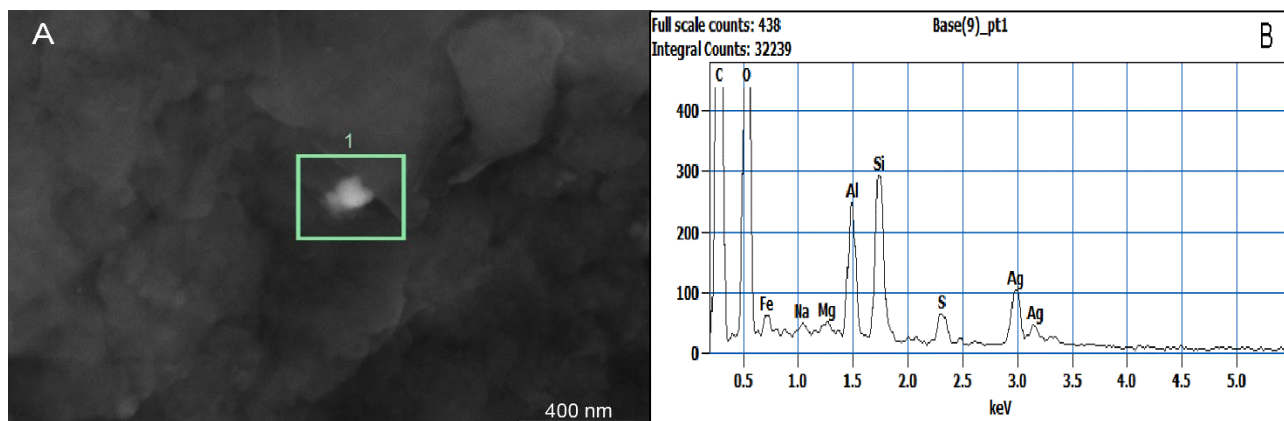


Figure 10. SEM-EDS soil samples after 14 days. Picture from SEM and EDS spectra from soil samples after 14 days. A) SEM image and the gate for EDS. B) EDS spectra from gate 1. The scale bar is 400 nm. Acc. Voltage is 10000 kV and the magnification is 200000x.

4.1.4 ICP-OES

The Cu from CuO NPs and CuSO₄ was quantified in the R-RPMI 1640 medium, where CuO NPs and CuSO₄ were dispersed. The results showed that the lower concentrations released most Cu⁺² ions after 6 hours of exposure (Figure 11). Then, the higher concentration (100 µg Cu mL⁻¹) did not release 100% of Cu⁺² ions after 48 h. It seemed there was a tendency that the ions were released after a few hours in the R-RPMI 1640 medium, and then the rest of the NPs remained stable, and they did not dissolve in the solution. The solution of CuSO₄ was assessed, although it is known that CuSO₄ dissolves quickly and releases the Cu⁺² ions. The CuSO₄ was the control of Cu⁺² ions to detect whether the effects were derived from NPs or the ions.

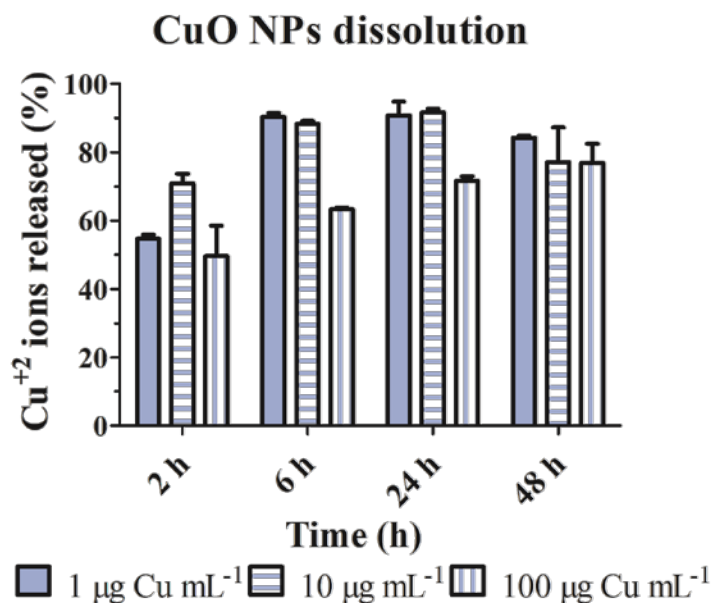


Figure 11. Dissolution of CuO NPs in R-RPMI 1640 medium. The Cu⁺² ions released in the R-RPMI 1640 medium after 2, 6, 24, and 48 h of exposure to the different CuO NPs concentrations used (1, 10 and 100 µg Cu mL⁻¹ CuO NPs). Values were measured by ICP-OES and shown as mean ± SD of three measurements with three replicates.

Similarly to CuO NPs, Ag₂S NPs were analysed by ICP-OES. The set-up experiment was the introduction of 5 mg Kg⁻¹ of Ag from Ag₂S NPs into the soil. The ICP-OES values confirmed that we inoculated the quantity of Ag⁺ ions we wanted to assess. Further, the control samples from the soil did not contain any Ag⁺ ions, which means there was no cross-contamination. Further, we observed that the concentration at 0 and 14 days varied similarly to both NPs and control ions treatment. According to the processed data, the nominal concentration remained at the start (0 days) while there was a lower concentration of Ag₂S NPs after 14 days (4.4 mg Ag Kg⁻¹; Table 4).

ICP-OES detected the quantity of Ag ingested by earthworms after 14 days exposed to Ag₂S NPs or AgNO₃. The values were dependent on the earthworms' weight. We observed that earthworms ingested Ag₂S NPs after 14 days (Table 4). We found 6.4 mg Ag Kg⁻¹ dry weight in the earthworms exposed to the Ag₂S NPs and 10.8 mg Ag Kg⁻¹ dry weight in earthworms exposed to AgNO₃ (Table 4). Hence, there was an uptake in both NPs and control ions treatment.

Treatment \ Time exposure	Soil (mg Ag kg ⁻¹)		Earthworm (mg Ag kg ⁻¹ dry weight)
	0 day	14 days	14 days
Control	0.0 ± 0.0	0.1 ± 0.0	0.0 ± 0.0
Ag ₂ S NPs	6.6 ± 0.8	4.4 ± 0.5	6.4 ± 0.3
AgNO ₃	4.9 ± 0.4	6.4 ± 0.7	10.8 ± 3.2

Table 4. The concentration of Ag⁺ ions was detected in the soil (0 and 14 days) and in the earthworms after 14 days of exposure. Values showed the mean ±SD; n=3

4.2 Coelomocytes cultivation

The cultivation of coelomocytes was optimised, and it was established that coelomocytes could stay alive in the R-RPMI 1640 medium up to 24 h. Then, the *in vitro* experiments were performed using 2, 6, and 24 h as the exposure times. The concentrations of TiO₂ and CuO NPs varied from the lowest concentration to the highest one (1, 10, and 100 µg mL⁻¹). The coelomocytes extracted from the earthworms exposed to Ag₂S NPs were not cultivated.

4.3 Electron microscopy

The coelomocytes exposed to TiO₂ NPs and CuO NPs were observed by SEM and TEM to detect and localize the NPs in the cells or their surroundings.

TiO₂ NPs (100 µg mL⁻¹) were localized on the coelomocytes membranes by SEM (Figure 12 A). The EDS microanalyses confirmed the presence of Ti (arrow blue, spot 2; Figure 13 A) in the cluster of TiO₂ NPs. EDS spot 4 (Figure 13 A), which is only coelomocytes, was also measured, and no Ti peak was detected, which is in concordance with the observations (Figure 13 B). The EDS spectra confirmed that the clusters with no coelomocyte shapes were TiO₂ NPs (Figure 13 A and B). Further, the 10 µg mL⁻¹ TiO₂ NPs were detected on the coelomocytes' surface, although the frequency was lower.

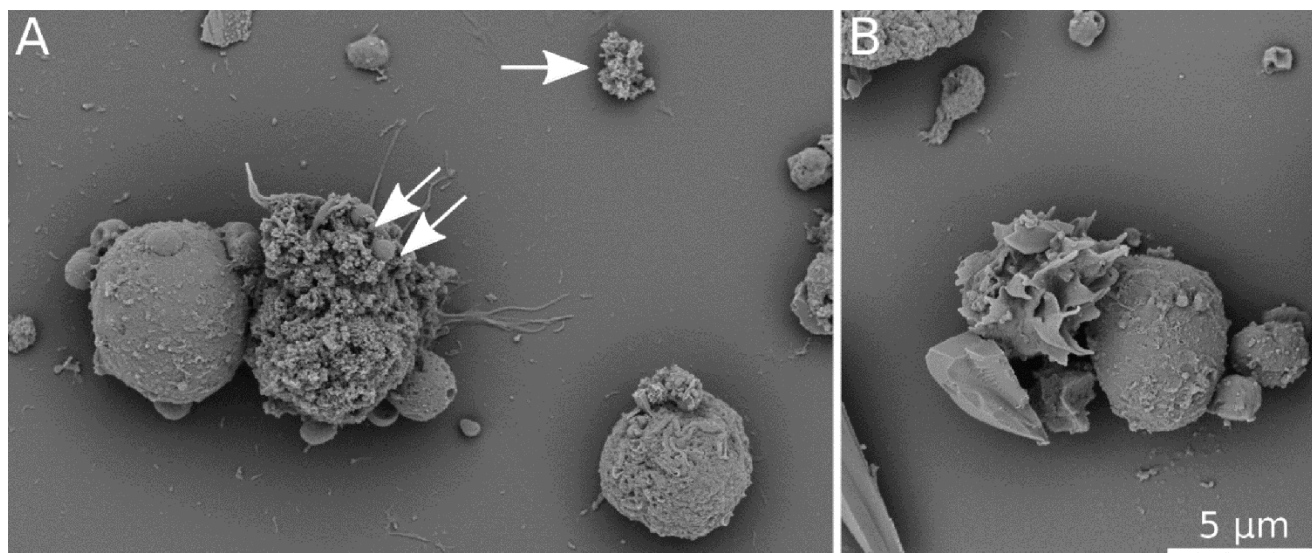


Figure 12. Scanning electron microscopy of coelomocytes. (A) Coelomocytes exposed to $100 \mu\text{g mL}^{-1}$ TiO_2 NPs for 2 h; (B) control cells cultured in R-RPMI 1640 medium. Images were recorded with B + C segments of a CBS detector at 3 kV. The white arrow indicates a TiO_2 NPs cluster on sample support. Clusters of the same morphology can be seen on the cell surface (white double arrow). The scale bar represents 5 μm .

Through SEM and TEM, the interaction between $100 \mu\text{g Cu mL}^{-1}$ of CuO NPs and coelomocytes was observed (Figure 14-15). EDS in SEM highlighted that the objects observed on coelomocytes' surface membranes were CuO NPs (Figure 15). As it was observed in Figure 11, the $1 \mu\text{g Cu mL}^{-1}$ CuO NPs were mostly dissolved in the R-RPMI 1640 medium. The $100 \mu\text{g Cu mL}^{-1}$ CuO NPs tended to aggregate; thus, these aggregates were located around the coelomocytes' surface membrane (Figure 14 A is control coelomocytes; Figure 14 B, C, D; white arrows). Furthermore, processing the picture, we observed that the concentration of NPs tended to decrease, which correlated with the dissolution analyses performed (Figure 11).

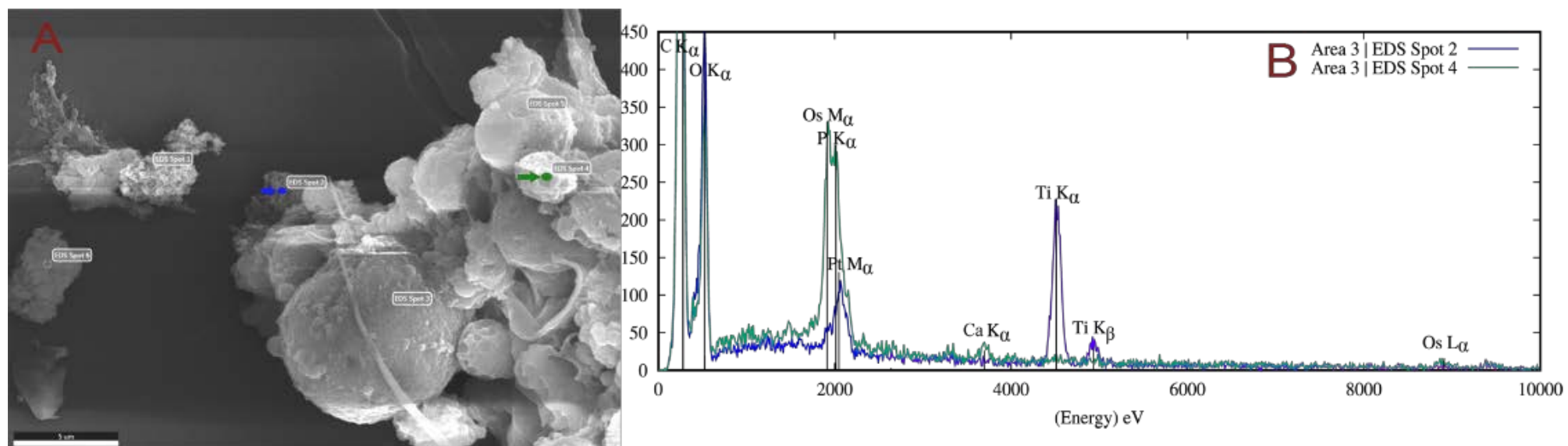


Figure 13. EDS pictures and spectra. A) Coelomocytes with $100 \mu\text{g mL}^{-1}$ TiO_2 NPs after 2 h exposure. The Blue arrow indicates TiO_2 NPs (EDS spot 2) and green arrow indicates coelomocytes (EDS spot 4). B) Spectra analyses from EDS spots 2 (blue) and 4 (green). The scale bar indicates $5 \mu\text{m}$.

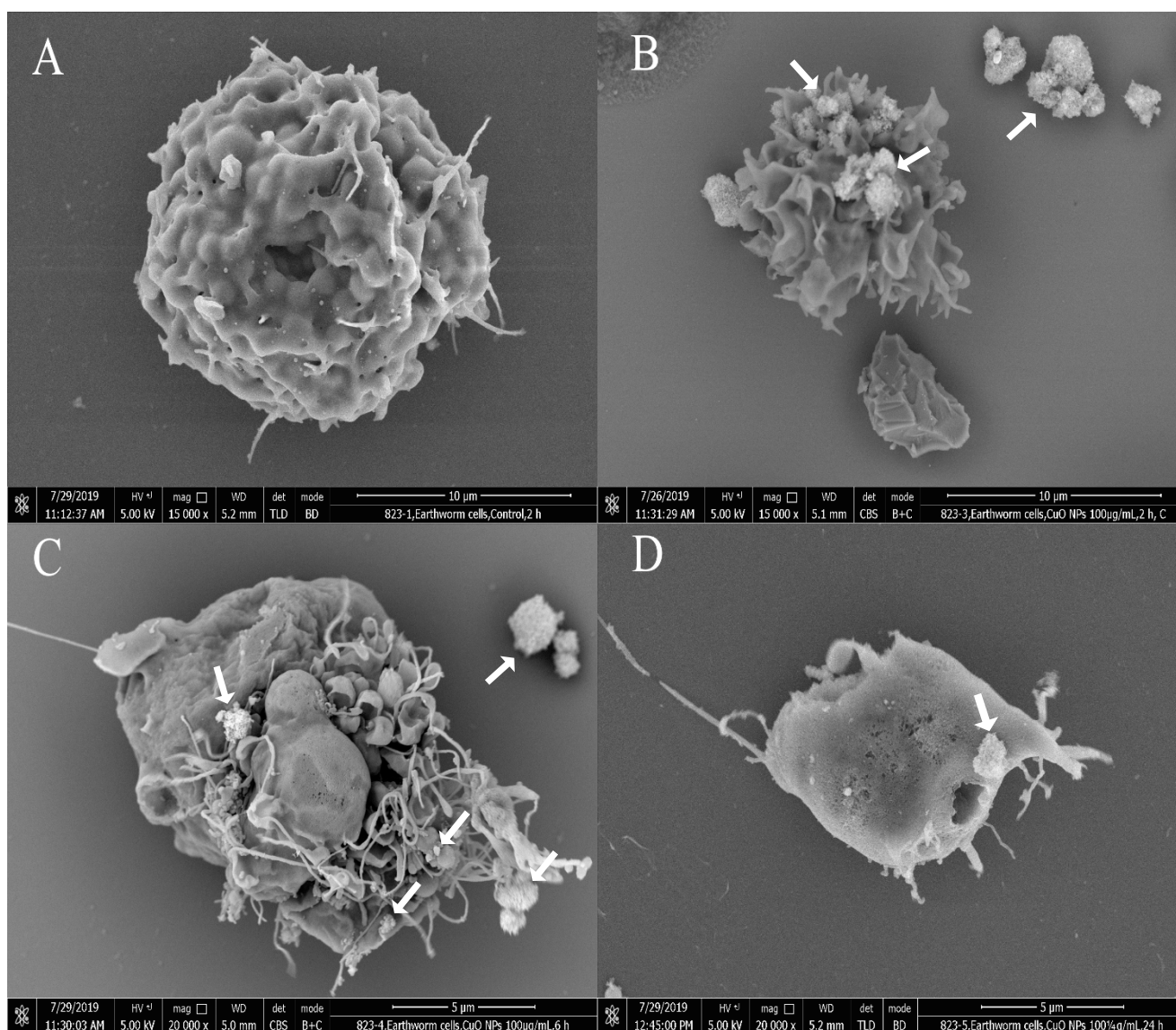


Figure 14. Scanning electron microscopy images of CuO NPs. A) Non-treated coelomocytes in R-RPMI 1640 medium after 2 h exposure, B-D) coelomocytes incubated with $100 \mu\text{g Cu mL}^{-1}$ CuO NPs for 2, 6, and 24 h. The scale bars represent $10 \mu\text{m}$ A-B) and $5 \mu\text{m}$ C). The white arrows indicate the location of CuO NPs on the coelomocyte surface.

The elemental composition of various spots was analysed (Figure 15). The EDS spot 3 were CuO NPs, EDS spot 7 were coelomocytes, and EDS spot 10 was the background-coated coverslip (Figure 15 A). Within those spots, it was observed that only EDS spot 3 had a peak of Cu. Neither EDS spot 7 nor 10 had any peak of Cu. The cluster observed in Figure 15 A on EDS spot 3, 6, and 8 was CuO NPs. Then, it also observed CuO NPs on the coelomocytes surface (Figure 15 B), and it was analysed the EDS spot 5 (Figure 15 B). The spot 5 showed a high peak of Cu ($K\alpha$, 8.048 keV) and the peak of carbon ($K\alpha$ 0.277 keV), showing that the CuO NPs were lying over the coelomocytes' surface membrane. Due to the elemental composition analyses, it

Chapter 4. Results

could determine the cluster were CuO NPs and also that CuO NPs were on the surface of coelomocytes. Further, spots on the background were taken to ensure there was no signal coming from the background or the coverslip (EDS spot 12, Figure 15 B). Later, an ultrathin section of coelomocytes exposed to $100 \mu\text{g Cu mL}^{-1}$ CuO NPs after 2 and 6 h were analysed (Figure 16).

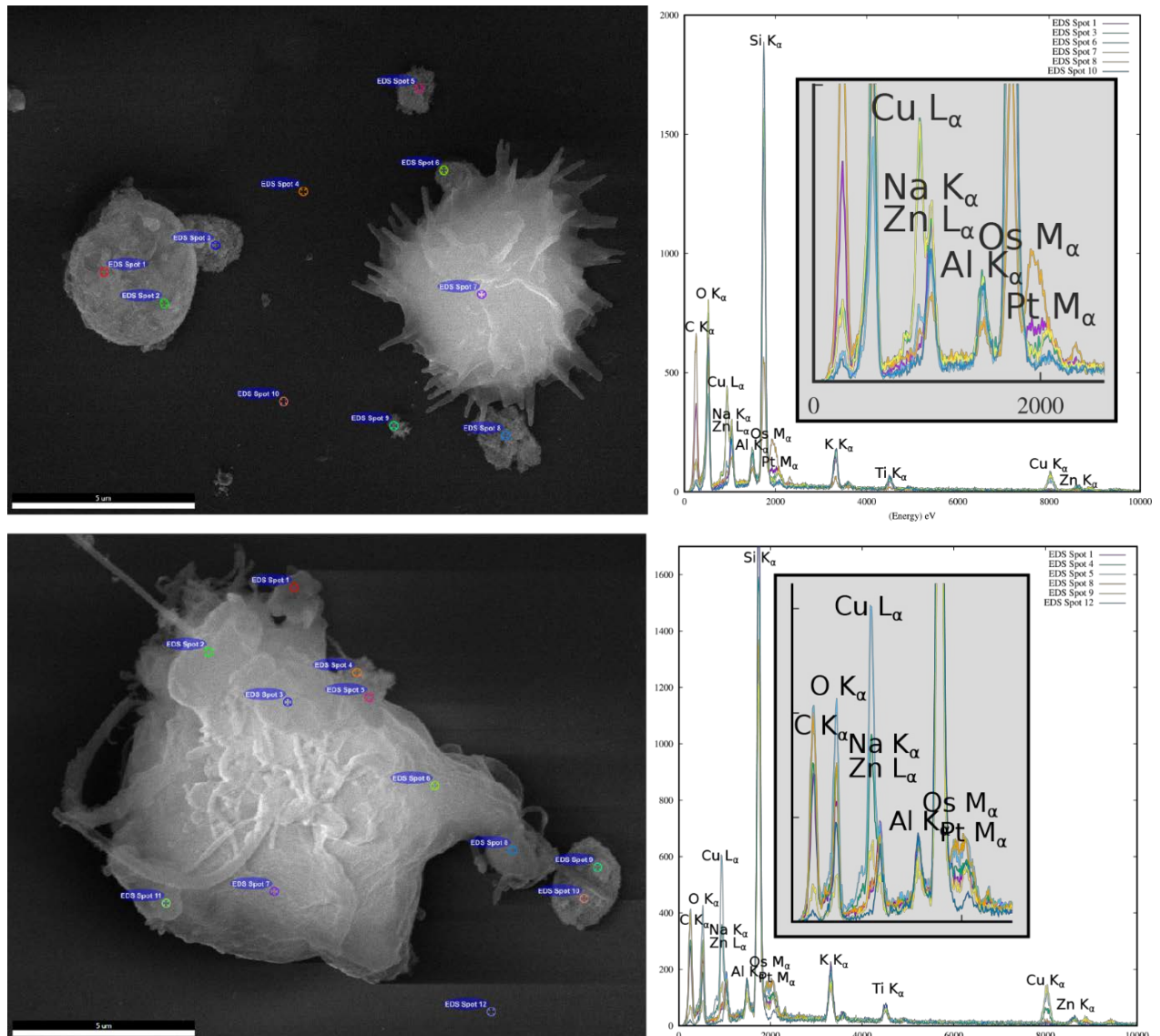


Figure 15. EDS spectra of coelomocytes exposed to CuO NPs. A) EDS analysis of coelomocytes and cluster of CuO NPs (EDS spot 8) and B) EDS analysis of coelomocytes with identified CuO NPs on their surface (EDS spot 5). The scale bar indicates 5 μm .

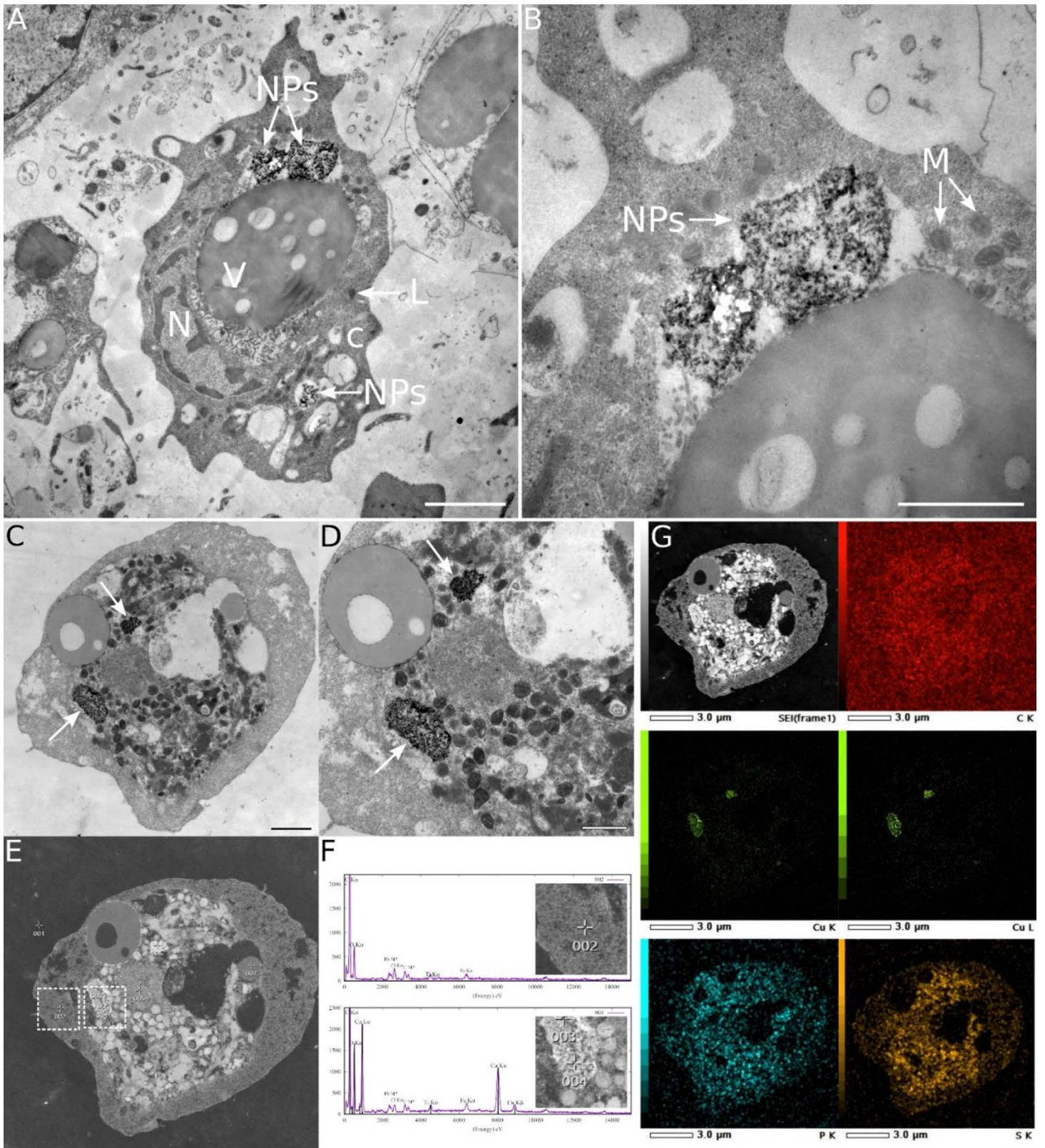


Figure 16. Transmission electron microscopy and STEM/EDS microanalysis of coelomocytes exposed to CuO NPs. Ultrathin sections of coelomocyte exposed with $100 \mu\text{g Cu mL}^{-1}$ CuO NPs after 2 h mounted onto Cu-grid (A and B). C and D: Ultrathin sections of the coelomocytes exposed with

Chapter 4. Results

100 $\mu\text{g Cu mL}^{-1}$ CuO NPs after 6 hours mounted onto Ti-grid. The arrows point to the CuO NPs clusters in the cytoplasm, Philips CM100 electron microscope. E: STEM HAADF image of the same section as in panels C and D; JEOL F200 electron microscope. The dashed squares marked the areas from the spectra in D originate. F: An example of two characteristic spectra taken from cytoplasm near the CuO NPs cluster (upper) and directly from the CuO NPs cluster (lower). G: Six panels that represent selected EDS maps. All spectra and elemental maps were recorded in JEOL F200 using JED-2300 X-ray spectrometer with a windowless SDD detector. The scale bars represent 2 μm in A and C panels and 1 μm in B and D panels. M -mitochondria, N - cell nucleus, L - lysosome, V - vacuoles, NPs - nanoparticles, and C - cytoplasm.

It was demonstrated that NPs were uptaken by coelomocytes (Figure 16). The NPs were localized in the cytoplasm, but they were not inside the mitochondria or nucleus (Figure 16 A and B) after 2 h of exposure. Later, at 6 h, an ultrathin section of coelomocytes was also evaluated, and similar to Figures 16 A and B, the NPs clusters were localized in the cytoplasm, and no inside the mitochondria or nucleus of the coelomocytes (Figure 16 C, D, and E). Then, in order to prove that the observed clusters were CuO NPs, the EDS spectra was performed. The dashed squares were the EDS spots analyzed. The main Cu K α (8.048 keV) and Cu L α (0.929 keV) peaks are clearly shown in the lower spectrum, confirming the presence of Cu in the electron-dense aggregates in the cytoplasm unequivocally (Figure 16 F). The other detected elements originate from sample processing (Pb and U from contrasting, according to (Reynolds, 1963) or from supporting grid (Ti) or microscope pole pieces (Fe). Carbon and oxygen are typical for the biological matter. The Cu maps (K α and L α) confirmed the copper's localization in the electron-dense clusters marked with arrows in panels C and D (Figure 16 F). Then, the elemental maps based on Figure 16 C-E confirmed that the NPs highlighted by dashed squares (Figure 16 E) or arrows (Figure 16 C) contained Cu peaks (Figure 16 G) while the rest of the coelomocyte was composed of C element and P element (Figure 16 G).

4.4 Cellular studies

The cellular studies were carried out with the flow cytometer except for the analyses performed in the *in vivo* experiment (Ag₂S NPs). The flow cytometer allowed the assessment of the subpopulation distribution. The combination of FSC and the SSC showed that ECs were on the top of the image due to high autofluorescence (Figure 17). This population was discarded in the studies because their autofluorescence interfered with the dyes' fluorescence. Thus, control samples with and without dyes were the same. It was distinguished the HAs and GAs, both amoebocytes populations. HAs are tinier cells with egg-shape and no granules on their surface, which are labelled as HAs in Figure 17. The GAs have a granular surface and

Chapter 4. Results

bigger size than HAs. That is the reason GAs were localized higher in the log SSC axis and the FSC axis (Figures 17 A and **Annex I. Figure 34**). Every experiment performed was also analyzed without the coelomocytes in order to see if the NPs would interfere. CuO NPs (Figure 17 A) did not have the NPs themselves in the gates where the coelomocytes were found (Figure 17 B). The viability of the cells was measured with the PI, which interacts with the nucleosides, so when emission wavelength was emitted, it meant that the coelomocytes were dead (**Annex I. Figure 34**). Every analysis performed afterwards was based on the detected alive coelomocytes (**Annex I. Figure 35-36**). The dead coelomocytes were discarded. HAs and GAs viability remained similar in both non-exposed coelomocytes and the TiO₂ NPs exposed to coelomocytes. Viability changed in the case of CuO NPs (Figure 28).

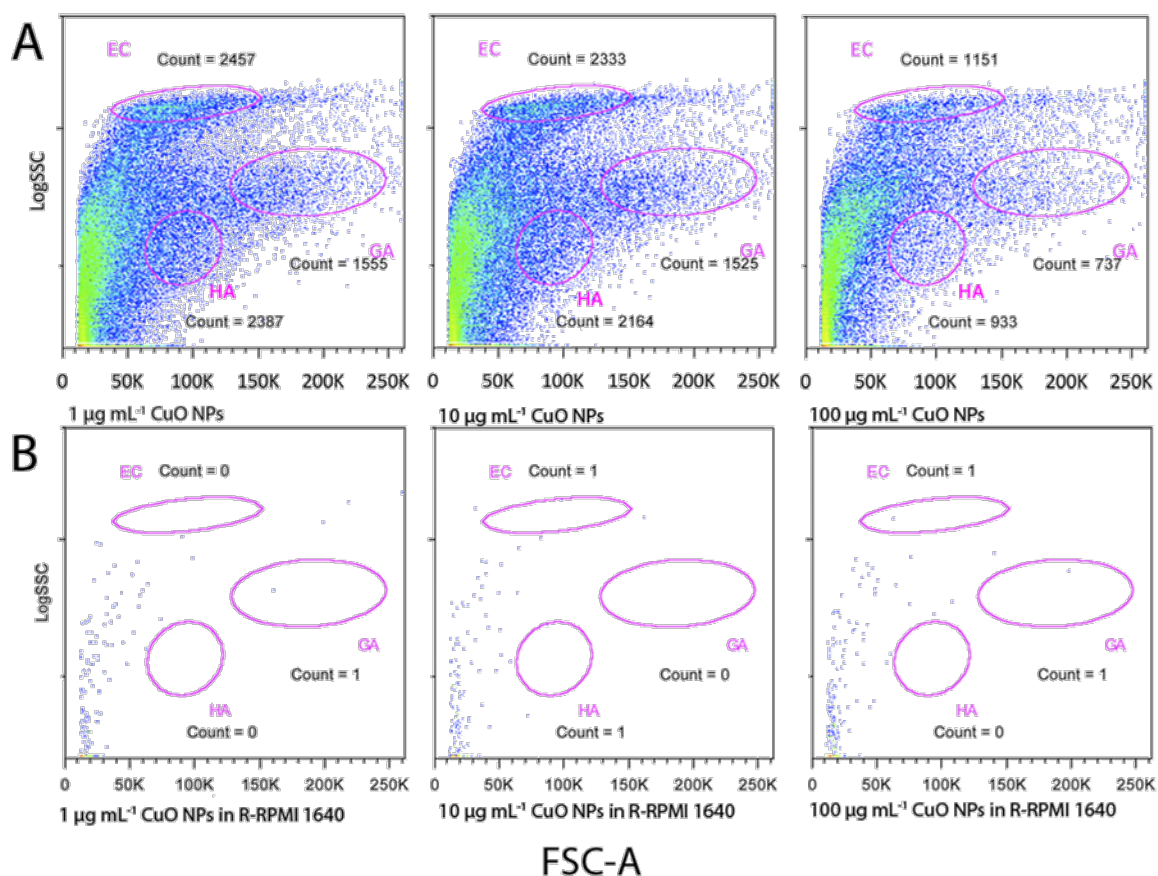


Figure 17. Coelomocytes subsets. A) Subsets of coelomocytes exposed to 1, 10, and 100 µg Cu mL⁻¹ CuO NPs. B) R-RPMI 1640 medium with 1, 10, and 100 µg Cu mL⁻¹ CuO NPs. EC: Eleocytes. GA: Granular amoebocytes. HA: Hyaline amoebocytes. Counts: number of events counted by flow cytometer.

Chapter 4. Results

The viability of coelomocytes from the earthworms of the *in vivo* experiment was measured by trypan blue viability assay after 14 days of exposure. The results showed no mortality of coelomocytes at any of the exposures (control, Ag₂S NPs or AgNO₃; Figure 18). The viability was 71.3 ± 13.9%, 76.7 ± 11.3% and 78.5 ± 7.2% for control, Ag₂S NPs and AgNO₃, respectively. The statistical difference was observed only in AgNO₃ exposure compared to the control.

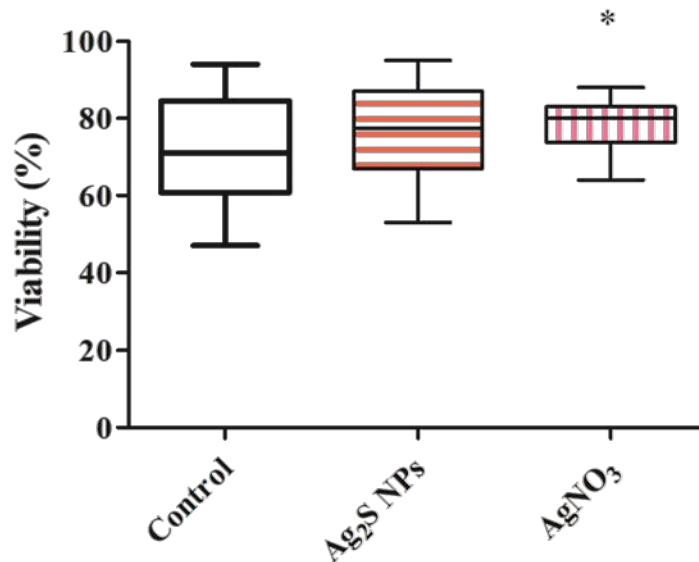


Figure 18. Viability of coelomocytes. Viability of cells exposed to Ag₂S NPs after 14 days exposure. Values are mean (%) ± SEM. No statistical difference was observed ($p > 0.05$ according to one-way ANOVA and Bonferroni post-hoc test).

4.5 Oxidative stress

4.5.1 ROS and NO production

The ROS production was analysed by the intensity emission of the cell-permeant tracer DCF-DA. Differences between NPs were observed in both HAs and GAs (Figure 19 A-B). In addition, it was observed that TiO₂ NPs (Figure 19 A.1 and B.1) emitted more intensity in HAs and GAs than CuO NPs or CuSO₄ (Figure 19 A.2-3 and B.2-3). Although intensities were different independently of the subpopulations, there were no statistical differences between the different treatments used (TiO₂ NPs, CuO NPs and CuSO₄). Moreover, independently of the exposures, it observed that HAs exerted approximately two times lesser fluorescence intensity (Figure 19 A) than GAs (Figure 19 B).

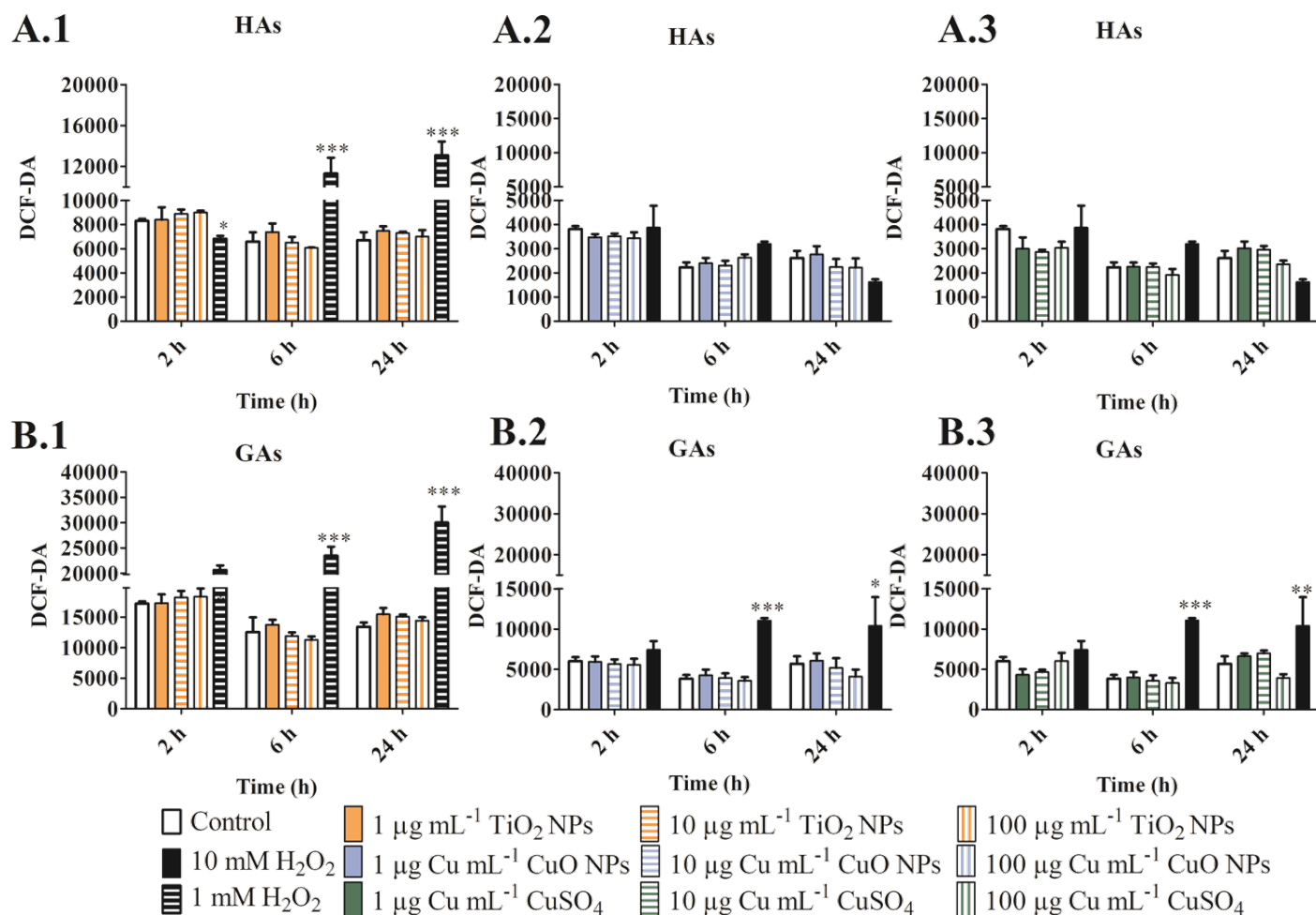


Figure 19. ROS production in HAs and GAs. A) ROS production of HAs exposed TiO₂ NPs (A.1), CuO NPs (A.2), and CuSO₄ (A.3; 1, 10 and 100 µg mL⁻¹) after 2, 6, and 24 h. B) ROS production of GAs exposed to TiO₂ NPs (B.1), CuO NPs (B.2), and CuSO₄ NPs (B.3; 1, 10, and 100 µg mL⁻¹) after 2, 6, and 24 h. Positive control was 1 mM H₂O₂ for TiO₂ NPs (A.1 and B.1) and 10 mM H₂O₂ for CuO NPs (A.2 and B.2) and CuSO₄ (A.3 and B.3). The results are shown as the mean of fluorescence intensity (DCF-DA) ±SEM of three independent experiments with 3 replicates in each. * p<0.001, ** p<0.01, and * p<0.05 according to two-way ANOVA and Bonferroni post-hoc test.**

NO production was analysed for the *in vivo* experiment. The values obtained were 32.9 ± 2.6, 28.4 ± 6.5, and 29.9 ± 3.1 µM NO for control soil, Ag₂S NPs, or AgNO₃, respectively (Figure 20). Although statistically

Chapter 4. Results

significant differences were not observed, greater variances were detected in the coelomocytes exposed to Ag₂S NPs. The variances could indicate an imbalance in NO metabolism.

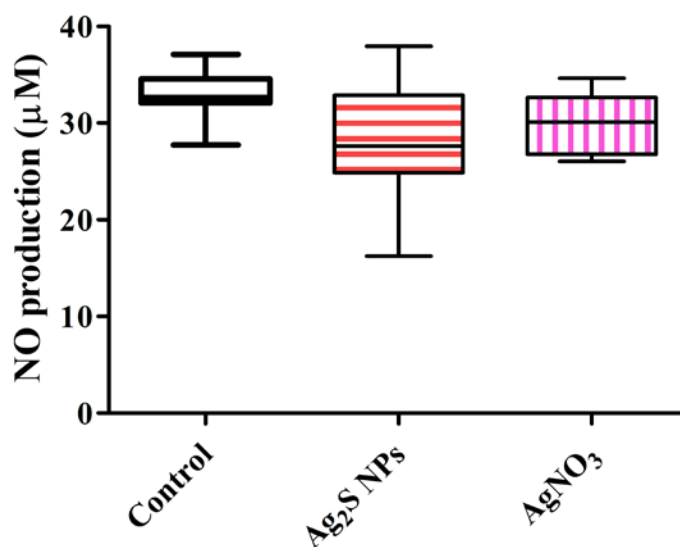


Figure 20. NO production. NO production (μM) by coelomocytes from earthworms exposed to control soil, 5 mg Ag Kg^{-1} from Ag₂S NPs or AgNO₃. No significant differences were observed ($p > 0.05$ according to one-way ANOVA and Bonferroni post-hoc test).

4.5.2 MDA production

The malondialdehyde (MDA) is a subproduct of lipid peroxidation. This product was assessed both, in the *in vivo* and *in vitro* experiments. Results of the *in vitro* experiments (TiO₂ NPs, CuO NPs and CuSO₄) are shown in Figure 21. The concentration of $1 \mu\text{g mL}^{-1}$ for the three exposures was discarded due to the low levels under the detection limit. The MDA production was lower than 200 % in the case of TiO₂ NPs (Figure 21 A) at any of the concentrations assessed. Contrary to ROS production results, it was observed that CuO NPs (Figure 21 B) and CuSO₄ (Figure 21 C) produced more MDA independently of the concentration exposures. In the case of the CuO NPs and CuSO₄ (Figure 21 B-C), the MDA production increased in a dose-dependent manner. The highest peak was found after 6 h (Figure 21 B-C). Then, the MDA production decreased after 24 h (Figure 21 B-C). The highest MDA levels were 10 and 13 times higher than in the control samples for CuO NPs and CuSO₄ ($100 \mu\text{g Cu mL}^{-1}$) after 6 h exposure (Figure 21 B-C). It was showed an inverse correlation between ROS and MDA production (Figures 19 and 20).

Chapter 4. Results

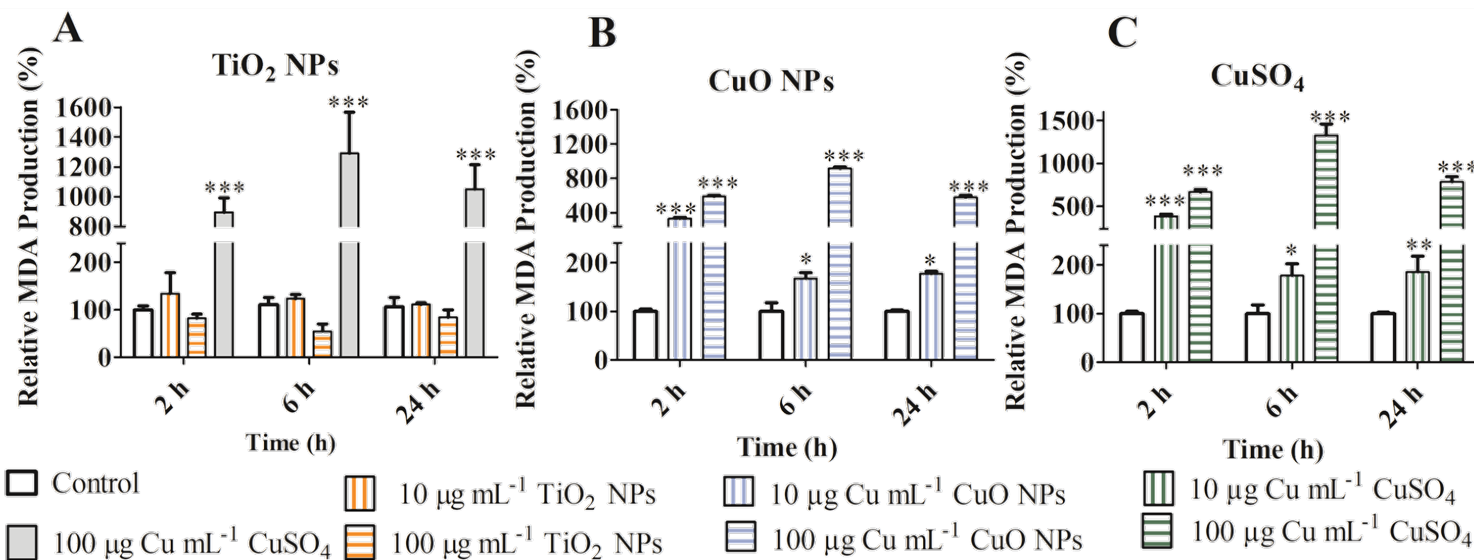


Figure 21. Relative MDA production. Relative MDA production in coelomocytes exposed to TiO₂ NPs (A), CuO NPs (B), and CuSO₄ NPs (C; 10, 100 µg mL⁻¹) for 2, 6 and 24 h. Values are expressed as mean (%) ± SD of three independent experiments with their three replicates in each. *p<0.001, **p<0.01 and *p<0.05 according to two-way ANOVA and Bonferroni post-hoc test.**

Statistically significant differences in MDA production were observed at different time exposures (2, 6, and 24 h) for CuO NPs and CuSO₄ (Figure 21 B-C). Moreover, it was observed that the highest production of MDA was at the 100 µg Cu mL⁻¹ concentration.

MDA production measured during the *in vivo* experiment did not reveal statistically different values compared to the control earthworms, according to the Kruskal-Wallis and the Dunn's post-hoc test. The values observed were 21.4 ± 8.8, 22.4 ± 3.9 and 23.3 ± 13.9 nM MDA for control, Ag₂S NPs or AgNO₃, respectively (Figure 22).

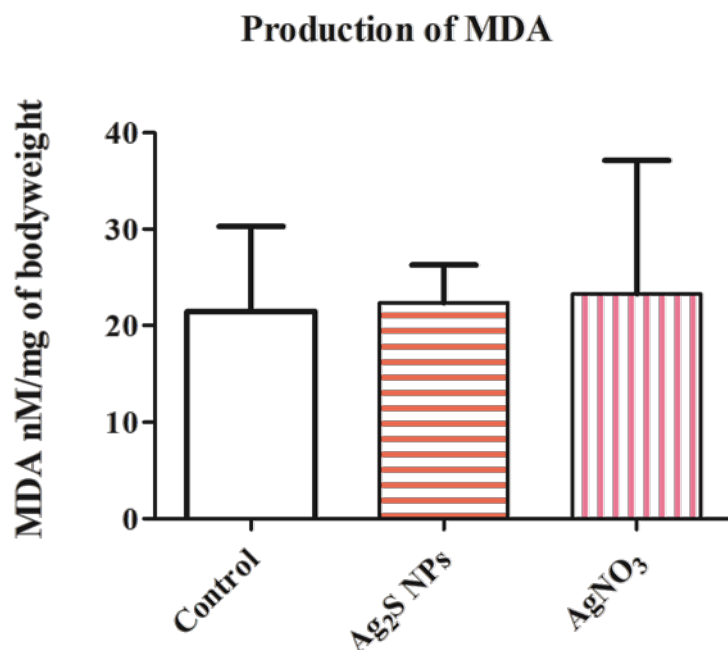


Figure 22. MDA production. MDA production (nM mg⁻¹ of bodyweight) of earthworms exposed to control soil, and 5 mg Ag Kg soil as Ag₂S NPs or AgNO₃ after 14 days exposure. Results are expressed as mean (nM mg⁻¹ bodyweight) ± SD. No significant differences were observed ($p > 0.05$, Kruskal-Wallis and Dunn's post-test). N= 3

4.6 Genotoxicity and immune biomarkers

Genotoxicity was assessed by the alkaline comet assay. Different parameters such as % tail DNA, % head DNA, and % olive tail were measured to evaluate the DNA damage. The plot showed the DNA damage from % of the DNA tail because the tail contains the fragmented DNA coming from the oxidative stress within others. A total of 100 comets were assessed in each exposure, control samples, and positive control (100 mM H₂O₂).

Among the different exposures, the highest DNA damage was coming from the Cu⁺² ions of CuSO₄. TiO₂ NPs did not cause any DNA damage in coelomocytes, as it could be seen in Figure 23 A. There were no statistical differences ($p > 0.05$) between the different concentrations and time exposure of TiO₂ NPs (Figure 23 A). However, changes were observed between CuO NPs and CuSO₄ (Figure 23 B-C). There was an increase of % DNA damage along the different exposure times (Figure 23 B-C) being statistically different after 6 and 24 h. Coelomocytes exposed to CuSO₄ caused even greater DNA damage (Figure 23 C) in comparison with 1 and 10 µg Cu mL⁻¹ CuO NPs after 24 h (Figure 23 B); and 100 µg Cu mL⁻¹ CuO NPs (Figure 23 B).

Chapter 4. Results

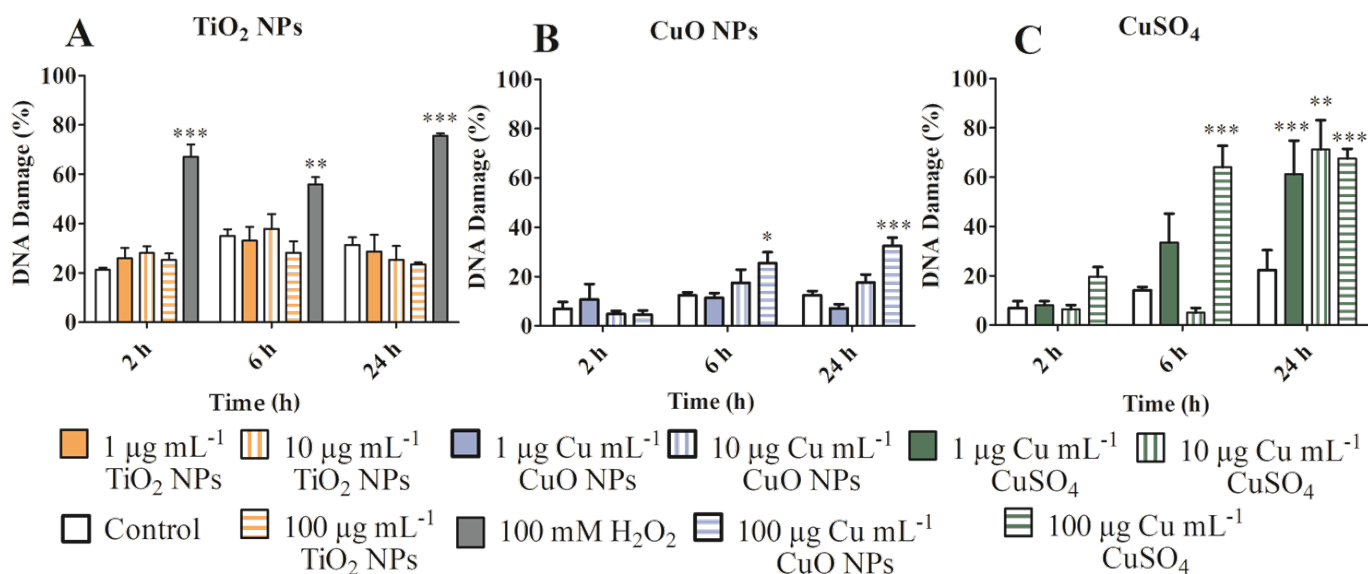


Figure 23. DNA Damage (%). DNA damage (%) in the coelomocytes exposed to TiO₂ NPs (A), CuO NPs (B) and CuSO₄ (C; 1, 10 and 100 µg mL⁻¹) after 2, 6 and 24 h. Data are expressed as the median of the % comet tail (N= 100 comets) ± SEM of three experiments with three replicates. *** p<0.001 and * p<0.05 according to two-way ANOVA and Bonferroni post-hoc test.

The phagocytic activity was measured *in vitro* for both subpopulations of amoebocytes (HAs and GAs). The phagocytic activity was similar between HAs and GAs in the exposure of TiO₂ NPs (Figure 24 A.1 and B.1). The phagocytic activity remained at approximately 50% after 2 and 6 h in control and the different concentration of TiO₂ NPs (1, 10, and 100 µg mL⁻¹; Figure 24 A.1) for the HAs and GAs (Figure 24 B.1). After 24 h, the phagocytic activity decreased slightly for HAs and GAs, although no statistical differences (p > 0.05) were found for TiO₂ NPs (Figure 24 A.1 and B.1; 1, 10, and 100 µg mL⁻¹) and the control. However, this trend was not observed when coelomocytes were exposed to CuO NPs (Figure 24 A.2 and B.2). Approximately 55- 60% of HAs (Figure 24 A.2) and 47- 50% of GAs (Figure 24 B.2) were phagocytic after 6 h exposure. Then, percentages decreased after 24 h exposure being 25% phagocytic activity for 100 µg Cu mL⁻¹ CuO NPs (Figure 24 A.2 and B.2). The results showed a similar tendency with CuSO₄ (Figures 24 A.3 and B.3). Statistical differences were observed only in HAs (Figure 24 A.3) after 6 and 24 h exposure to 100 µg Cu mL⁻¹ of CuSO₄. Thus, slight differences were observed between both subpopulations of amoebocytes leading to a possible sensitiveness of HAs.

Chapter 4. Results

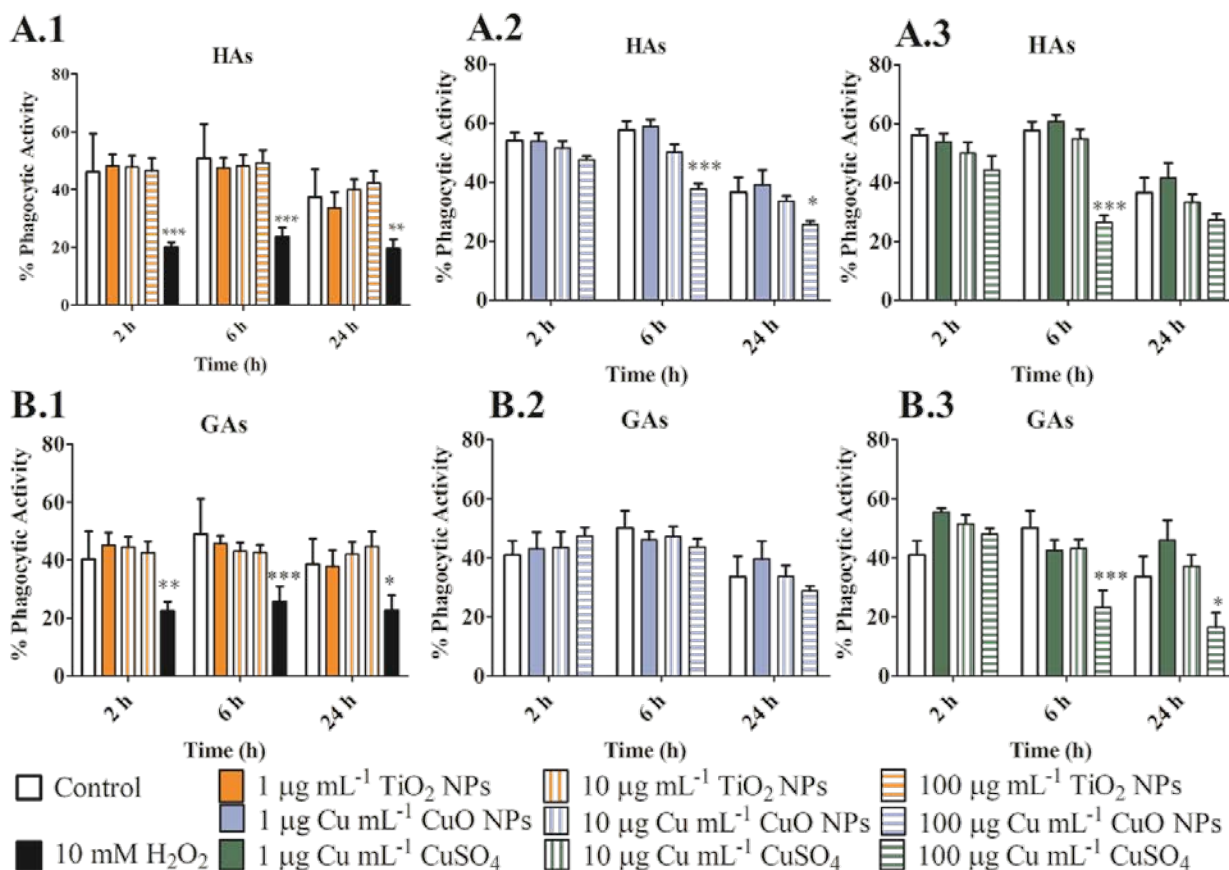


Figure 24. Phagocytic activity. Phagocytic activity was measured for HA (A) and GA (B) after exposure to 1, 10, and 100 $\mu\text{g mL}^{-1}$ TiO₂ NPs (A.1 and B.1), CuO NPs (A.2 and B.2) and CuSO₄ (A.3 and B.3) for 2, 6 and 24 h. Values are shown as mean (%) of phagocytic activity \pm SEM of three experiments with three replicates. *** $p < 0.001$ and * $p < 0.05$ according to two-way ANOVA and Bonferroni post-hoc test.

Apoptosis was evaluated for the *in vitro* experiments (**Annex I. Figure 36**). The apoptosis measured the early apoptosis (Figure 25), the late apoptosis (Figure 26), the necrosis (Figure 27), and the viable cells (Figure 28). The apoptosis is a cell programme death that starts with viable cells going to early and late apoptosis; then, it can end in the necrosis.

At the early apoptosis, it could observe no significant difference between the different exposures of TiO₂ NPs and the control in both HAs and GAs (Figure 25 A.1 and B.1). However, significant differences were observed in 100 $\mu\text{g Cu mL}^{-1}$ CuO NPs at 2 and 24 for HAs (Figure 25 A.2). Similarly, results were also observed with CuSO₄ at the same concentration and times for HAs (Figure 25 A.3). However, for the GAs, the significant differences were only observed at 100 $\mu\text{g Cu mL}^{-1}$ for CuO NPs and CuSO₄ (Figure 25 B.2

Chapter 4. Results

and B.3). Moreover, it was observed there were not changes between HAs and GAs (Figure 25 A and B) and both had similar results for early apoptosis.

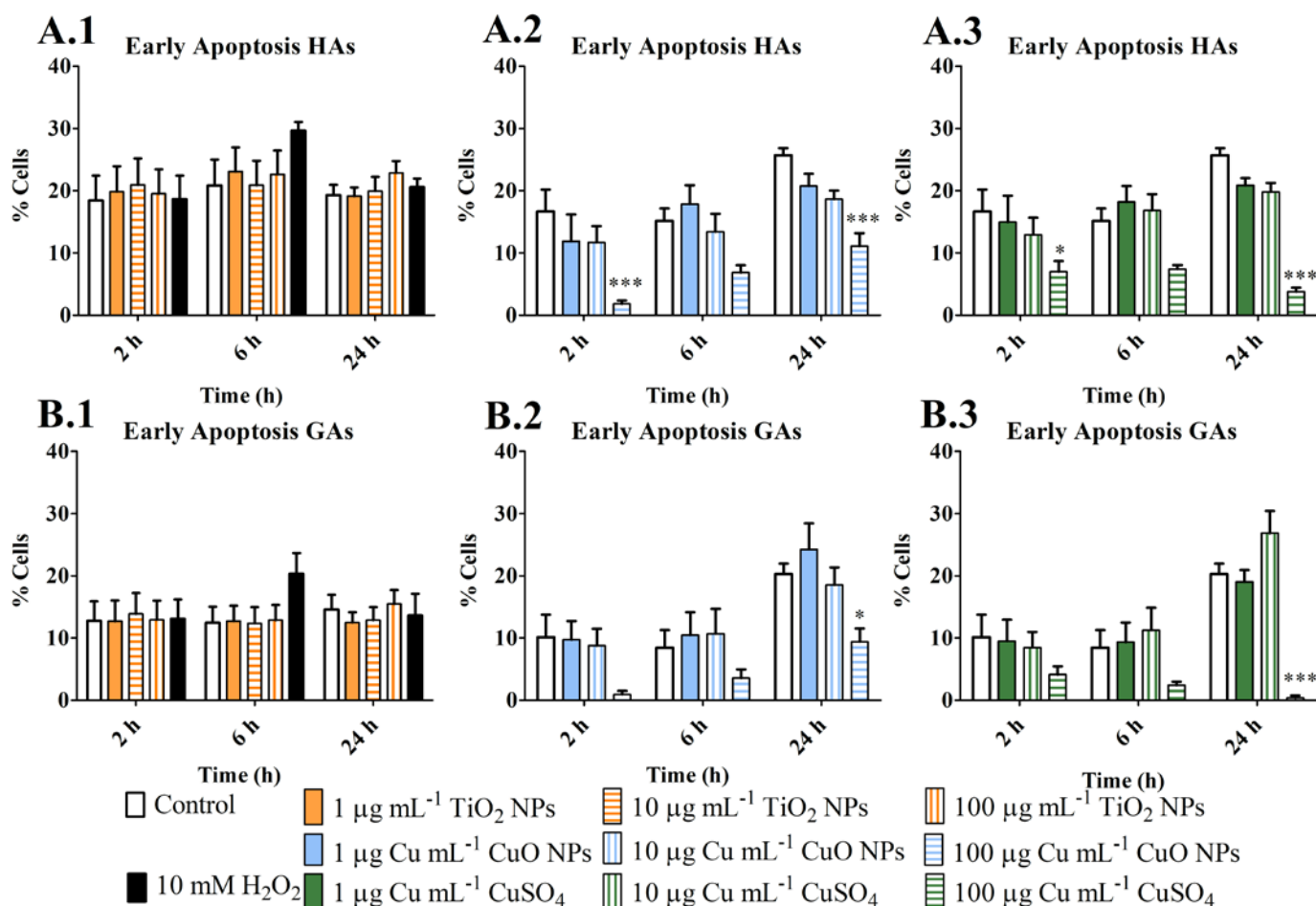


Figure 25. Early apoptosis. A) Early apoptosis of HAs and B) early apoptosis of GAs after exposure to 1, 10, and 100 µg mL⁻¹ of TiO₂ NPs (A.1 and B.1), CuO NPs (A.2 and B.2), and CuSO₄ (A.3 and B.3) for 2, 6 and 24 h. The values are mean (%) of cells ± SEM of three independent experiments with 3 replicates in each. * p<0.001 and * p<0.05 according to two-way ANOVA and Bonferroni post-hoc test.**

At the late apoptosis, there were no significant differences in the different concentrations of TiO₂ NPs for HAs and GAs (Figure 26 A. and B.). However, similar to early apoptosis, significant differences were observed in 100 µg Cu mL⁻¹ CuO NPs at 2 and 24 for HAs (Figure 26 A.2). On the contrary, a significant difference in 100 µg Cu mL⁻¹ CuSO₄ at 24 h for HAs was detected (Figure 26 A.3). Looking at the results, it observed that early and late apoptosis in GAs had a similar significant difference for 100 µg Cu mL⁻¹ CuO NPs and CuSO₄ (Figure 26 B.2 and B.3) at 24 h.

Chapter 4. Results

The necrosis, when cells are only stained with PI, was further evaluated. It was observed that both HAs or GAs tendency was similar. Similar to early and late apoptosis, it showed that the exposure to the different concentrations of TiO₂ NPs for HAs and GAs did not cause any statistical significance in the necrosis (Figures 27 A.1 and B.1). The positive controls (10 mM H₂O₂) showed statistical significance in the necrosis (Figures 27 A and B). However, the highest necrosis percentage of HAs and GAs was caused by the exposure to 100 µg Cu mL⁻¹ CuSO₄ at 24 h (Figures 27 A.3 and B.3). Remarkably, the CuO NPs also showed statistical significance in the 100 µg Cu mL⁻¹ at the different exposure times (2, 6 and 24 h; Figure 27 B.2) in the GAs. It could highlight that this concentration (100 µg Cu mL⁻¹ CuO NPs) had a lower percentage of cells in early apoptosis (Figure 25 B.2).

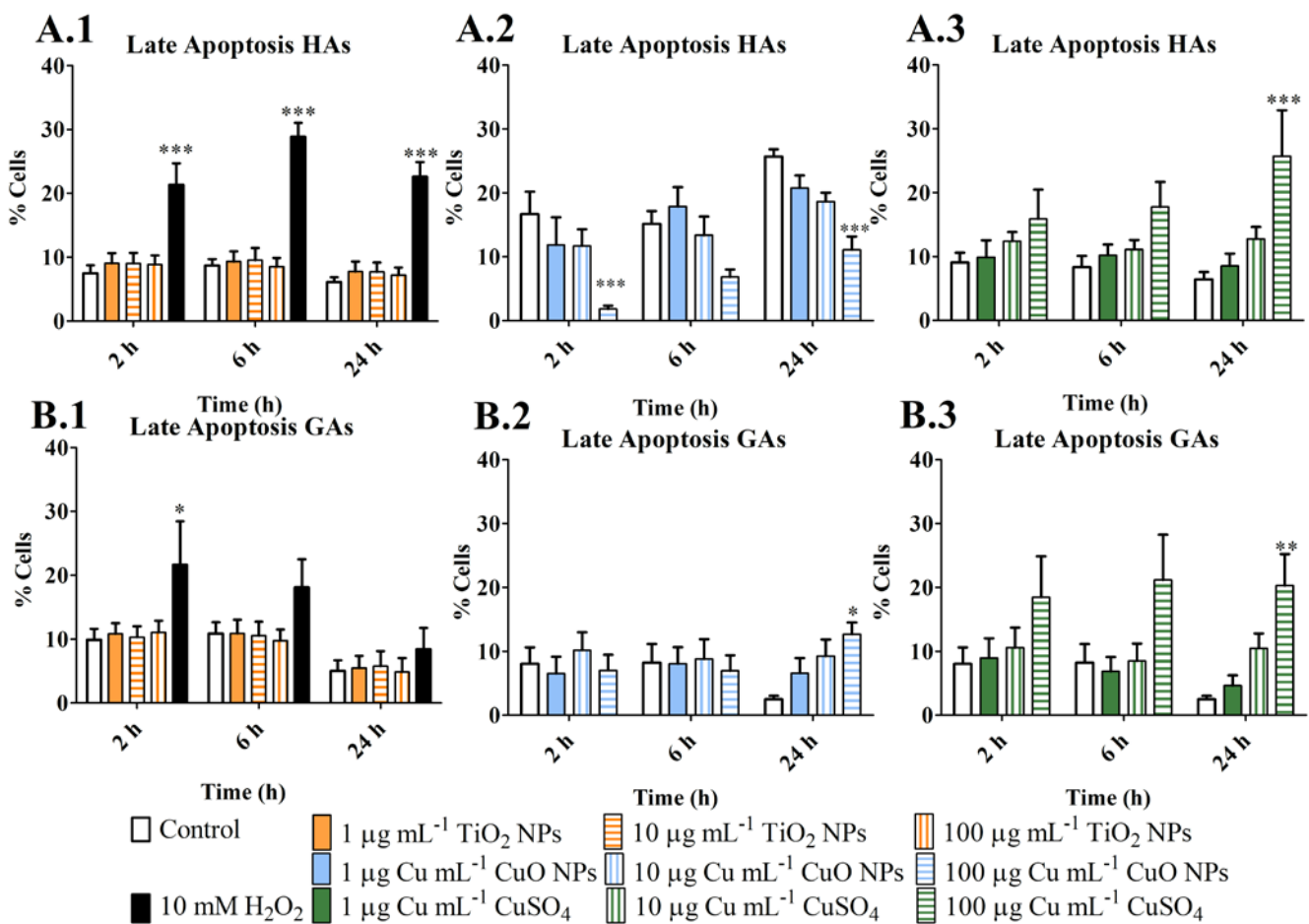


Figure 26. Late apoptosis. A) Late apoptosis of HAs and B) late apoptosis of GAs after exposure to 1, 10 and 100 µg mL⁻¹ of TiO₂ NPs, CuO NPs and CuSO₄ for 2, 6 and 24 h. The values are mean (%) of cells ±SEM of three independent experiments with 3 replicates in each. * p<0.001 and * p<0.05 according to two-way ANOVA and Bonferroni post-hoc test.**

Chapter 4. Results

The cell death programme goes from viability to early apoptosis, then late apoptosis and the last step is necrosis. It observed that due to the low percentage of cells in early and late apoptosis and necrosis from the different concentrations of TiO₂ NPs after 2, 6, and 24 h for HAs and GAs, the viability of the cells remained at approximately 70-75 % (Figure 28 A.1 and B.1). However, when it was observed the results from 100 µg Cu mL⁻¹ CuO NPs and CuSO₄ at 2, 6 and 24 h for HAs (Figure 28 A.2 and A.3) and GAs (Figure 28 B.12 and B.2), there was a decreased tendency of the viability. Thus, it was corroborated by the high necrosis observed (Figures 27 A and B) and the early and late apoptosis (Figures 25 and 26).

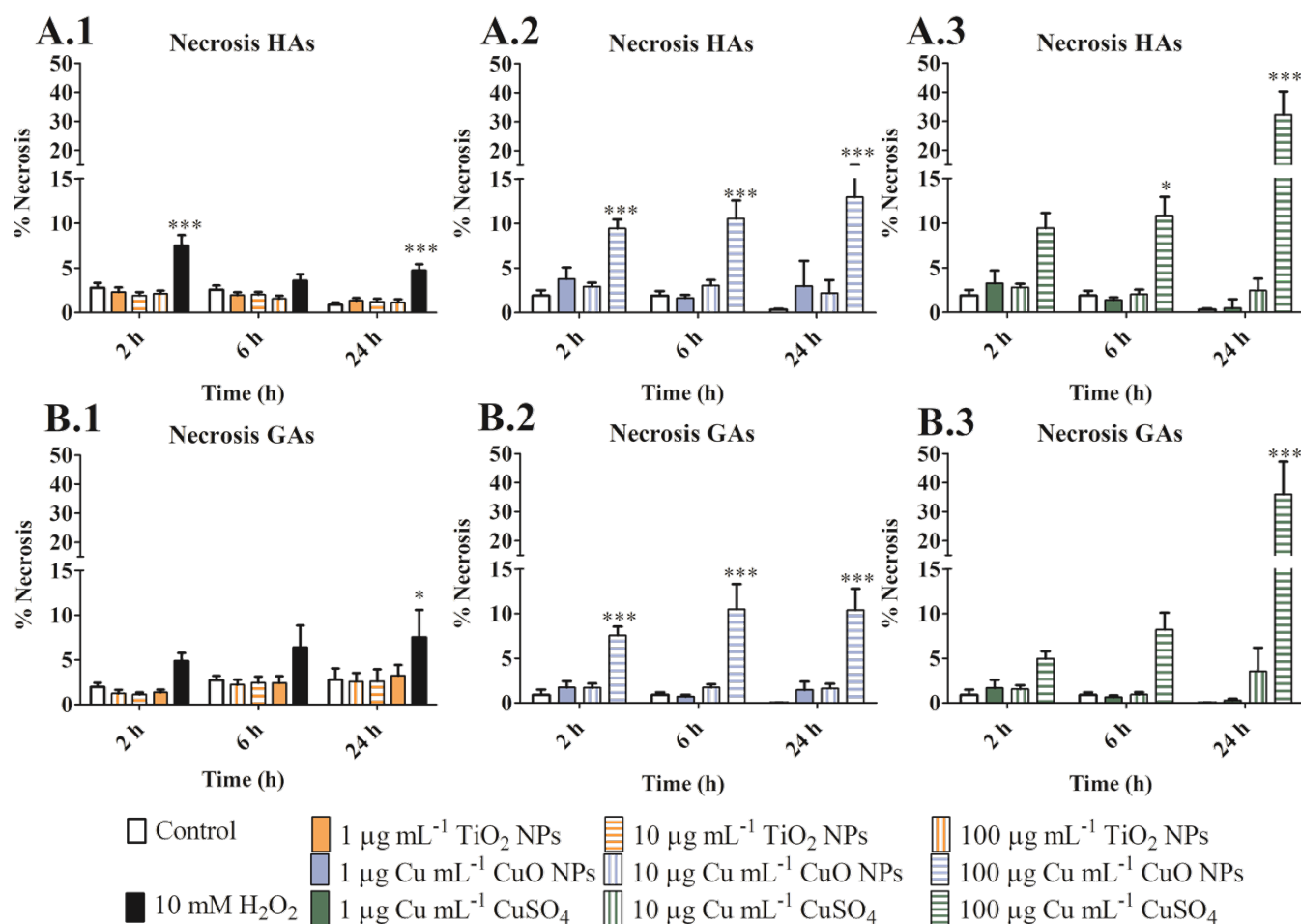


Figure 27. Necrosis. A) Necrosis of HAs and B) Necrosis of GAs after exposure to 1, 10, and 100 µg mL⁻¹ of TiO₂ NPs, CuO NPs and CuSO₄ for 2, 6 and 24 h. The values are mean (%) of cells ±SEM of three independent experiments with 3 replicates in each. * p<0.001 and * p<0.05 according to two-way ANOVA and Bonferroni post-hoc test.**

Chapter 4. Results

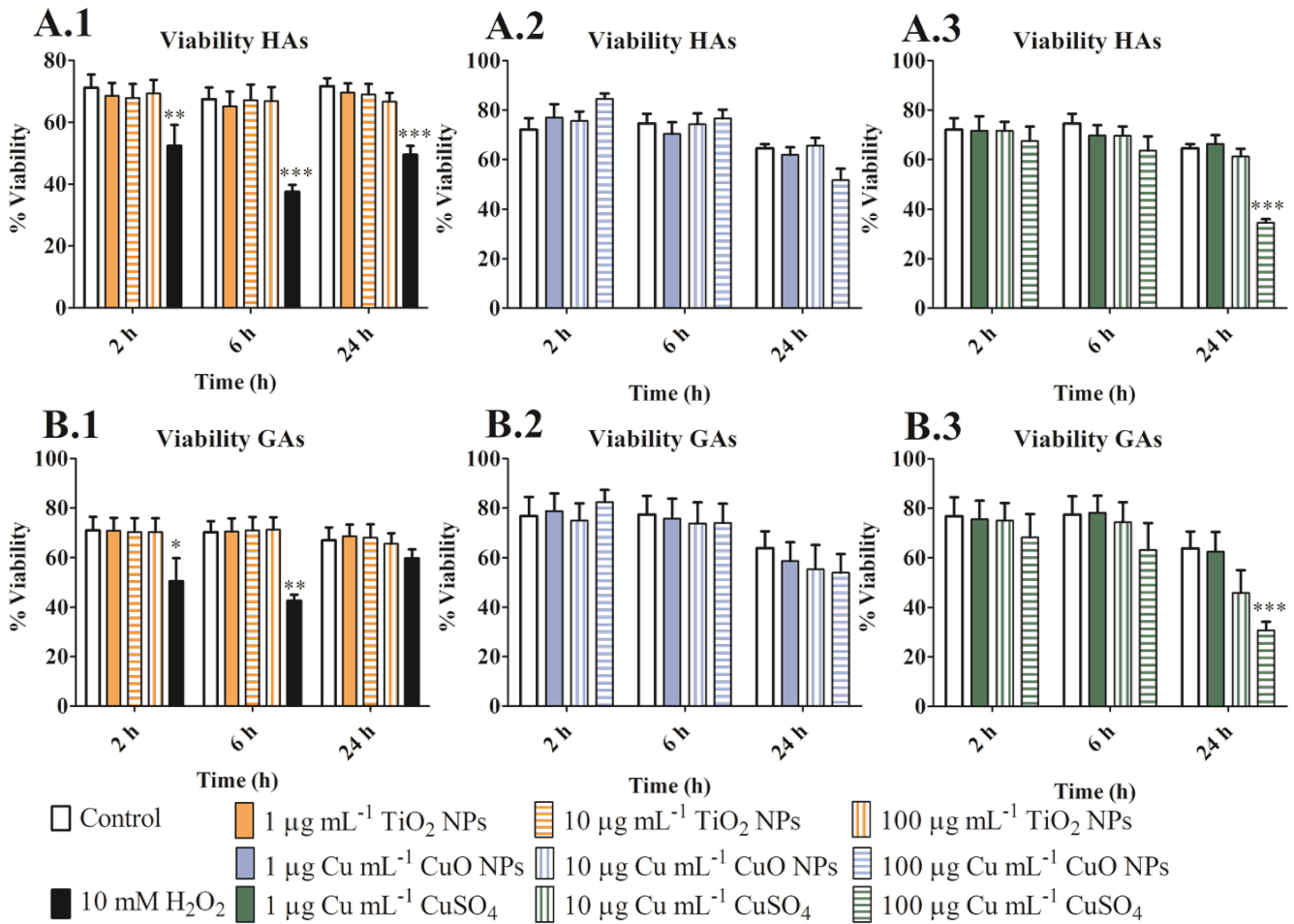


Figure 28. Viability. A) Viability of HAs and B) viability of GAs after exposure to 1, 10, and 100 $\mu\text{g mL}^{-1}$ of TiO_2 NPs, CuO NPs and CuSO_4 for 2, 6 and 24 h. The values are mean (%) of cells \pm SEM of three independent experiments with 3 replicates in each. * $p < 0.001$ and * $p < 0.05$ according to two-way ANOVA and Bonferroni post-hoc test.**

Finally, the last endpoint measured was phenoloxidase activity (PO) in the *in vivo* experiment. The PO activity was $111.7 \pm 42.4\%$, $130.4 \pm 38.1\%$ and $145.8 \pm 65.4\%$ for control, Ag_2S NPs and AgNO_3 , respectively (Figure 29). There was no statistical significance between the control earthworms and the earthworms exposed to the Ag_2S NPs and the control Ag^+ ions (AgNO_3).

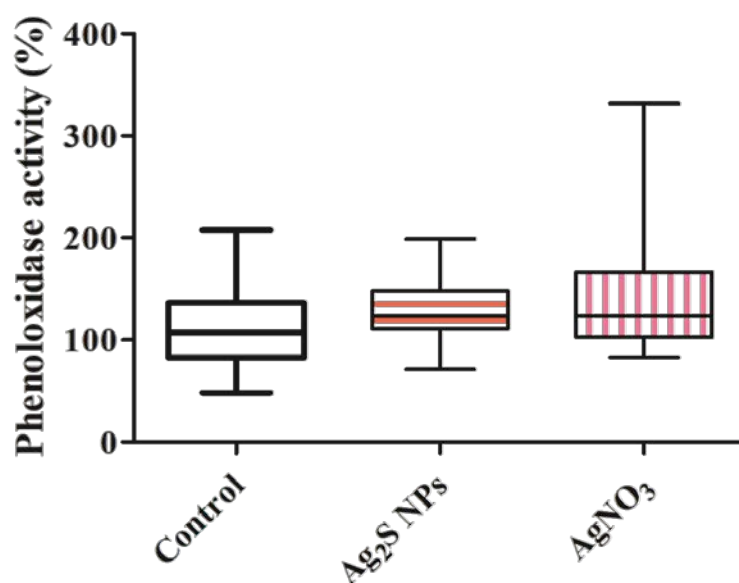


Figure 29. Phenoloxidase activity (%) of coelomocytes. Phenoloxidase activity (%) of coelomocytes exposed to 5 mg Ag Kg⁻¹ soil in form of Ag₂S NPs or AgNO₃. No significant differences were observed ($p > 0.05$) according to one-way ANOVA and Bonferroni post-hoc test (N= 15 per exposure and 4 technical replicates in each).

4.7 mRNA analyses

Observed changes in mRNA levels of the selected molecules after the exposure to 1 and 10 $\mu\text{g mL}^{-1}$ TiO₂ NPs, CuO NPs and CuSO₄ were evaluated. 10 different molecules were chosen due to their defense function in the earthworms. Few of them were up/downregulated after the different exposures (Table 5, 6 and 7). 100 $\mu\text{g Cu mL}^{-1}$ as a form of CuO NPs and CuSO₄ was discarded from the analyses. The quality of RNA from the highest concentration was poor, which could be related to the high mortality observed (Figures 23 and 28).

TiO₂ NPs exhibited similar changes as CuO NPs and CuSO₄ (Tables 5, 6, and 7). Metallothioneins were upregulated along the exposure times after 1 $\mu\text{g mL}^{-1}$ TiO₂ NPs exposure while metallothioneins were only upregulated at 6 h exposure after 10 $\mu\text{g mL}^{-1}$ exposure (Table 5). Regarding oxidative stress molecules, MnSOD was downregulated at 6 h exposure for after 10 $\mu\text{g mL}^{-1}$ TiO₂ NPs exposure.

TiO₂ NPs produced changes in mRNA levels of the immune and signal transduction molecules. It was detected upregulation of Fet/Lys and lumbricin when coelomocytes were exposed to 10 $\mu\text{g mL}^{-1}$ TiO₂ NPs after 6 h. In addition, MEKK 1 was upregulated after 1 $\mu\text{g mL}^{-1}$ TiO₂ NPs exposure at 24 h and after 10 $\mu\text{g mL}^{-1}$

Chapter 4. Results

mL⁻¹ TiO₂ NPs exposure at 6 h (Table 5). Then, downregulation of PKC 1 was detected after the exposure of coelomocytes with 10 µg mL⁻¹ TiO₂ NPs after 6 and 24 h (Table 5).

Function	Gene	TiO ₂ NPs (µg mL ⁻¹)	Normalized gene expression (relative to control)		
			2 h	6 h	24 h
Metal detoxification	Metallothionein	1	5.16±1.73**	2.00±0.32*	2.71±0.20*
		10	1.11±0.2	1.97±0.22**	1.00±0.25
Heavy metal detoxification	Phytochelatin	1	1.38±0.09	1.02±0.04	1.18±0.08
		10	1.00±0.02	0.82±0.02	0.80±0.01
Oxidative stress	MnSOD	1	1.47±0.12	0.85±0.19	0.58±0.05
		10	0.93±0.09	0.53±0.01*	0.72±0.01
	CuZnSOD	1	0.68±0.05	0.84±0.22	0.98±0.04
		10	0.96±0.07	0.71±0.04	0.87±0.01
	CAT	1	1.41±0.19	0.87±0.03	0.66±0.03
		10	1.04±0.13	0.71±0.02	0.8±0.2
Immunity	EMAP II	1	0.90±0.07	0.94±0.1	0.86±0.02
		10	0.84±0.09	1.21±0.01	1.33±0.20
	Fet/Lys	1	0.64±0.08	0.62±0.13	0.70±0.04
		10	0.65±0.05	2.20±0.2**	0.81±0.19
	Lumbricin	1	1.33±0.05	0.75±0.10	1.84±0.02
		10	0.84±0.10	2.10±0.43*	1.92±0.55
Signal Transduction	MEKK 1	1	1.40±0.19	1.47±0.44	1.73±0.04*
		10	1.00±0.15	1.96±0.11*	1.33±0.03
	PKC 1	1	1.52±0.30	1.08±0.19	1.43±0.06
		10	1.10±0.16	0.33±0.04**	0.58±0.11*

Table 5. The mRNA levels of different molecules in coelomocytes exposed to 1 and 10 µg mL⁻¹ TiO₂ NPs. mRNA changes were tested by two-way ANOVA with the Bonferroni post-hoc test (* p < 0.05, ** p < 0.01, * p < 0.001). The control is relative to 1.00. Values <1.00 correspond to gene downregulation, and values > 1.00 correspond to gene upregulation.**

Chapter 4. Results

Two reference genes (RPL13, RPL17) were selected as internal controls for the normalization of the other gene expression. The mRNA fold change level was related to the change in the settled controls.

It was observed upregulation of metallothioneins after the exposure to CuO NPs (Table 6). At both concentrations, there was an increase along the exposure times. Although 1 $\mu\text{g Cu mL}^{-1}$ exhibited high upregulation, 10 $\mu\text{g Cu mL}^{-1}$ had the greatest upregulation after 24 h exposure to CuO NPs (Table 6).

Even though metallothioneins were upregulated, the molecules associated with the antioxidative system were downregulated. MnSOD was downregulated after 2 h exposure to 1 $\mu\text{g Cu mL}^{-1}$ and CuZnSOD. Then, MnSOD remained downregulated after 24 h. However, CAT was only downregulated after 24 h when coelomocytes were exposed to 10 $\mu\text{g Cu mL}^{-1}$. Except for metallothioneins and the molecules involved in the oxidative system, the rest of the molecules remained unchanged. In conclusion, the exposure to both CuO NPs concentrations did not exhibit induction nor suppression of the signalling or immune molecules (Table 6).

Function	Gene	CuO NPs ($\mu\text{g Cu mL}^{-1}$)	Normalized gene expression (relative to control)		
			2h	6h	24h
Metal detoxification	Metallothionein	1	5.27±0.88**	2.63±0.06*	5.44±0.12**
		10	0.87±0.11	1.22±0.06	13.36±0.35***
Heavy metal detoxification	Phytochelatin	1	0.984±0.14	0.81±0.18	1.03±0.16
		10	0.9±0.12	1.52±0.08	1.03±0.15
Oxidative stress	MnSOD	1	0.30±0.08*	0.50±0.06	0.26±0.04**
		10	0.83±0.14	0.55±0.12	0.46±0.099
	CuZnSOD	1	0.26±0.04***	0.95±0.26	0.65±0.10
		10	0.82±0.12	1.04±0.10	1.11±0.20
	CAT	1	1.13±0.15	0.55±0.09	0.57±0.13
		10	0.84±0.11	1.25±0.10	0.52±0.07*
Immunity	EMAP II	1	0.66±0.13	0.70±0.09	0.91±0.19
		10	0.86±0.11	1.38±0.09	1.54±0.17
	Fet/Lys	1	0.44±0.06	0.77 ±0.11	0.69±0.11
		10	0.74±0.10	1.51±0.11	1.26±0.36

Chapter 4. Results

Signal Transduction	lumbricin	1	1.26±0.21	0.47±0.19	1.20±0.31
		10	1.03±0.14	2.08±0.5	0.74±0.09
	MEKK 1	1	0.96±0,10	0.66±0.07	0.69±0,18
		10	0.88±0.12	1.49±0.07	0.70±0.03
	PKC 1	1	1.70±0,28	0.64±0.09	0.94±0.18
		10	0.88±0.15	1.27±0.15	0.57±0.18

Table 6. The mRNA levels of different molecules in coelomocytes exposed to 1 and 10 $\mu\text{g Cu mL}^{-1}$ CuO NPs. mRNA changes were tested by two-way ANOVA with the Bonferroni post-hoc test (* $p < 0.05$, ** $p < 0.01$, * $p < 0.001$). The control is relative to 1.00. Values <1.00 correspond to gene downregulation, and values >1.00 correspond to gene upregulation. Two reference genes (RPL13, and RPL17) were selected as internal controls for the normalization of the other gene expression. The mRNA fold change level was related to the change in the settled controls.**

The Cu^{+2} ions control (CuSO_4) mRNA levels of assorted molecules were assessed (Table 7), and differences in comparison to CuO NPs exposure were found. Similar to CuO NPs, there was an upregulation of metallothioneins which was the greatest at 24 h for 10 $\mu\text{g Cu mL}^{-1}$. Concerning the oxidative stress molecules, there was an MnSOD suppression during the time exposure (2 and 6 h) for 1 and 10 $\mu\text{g Cu mL}^{-1}$ concentration. Similar to CuO NPs, 1 $\mu\text{g Cu mL}^{-1}$ led to the suppression of CuZnSOD at 2 h while catalase was downregulated for both 1 and 10 $\mu\text{g Cu mL}^{-1}$ concentration at 6 h.

Differences were observed in the mRNA levels of immune and signal transduction molecules which were upregulated and downregulated, respectively. While CuO NPs did not lead to any mRNA changes, the Cu^{+2} ions control (CuSO_4) exposure led to mRNA changes in some molecules (Tables 6 and 7). The EMAP II molecules levels were increased after 24 h and exposed to 10 $\mu\text{g Cu mL}^{-1}$. MEKK 1 and PKC 1 mRNA levels were downregulated at 2 h exposure to 1 and 10 $\mu\text{g mL}^{-1}$ Cu as a form of CuSO_4 , respectively (Table 7). The greatest concentration of Cu^{+2} ions decreased PKC 1 mRNA levels after 24 h exposure (Table 7). The results showed that the Cu^{+2} ions were able to invoke similar changes as CuO NPs, but they also produced changes in the remaining molecules.

Function	Gene	CuSO ₄		Normalized gene expression (relative to control)		
		($\mu\text{g Cu mL}^{-1}$)	2h	6h	24h	
Metal detoxification	Metallothionein	1	0.89±0.13	0.64±0.17	6.93±1.68***	
		10	0.97±0.19	2.54±0.19***	10.44±0.54***	
Heavy metal detoxification	Phytochelatin	1	1.21±0.20	0.73±0.33	0.8±0.31	
		10	0.98±0.12	0.90±0.06	0.88±0.18	
Oxidative stress	Mn-SOD	1	0.4±0.07^a	0.35±0.09*	0.29±0.08*	
		10	0.84±0.09	0.51±0.05**	0.39±0.05***	
	CuZn-SOD	1	0.29±0.08**	0.51±0.12	0.82±0.19	
		10	0.9±0.09	0.67±0.03	1.07±0.09	
	CAT	1	0.80±0.12	0.35±0.08*	0.58±0.16	
		10	1.01±0.20	0.49±0.05*	0.3±0.04**	
Immunity	EMAP II	1	0.71±0.1	0.57±0.13	0.55±0.3	
		10	0.68±0.09	1.21±0.08	1.71±0.09*	
	Fet/Lys	1	0.78±0.1	0.49±0.11	0.58±0.16	
		10	0.58±0.08	1.52±0.11	0.53±0.03	
	Lumbricin	1	1.11±0.15	0.57±0.15	1.18±0.56	
		10	1.04±0.14	1.05±0.12	0.75±0.06	
Signal Transduction	MEKK 1	1	0.63±0.08	0.44±0.1*	0.65±0.15	
		10	0.78±0.09	0.98±0.23	0.88±0.13	
	PKC 1	1	0.73±0.1	0.39±0.09	0.69±0.18	
		10	1.06±0.13	0.44±0.03**	0.29±0.05***	

Table 7. The mRNA levels of different molecules in coelomocytes exposed to 1 and 10 $\mu\text{g Cu mL}^{-1}$ CuSO₄. mRNA changes were tested by two-way ANOVA with the Bonferroni post-hoc test (* $p < 0.05$, ** $p < 0.01$, *** $p < 0.001$). The control is relative to 1.00. Values <1.00 correspond to gene downregulation, and values >1.00 correspond to gene upregulation. Two reference genes (RPL13, RPL17) were selected as internal controls for the normalization of the other gene expression. The mRNA fold change level was related to the change in the settled controls.

4.8 Weight loss and mortality

According to the OECD 207 guidelines (OECD, 1984), there were no dead earthworms found in the containers of control, Ag₂S NPs or AgNO₃ after the 14 days of exposure.

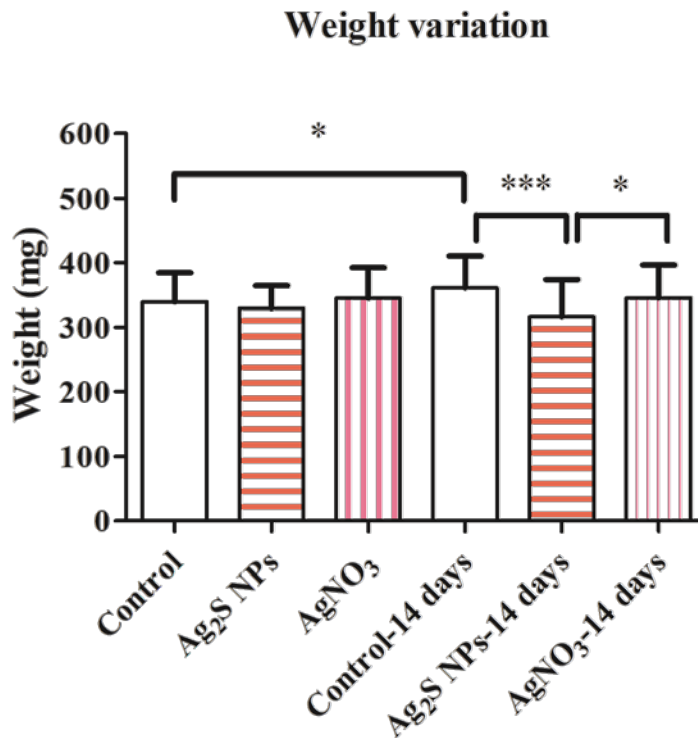


Figure 30. Weight loss of earthworms (mg). The body weight of the earthworms exposed to control, Ag₂S NPs or AgNO₃ at the start of the experiment and after 14 days of the experiment. Values were shown as mean (mg)±SD. * p<0.05, *** p<.001 according to one-way ANOVA and Bonferroni post-hoc test. N= 60 earthworms in each exposure.

At the start of the experiment, every earthworm was weighed, and their weight was approximately 300 mg. After 14 days of exposure, a significant difference was observed in their weight due to the weight increase of the earthworms (357.5 mg) which were in the control container (Figure 30).

After 14 days changes in the weight of the earthworms were detected in comparison with the control. The earthworms exposed to the Ag₂S NPs after 14 days decreased their weight (311 mg) in comparison with the control at the same time (Figure 30). Moreover, a slight statistical difference was also observed between the exposure of Ag₂S NPs and AgNO₃ after 14 days (311.6 and 341.4 mg, respectively; Figure 30). There was statistical significance for Ag₂S NPs and no statistical significance for AgNO₃ in comparison with the control (Figure 30). The weight loss clearly showed that it was produced by the Ag₂S NPs themselves.

Chapter 5



Final Discussion

5. Final Discussion

5.1 NPs Characterization

5.1.1 UV/Vis and primary size

This thesis has demonstrated that UV/Vis wavelength analysis is a useful technique for the characterization of NPs. When the UV/Vis wavelength is different between the NP stock (manufacturer data) and the NPs measured in the experimental set-up, there is a high probability that NPs have changed. However, the results obtained showed that the spectra absorbance of TiO₂ NPs and CuO NPs remained similar along the exposure times (Table 3). In the case of Ag₂S NPs, it was compared the UV/Vis spectra obtained to that one from the manufacturer so then it could confirm that Ag₂S NPs did not change prior to their dispersion in the soil.

Another potential concern is that NPs can have the same wavelength as some reagents from absorbances tests. Therefore, it is highly recommended to check the UV/Vis wavelength of NPs prior to performing any experiment to avoid problems of background noises. For this reason, in Figure 17 B, samples of NPs themselves were included in the flow cytometry analyses to eliminate any disturbances in our results.

According to the TEM images, primary sizes were 20 -100 nm and 5-15 nm for 500 µg mL⁻¹ TiO₂ NPs (Figure 8 A) and 100 µg Cu mL⁻¹ CuO NPs (Figure 8 B), respectively, while the Ag₂S manufacturer determined the size which was 20.4 nm (Figure 8 C). In addition, the TEM images showed that TiO₂ NPs, CuO NPs, and Ag₂S NPs were rounded in shape, which was in concordance with the manufacturer's information. Primary size has an important role because cells engulf NPs with sizes ranging between 20 - 50 nm (Sukhanova et al., 2018 and papers there in). Moreover, an inverse correlation between size and toxicity was demonstrated (Sukhanova et al., 2018 and papers there in). Thus, the greater the NPs size is, the toxicity decreases. The precipitation of NPs can also be related to the NPs size. For example, greater size of CuO NPs (approximately 50 nm) will remain in suspension lesser time in seawater (Keller et al., 2017).

Furthermore, the complexity of the exposure media is also important to consider due to the differences in bioavailability and binding within the NPs' cultivation medium (TiO₂ NPs and CuO NPs) and the soil medium (Ag₂S NPs).

5.1.2 NPs-Cultivation medium interaction

The cultivation media preparation depends on the type of cells assessed and whether the organisms are marine or terrestrial (Alijagic et al., 2019; Navarro Pacheco et al., 2021a; Swartzwelter et al., 2021 and papers there in). Coelomocytes were cultivated in R-RPMI 1640 medium with adjusted osmolarity (Navarro Pacheco et al., 2021a, 2021b; Semerad et al., 2020). The RPMI 1640 medium contained 5% FBS (heat-inactivated) and HEPES within others. Several studies have already shown that FBS could affect the stability of the NPs (Sukhanova et al., 2018 and papers there in; Wang et al., 2013). Moreover, HEPES would

Chapter 5. Final Discussion

also enhance the stability of the NPs. Therefore, the substances supplemented in the RPMI 1640 and RPMI 1640 medium itself can change the NPs dispersion leading to precipitation, aggregation, or dissolution (Wang et al., 2013). The differences in hydrodynamic size between distilled water and R-RPMI 1640 medium were observed (Table 3). TiO₂ NPs tended to be stable until 6 h, then samples started to aggregate (Table 3 A). Similar effects were observed by Bigorgne et al. (2012). They demonstrated that the addition of 10% FBS re-dispersed TiO₂ NPs while HEPES tended to aggregate TiO₂ NPs (Bigorgne et al., 2012).

CuO NPs dispersion, are unstable like most of the metal oxide NPs, as it could observe through the zeta potential in R-RPMI 1640 medium (Table 3 C), but they also tended to dissolve (Figure 11). Keller et al. (2017) explained that pH and salinity were the main precursors of CuO NPs stability. Variations in pH and salinity in the medium lead to aggregation and precipitation of CuO NPs (Keller et al., 2017). Salinity was excluded because of the osmolarity of coelomocytes and pH was controlled and remained at 7.02.

Moreover, it was observed there was a correlation between the concentration of CuO NPs and the dissolution. Lower concentrations tended to dissolve faster than the highest concentration (100 µg Cu mL⁻¹). The reason could be the high rate of aggregation found on 100 µg Cu mL⁻¹ CuO NPs (Figure 8 B) and confirmed by Keller et al. (2017). Keller and colleagues observed that aggregated Cu NPs had reduced surface area which slowed the dissolution rate of Cu NPs (Keller et al., 2017). Thus, it showed that the dissolution speed decreased when the NPs were strongly aggregated. Wang et al. realised that at pH 7.4, the solubility of CuO NPs increased when the NPs were dispersed in a medium which contained glutamine (amino functional groups) within other compounds (Wang et al., 2013). In addition, most of the effects caused by the exposure to CuO NPs were produced by Cu⁺² ions. Although ICP-OES confirmed the dissolution of CuO NPs, TiO₂ NPs did not undergo the dissolution process. However, they became active when they are irradiated with UVA light (Alijagic and Pinsino, 2017; Reeves et al., 2008). Non-UVA light irradiation was one of the main reasons that influenced the no greater toxic effects on coelomocytes. Bigorgne et al. (2012) prepared TiO₂ NPs with sonication but they also did not irradiated TiO₂ NPs prior to exposure with coelomocytes. Most of the toxicity effects discussed in several studies were related to the dissolution of NPs and the release of their ions (Gupta et al., 2014; Mincarelli et al., 2016; Navarro Pacheco et al., 2021a).

The zeta potential, which indicates the stability of NPs, showed that TiO₂ NPs were stable when they were dispersed in distilled water. However, these values dropped when they were dispersed in R-RPMI 1640 medium. CuO NPs were also unstable in R-RPMI 1640 medium (Table 3 B). Then, the hydrodynamic sizes confirmed the zeta potential values. It could observe that the size of NPs increased along exposure times, being the bigger sizes at 24 h exposure for TiO₂ NPs (Table 3 A). Remarkably, the size changes remained similar until 6 h exposures, although the zeta potential indicated the instability (Table 3 A).

Chapter 5. Final Discussion

Thus, these changes in size distribution and zeta potential showed that TiO₂ NPs started to precipitate after 6 h of exposure (Table 3 A). Magdelonová et al. (2012) indicated that different tested cell culture media did not influence TiO₂ NPs. The influence was mostly associated with the dispersion protocols used and the serum in the stock solution. For example, sonication of TiO₂ NPs for 30 min at 4 °C left small aggregates (Bigorgne et al., 2012). Dispersion protocols and serum affected the aggregation state and, thus, the size distribution of TiO₂ NPs (Magdolenova et al., 2012). Despite Magdolenová and colleagues' observations, Ji et al. (2010) suggested that the TiO₂ NPs dispersion could improve by adding serum albumin (BSA), but dispersion could also depend on phosphate concentration. The NPs dispersion and their stability could be improved by the serum which is one of the substances that the cell culture media contains for the viability of the cells. It could then confirm that the fetal bovine serum (FBS) added could not potentially improve the TiO₂ NPs dispersion, and therefore NPs tended to aggregate. However, 10% FBS in MEM medium enhanced the dispersion (Bigorgne et al., 2012). However, the phosphate concentration and salinity may also affect the dispersion (Keller et al., 2017). The preparation of the R-RPMI 1640 medium discarded the high salinity concentration.

Exceptionally, Ag₂S NPs did not show an aggregation state though the manufacturer confirmed that the formed colloid showed some degree of agglomeration (Figure 8 C). Consequently, most metal oxide and metal sulfide NPs commonly have some agglomeration degree.

5.1.3 NPs-soil interaction

Soil interaction would affect the availability and mobility of NPs due to several factors like pH, DOM, ionic strength, and also soil microbes. These factors could develop changes in the physicochemical properties of NPs, allowing them to be more disposable or soluble in the soil (Cornelis et al., 2014 and papers there in; Sukhanova et al., 2018 and papers there in). High pH would interact mostly with NPs because of the negative charge of the NPs' surface (Cornelis et al., 2014 and papers there in). Another factor is the aggregation, NPs strongly aggregated tended to sediment faster (Abbas et al., 2020). Then, the NPs could be more in contact to soil organisms.

The common soils used for *in vivo* exposures are OECD soil and LUFA soil. OECD soil is characterized by a mixture of sphagnum peat, sand, and clay soil (OECD, 2016, 1984). LUFA soil is commonly used for metal exposure studies due to the lack of dissolved organic matter (DOM), and pH neutral, allowing to discard some characteristics that would affect NPs dispersion. Hence, LUFA 2.1 soil was chosen to avoid any factors that modified or affected NPs dispersion.

Soil samples collected before and after the exposure proved the stability of Ag₂S NPs in the soil (Figures 9 and 10). The peaks of EDS revealed that the particles contained S and Ag (Figures 9 and 10). Moreover, the ICP-OES data showed the Ag⁺ ion concentration in earthworms and soil. The data confirmed that the

Chapter 5. Final Discussion

nominal concentration was 5 mg Ag Kg⁻¹ soil (Table 4). Moreover, the data showed an increase in Ag⁺ ion concentration in earthworms exposed to Ag₂S NPs and AgNO₃, while the concentration of Ag⁺ ion was lower in the soil after 14 days of exposure (Table 4). Hence, the data suggested that earthworms accumulated Ag in their body. These results are in line with those shown by Baccaro et al. (2018), who described that earthworms engulfed Ag, Ag₂S NPs and AgNO₃. The ingestion of different NPs with their ions released inside the earthworm enhanced toxicity effects and caused oxidative stress, genotoxicity and cytotoxicity (Gupta et al., 2014; Hayashi et al., 2012; Navarro Pacheco et al., 2021a). Regarding Ag₂S NPs, they are probably more stable than Ag NPs (Baccaro et al., 2018; Peixoto et al., 2020; Schultz et al., 2018). Their solubility is much lower in Ag₂S NPs than in Ag NPs, which is the reason that Ag₂S NPs would require more time to dissolve and release the Ag⁺ ions (Wang et al., 2015). Moreover, Peixoto et al. (2020) suggested that the potential effects derived from Ag⁺ ions from Ag₂S NPs would occur at long-time exposures.

To sum up, the toxic effects produced by NPs depend not only on the type of NPs but on the type of medium and the way they are dispersed. Therefore, the NPs characterization is key to predict the NPs' behaviour in the medium. According to this, the toxicity mechanisms vary depending on their dispersion and physicochemical characteristics, as it was also observed (Table 3 and Figure 8).

Moreover, several studies have enlightened the importance of creating standard NP guidelines for their characterization in cultivation medium (cellular studies) and the soil (Barhoum et al., 2022 and papers there in; Boraschi et al., 2020 and papers there in; Tortella et al., 2020). The proper characterization guidelines would aid in understanding the pre-conditions of the toxicity mechanisms and unify several NPs toxicity studies to have a broader comprehension of NPs' effects on different organisms in the environment.

5.2 Coelomocytes cultivation conditions

The *in vitro* testing is focused on the effects of the NPs at the cellular level. Coelomocytes explained in the introduction (**1.4.3.1 Cellular response**) are extruded by chemical irritative substances or mild electrical stimulation (TiO₂ NPs and CuO NPs, and Ag₂S NPs, respectively). However, irritative substances are more suitable for cell viability and allow larger RNA yields. That is why they were used in a number of studies (Navarro Pacheco et al., 2021b, 2021a; Semerad et al., 2020).

Our studies focused on amoebocytes (HAs and GAs) which have an immune function in the earthworm *E. andrei*. The main characteristics of coelomocytes are that they are primary cells; thus, coelomocytes do not have long survival rates after a few hours or days out of the earthworm. Similarly to Yang et al. (2017) the optimal rates are up to 24 h; then, the survival decreases exponentially in RPMI 1640 medium (Yang et

Chapter 5. Final Discussion

al., 2017). The optimal conditions for coelomocytes are 20 °C and darkness (TiO₂ NPs, CuO NPs and CuSO₄). They are able to survive in RPMI 1640 medium with 176 mOsm. The osmolarity is among the main characteristics of coelomocytes survival, and 176 mOsm is the threshold where cells may stay alive. Thus, RPMI 1640 medium was diluted with Milli-Q water (0.05 μS cm⁻¹), and called R-RPMI 1640 medium. Some studies have suggested that RPMI 1640 medium is the most appropriate among other mediums (Leibovitz' L15, BME; Garcia-Velasco et al., 2019; Yang et al., 2017). The RPMI 1640 medium used in our studies is also enriched with FBS, HEPES, Na-pyruvate, L-glutamine, and antibiotic-antimycotic substances that enhance the survival of the cells (Navarro Pacheco et al., 2021a, 2021b; Semerad et al., 2020). The amino acid groups like glutamine, glucose, HEPES and/or FBS that enrich the medium could affect the availability, dissolution, or stability of NPs inside the medium (**5.1.2 NPs-Cultivation medium interaction**; Wang et al., 2013). Another important thing to consider is the salts concentration, as they may force NPs to precipitate, which usually happens when the test is performed with marine organisms like sea urchins, mussels, etc. (Alijagic et al., 2020; Swartzwelter et al., 2021 and papers there in). For these reasons, the coelomocytes analyses were carried out in a short period (2, 6 and 24 h; in R-RPMI 1640 at 176mOsm).

5.3 Electron microscopy

The scanning electron microscope detected TiO₂ NPs and CuO NPs on the cell surface (Figures 12-15). The EDS analyses confirmed the presence of Ti from 100 μg mL⁻¹ TiO₂ NPs (spot 2) in the coelomocytes after 2 h exposure (Figure 13 B). However, it was only observed at 100 μg mL⁻¹; lesser concentrations did not show similar features due to the EDS microanalyses detection limit. According to Bigorgne et al. (2012) TiO₂ NPs were engulfed by coelomocytes and observed in the coelomocytes' cytoplasm. It could not be detected TiO₂ NPs inside the coelomocytes, and it could be probably caused by the large aggregates formed. The probable route of internalization of TiO₂ NPs would be via phagocytosis or endocytosis (Bigorgne et al., 2012; Gupta and Tripathi, 2011 and papers there in). The EDS analyses also confirmed the presence of Cu on the surface of coelomocytes (Figure 15 A, spot 8; Figure 15 B, spot 5).

In the case of CuO NPs, the NPs were found inside the coelomocytes (Figure 16 A-D) after 2 h exposure to 100 μg Cu mL⁻¹ CuO NPs. Similarly to Bigorgne et al., (2012) the NPs were located in the cytoplasm, but they were not found in the nucleus or mitochondria (Figure 16 A-E) . Bigorgne and colleagues observed that the main coelomocytes that had internalised TiO₂ NPs were amoebocytes (HAs and GAs; Bigorgne et al., 2012). Undoubtedly, the STEM/EDS microanalysis verified elemental Cu in those aggregates (Figure 16 E-G). Then, those clusters of CuO NPs could be the internal source of Cu⁺² ions that could induce cellular damage. This mechanism, called the "Trojan horse" effect, was suggested and described for human lung epithelial cells exposed to Co₃O₄ NPs and earthworm coelomocytes exposed to Ag NPs (Hayashi et al., 2016; Limbach et al., 2007). Similarly, Gupta et al. (2014) described that coelomocytes could scavenge ZnO

Chapter 5. Final Discussion

NPs, and then adverse effects in DNA damages were detected. The bigger sizes of these NPs (100 nm) were found in the endosome inside the coelomocytes (Gupta et al., 2014). The route of internalization was not described but it is suggested that it would depend on the NPs size engulfed. Phagocytosis occur in sizes ranged between 0.1-1 μm for TiO_2 NPs (Bigorgne et al., 2012). The other route is the receptor-mediated endocytosis which is subdivided into three types: clathrin-mediated endocytosis (<200 nm), caveolae-mediated endocytosis (200 nm-1 μm) and macropinocytosis (>1 μm) (Bigorgne et al., 2012). For example, caveolae route for uptaking NPs is particularly used by adipocytes, fibroblast muscle and endothelial cells (Azhdarzadeh et al., 2015). On the other hand, macropinocytosis has been suggested as a route to endocytose 100 nm ZnO NPs in coelomocytes (Gupta et al., 2014). However, there is a lack of knowledge of the most probable route of NPs internalization in earthworms (Gupta et al., 2014)

Hence, both TiO_2 NPs and CuO NPs showed that the amoebocyte population's phagocytic ability can lead to NPs scavenging and endocytosing. Consequently, amoebocytes may be more sensitive to NPs exposure due to their phagocytic activity. Gupta et al. (2014) also confirmed that coelomocytes were able to endocytose ZnO NPs, causing DNA damage.

5.4 Cellular studies

Immunotoxicity is a term that refers how certain chemicals affect the immune system. In the immune system, coelomocytes play a protective role and trigger several defence mechanisms. However, some NPs could cause potential damage to these cells, leading to a general immunodepression of the animal.

The viability was one of the main analyses to evaluate the state of coelomocytes. Therefore, in every biomarker, the viability of the coelomocytes was assessed. According to this, the results were expressed as the viable coelomocytes which were phagocytosing or producing ROS.

TiO_2 NPs did not cause mortality (Figure 28 A.3 and B.3) of HAs and GAs, which is in line with the results shown by Bigorgne et al. (2012). Then, the reason why both NPs did not cause high mortality rates could be related to the lack of ions released. Several studies suggested that high solubility leads to ions release, which increase oxidative stress, and then decrease the viability (Gautam et al., 2018; Navarro Pacheco et al., 2021a; Semerad et al., 2020). Thus, the viability results from TiO_2 NPs and Ag_2S NPs can be caused by the low solubility and the low release of ions. CuO NPs and CuSO_4 had low viability (Figure 28 A.1, A.2 and B.1, B.2) at $100 \mu\text{g Cu mL}^{-1}$ for HAs and GAs. Their low viability could be associated with the solubility and ions released (Figure 11). Isani et al. (2013) also observed low viability and other adverse toxic effects when trout erythrocytes were exposed to CuO NPs. Isani and colleagues suggested that CuO NPs had low solubility so partially damages could not come from Cu^{+2} ions (Isani et al., 2013). However, our dissolution studies showed that CuO NPs were soluble (Figure 11). Sémerad et al. (2020) showed also that control ions

Chapter 5. Final Discussion

of Fe produced stronger damages than nZVI NPs themselves. Probably, the coating of nZVI NPs protected the NPs not to release the Fe ions (Semerad et al., 2020).

The viability of coelomocytes exposed to Ag₂S NPs was analysed according to the trypan blue viability test (Figure 18). Coelomocytes were healthy, reaching 71-78% viability in each treatment (control, Ag₂S NPs or AgNO₃). Our results differed from previous studies, where Ag NPs dropped coelomocytes viability after 24 h of exposure to 0.05 mg Ag Kg⁻¹ (Curieses Silvana et al., 2017). However, the effects derived from sulfidized Ag NPs (Ag₂S NPs) have not been studied (Curieses Silvana et al., 2017).

Several biomarkers were used to assess the potential damages caused by the chosen NPs (TiO₂ NPs, CuO NPs and Ag₂S NPs). Several studies have already used oxidative stress markers (ROS; NO; and lipid peroxidation; Table 1; Curieses Silvana et al., 2017; Hayashi et al., 2016; Mincarelli et al., 2016; Navarro Pacheco et al., 2021b; Qi et al., 2018; Semerad et al., 2020). Other studies conducted mRNA analyses observed whether the cells up/downregulated several important molecules or performed genotoxicity assays (Bigorgne et al., 2012; Gupta et al., 2014; Hayashi et al., 2012; Isani et al., 2013; Mincarelli et al., 2019, 2016; Navarro Pacheco et al., 2021a). We have tried to connect the different assays to understand the possible mechanisms of toxicity and the observed effects. As the thesis focused on the immune system, it was assessed the phagocytic and phenoloxidase activity. Phagocytic cells could interact as nanoscavengers, and thus, they are among the most sensitive cells to NPs (Bigorgne et al., 2012; Gupta et al., 2014).

5.5 Oxidative stress

5.5.1 ROS and NO production

Several studies mentioned that oxidative stress is usually generated when the cells and microorganisms are exposed to NPs (Table 1). Oxidative stress as a biomarker has been assessed in different species (Swartzwelter et al., 2021 and papers there in). Generally, the excessive production of free radicals (ROS) leads to cell damage. ROS production is an innate immune mechanism to remove foreign materials. This process is also observed in human neutrophils and macrophages, which produce ROS that kills the microbes and other cells (Abbas et al., 2021).

In comparative immunology, every species has an innate immune system (Figure 4), which is more or less evolutionary developed. Thus, oxidative stress is a promising biomarker for understanding immunotoxicity and comparing it with other species. Terrestrial and marine organisms shared the production of ROS as NPs adverse effects (Gautam et al., 2018; Isani et al., 2013; Swartzwelter et al., 2021 and papers there in).

Chapter 5. Final Discussion

ROS and NO are biomarkers of oxidative stress. Both produced free radicals that interact with their surroundings, including lipids, other cells, etc. NO is also produced by human macrophages that kill microbes (Abbas et al., 2021). ROS was measured for TiO₂ NPs and CuO NPs experiments, while NO was measured for Ag₂S NPs exposure. ROS production is often triggered after exposure to NPs (Huerta-García et al., 2014; Semerád et al., 2019).

Surprisingly, the ROS production was not induced by the exposure to CuO NPs and CuSO₄ (Figure 19 A.2-3 and B.2-3), which was detected by the unchanged ROS production in both HAs and GAs (Figure 19 A.2-3 and B.2-3). Gautam et al. (2018) observed a decrease of NO production when coleomocytes were exposed to CuO NPs. Liang et al. (2017) also showed an increased production of ROS when earthworms were exposed to 1000 mg Kg⁻¹ soil of nZVI NPs. Exposure of earthworms with MWCNTs increased the production of ROS (Yang et al., 2017). Moreover, some studies suggested that oxidative stress like ROS was commonly produced after NPs exposure to different organisms (Boraschi et al., 2020 and papers there in; Garcia-Velasco et al., 2016; Swartzwelter et al., 2021 and papers there in). Although ROS production was not observed, it detected an increasing accumulation of brown bodies during the cells' exposure to 100 µg Cu mL⁻¹ of CuO NPs (Figure 31). Furthermore, it was observed how brown bodies formation increased after 24 h (Figure 31 D). In comparison with the control, , the brown bodies formation increased significantly after 24 h (Figure 31 C-D). After 2 h exposure, control and CuO NPs exposure had similar levels of brown bodies produced (Figure 31 A-B).

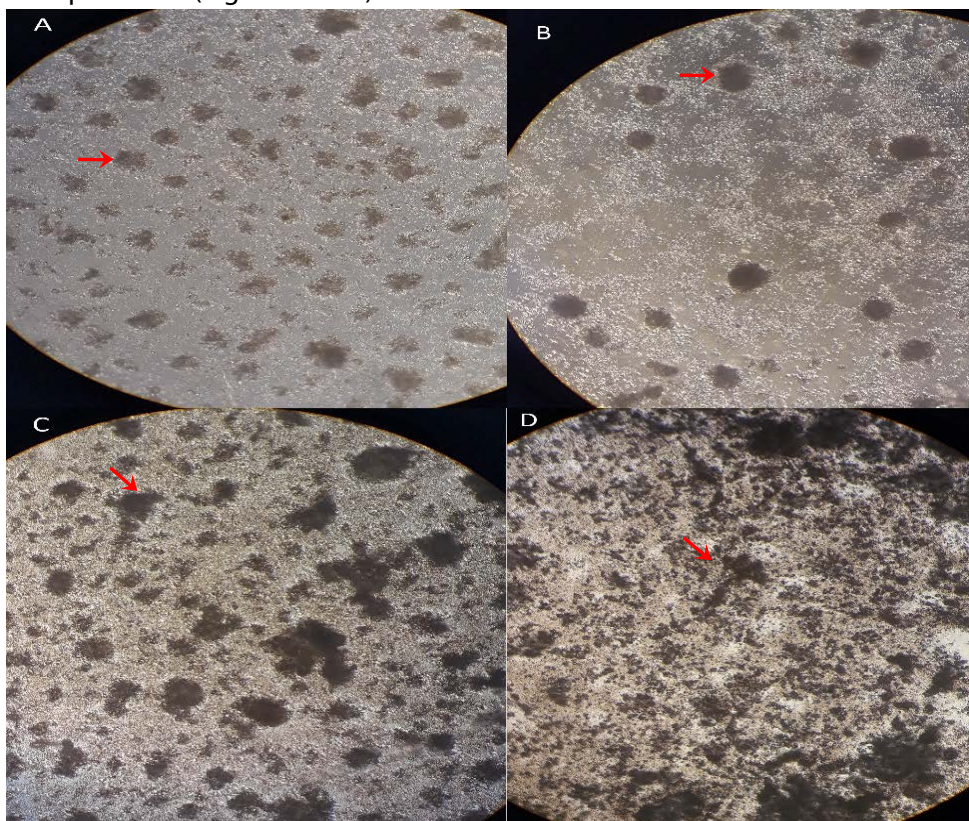


Figure 31. Brown bodies formation. A) Non-treated coelomocytes in R-RPMI 1640 medium after 2 h, B) non-treated coelomocytes in R-RPMI 1640 medium, C) coelomocytes incubated with $100 \mu\text{g Cu mL}^{-1}$ CuO NPs for 2 h D), 24 h incubation of coelomocytes with $100 \mu\text{g Cu mL}^{-1}$ CuO NPs. The number of brown bodies increased along the whole surface of the plate. Cells (treated with CuO NPs and without) were incubated at the same time and under conditions (20°C in darkness). Red arrows indicate brown bodies formation.

It was described that lipofuscin deposition in brown bodies could inhibit ROS generation (Valembois et al., 1994). Valembois and colleagues suggested that both lipofuscin and melanin pigments in brown bodies would neutralize on-self or altered-self tissues (Valembois et al., 1994). Homa et al. (2016) also showed that the increasing number of brown bodies formed was correlated with lipofuscin accumulation. Thus, the ROS was probably generated in CuO NPs and CuSO_4 exposure, but it was suppressed entirely due to the formation of brown bodies. Besides that, ROS production could be affected and suppressed by metallothioneins induction (Table 5-6), which counteracts ROS production (Hayashi et al., 2012).

Similarly to CuO NPs, TiO_2 NPs did not increase the ROS production compared to control coelomocytes (Figure 14). Probably, the ROS could be elicited by the metal ions released from that metal NPs like Ag, nZVI or ZnO NPs, which induced significantly greater ROS production (Garcia-Velasco et al., 2016; Gupta et al., 2014; Semerad et al., 2020). For example, nZVI NPs did not produce ROS until 24 h. It could be potentially explained by the possibility that NPs were engulfed by the immune cells, and when the coating was degraded, the Fe ions were released and intracellular ROS species were generated (Semerad et al., 2020). Furthermore, nZVI NPs showed that ROS species have a shorter life span (Semerad et al., 2020). Generally, it is explained that ROS species are produced and degraded within minutes and hours, depending on the cells (Ayala et al., 2014). Their short life may be explained by their binding to other molecules in the surrounding, becoming toxic, and killing the foreign particles and the host cells. Last but not least, the activation of the antioxidative stress system can scavenge the ROS species generated. The antioxidative system of earthworms is described in the **5.7 mRNA analyses**, where the up/down-regulation of the main molecules related to the antioxidative system were observed.

Remarkably, HAs exerted approximately two times lesser ROS production than granular amoebocytes after the exposure to TiO_2 NPs, CuO NPs or CuSO_4 (Figure 19 A-B). The reduced ROS production suggests that HAs could be more resistant to oxidative stress than GAs, or they could produce less ROS due to their size, or the production could be affected by their different metabolisms.

Although both are oxidative stress biomarkers and coelomocytes were exposed to NPs, it have observed that NO production was not the most optimal biomarker to be assessed in *E. andrei*. Along the optimisation process, it was observed that the NO production basal levels from *E. andrei* were under the

Chapter 5. Final Discussion

detection limit. Thus, L-arginine was used to enhance the NO production in order to detect it. It can be due to different NO production among individual earthworms. Further, Gautam et al. (2018) observed the increased NO production when the earthworm *Metaphire posthuma* was exposed to Cu NPs. Cook et al. (2015) also observed an increased production of NO when *Eisenia hortensis* coelomocytes were exposed to bacteria (Cook et al., 2015). Thus, it remarks that may NO production differs depending on the type of earthworm used for the assessment.

The differences between Gautam et al. (2018) and our results highlight that ions effects could have a crucial role in NO production. While CuO NPs and CuSO₄ release Cu⁺² ions, Ag₂S NPs are not completely soluble. Although the results did not indicate changes in NO generation, the variances in Ag₂S NPs suggested a possible imbalance of NO metabolism (Figure 20).

5.5.2 MDA production

Ayala et al. (2014) also suggested that mainly OH⁻ (ROS) interact with lipids and generate the MDA, a subproduct of lipid peroxidation apart from other molecules. MDA is considered more toxic than ROS species, and this molecule can also bind the DNA bases causing damage and mutations (Ayala et al., 2014 and papers there in). MDA production, called lipid peroxidation, was measured for coelomocytes exposed to TiO₂ NPs, CuO NPs and Ag₂S NPs. It was observed the link between ROS and MDA when coelomocytes were exposed to TiO₂ NPs (Figures 19 A.1 and B.1, and 21 A). Hence, it corroborates the linkage that Ayala suggested between ROS interacting with fatty acids and leading to MDA production. It was described that excess ROS leads to the MDA production (Zhang et al., 2018). However, no MDA production was observed due to the non-reactivity of TiO₂ NPs. The irradiation of UVA light could increase the reactivity of TiO₂ NPs and its production of oxidative stress leading to an increase in the toxicity effects (Reeves et al., 2008).

Similar results were observed in the TiO₂ NPs exposure on THP-1 human cells and sea urchin cells (Alijagic et al., 2019; Poon et al., 2020). In this thesis, the cultivation conditions were dark, which could explain the absence of oxidative stress. Lipid peroxidation was also measured after CuO NPs and CuSO₄ exposure, showing significantly higher MDA production during the experiment for 10 and 100 µg Cu mL⁻¹ concentrations (Figure 21 B and C). Although ROS production was not induced, it can not discard that MDA was produced by free radicals derived from Fenton-like copper redox. The Fenton-like redox occurs when Cu⁺² ions or Fe⁺², Fe⁺³ ions react with H₂O₂ in the environment and produce OH⁻ (Pham et al., 2013). Yirsaw et al. (2016) also suggested that via Fenton-like redox Fe could produce reactive species (OH⁻, H₂O₂, O₂⁻). Later OH⁻ interact and affect the fatty acids of the cell membrane. For example, 200 mg L⁻¹ MWCNTs produced MDA after the exposure with earthworms (Yang et al., 2017). Yirsaw et al.(2016) also observed

Chapter 5. Final Discussion

the increased production of MDA and they suggested that oxidative stress could interact with cellular compounds like lipids to produce MDA.

Similarly to TiO₂ NPs (Figure 21 A), Ag₂S NPs exposure led to similar NO and MDA production values (Figures 20 and 22). However, MDA production did not differ among Ag₂S NPs or AgNO₃ and control samples. Although nZVI NPs and the control ions samples could produce ROS and MDA production (Semerad et al., 2020), other metal NPs like TiO₂ NPs and Ag₂S NPs do not release ions. Then, oxidative stress was not produced due to no production of ROS and MDA (Figure 19-22). The adverse effects could be derived from the ions instead of NPs. However, AgNO₃ (control Ag⁺ ions) did not induce NO or MDA production, although induction was expected. The most probable explanation would be that the Ag⁺ ions amount was not sufficient to exert some effects on earthworms, as was observed in another study (reproduction EC50 42-46.9 mg Kg⁻¹; Schlich et al., 2013). Further, Ag⁺ ions could also be transformed into Ag particulate as it was described by Baccaro et al. (2018). Thus, if the Ag⁺ ions became Ag particulate and earthworms excrete it, there are no Ag⁺ ions to produce NO or MDA, activating the oxidative stress in earthworms.

MDA production seems to be the best biomarker among the other biomarkers to assess oxidative stress. It is sensitive enough to be detected even at low exposure levels (Liang et al., 2017). The reason is that not only intracellular ROS could be produced, but in the case of Fe and Cu, also the Fenton-like redox exists, which can produce enough quantity of free radicals to interact with the lipids (Pham et al., 2013; Wang et al., 2013).

5.6 Genotoxicity and immune biomarkers

The alkaline comet assays were carried out to observe the possible DNA damage. The MDA produced by the lipid peroxidation probably interacts with nucleosides (Ayala et al., 2014 and paper there in). This interaction lead to the DNA damages visible as DNA comets. The comets consist of two parts, the comet

Chapter 5. Final Discussion

head and the comet tail. The comet head is the nucleus with compacted DNA inside. If there are DNA breaks, the shorter fragments of DNA move faster and form the comet tail (Figure 32).

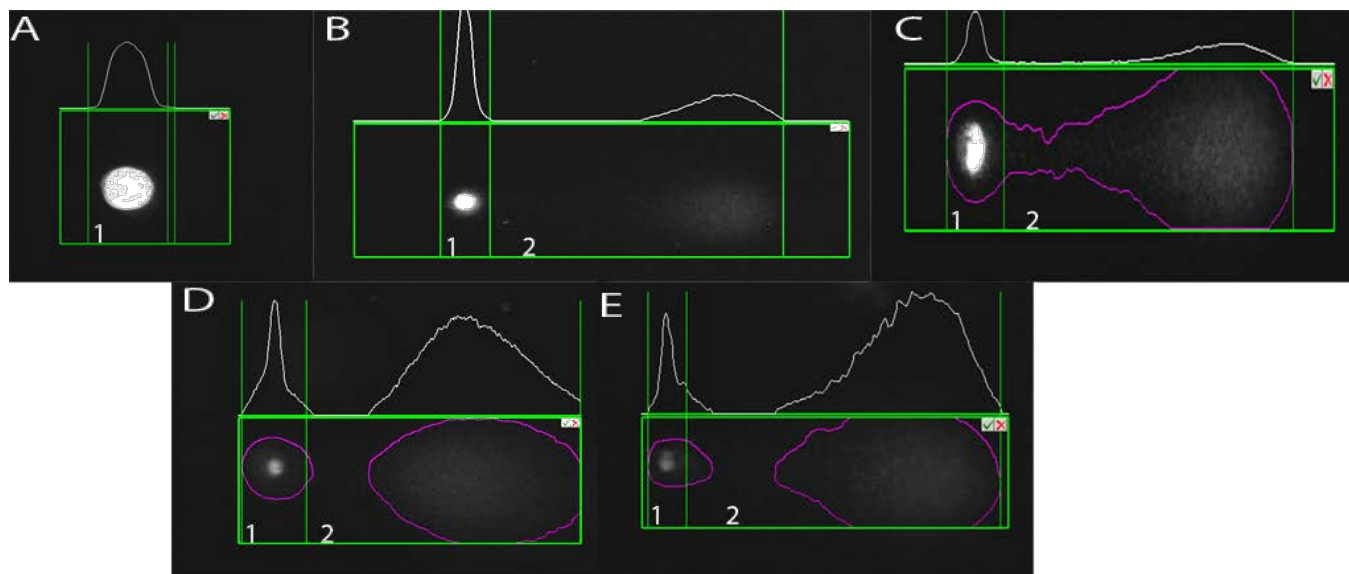


Figure 32. Illustrative DNA comet. Image of comet analyses where the intensity in the head (1) and in the tail (2) of the comet is analysed for control coelomocytes (A), 100 µg mL⁻¹ TiO₂ NPs (B), CuSO₄ (C), CuO NPs and (D) 100 mM H₂O₂ (E) at 24 h exposure.

The comet assay was carried out under different concentrations (1, 10, and 100 µg mL⁻¹) of TiO₂ NPs (Figure 32 B), CuO NPs (Figure 32 D) and CuSO₄ (Figure 32 C). Exposure of coelomocytes to TiO₂ NPs resulted in slight DNA damage compared to the control coelomocytes (Figure 23 A). Further, the relationship between ROS, MDA, and DNA damage was observed for TiO₂ NPs (Figures 19, 21 and 23). As it was described previously, ROS may induce MDA, and then MDA may interact with DNA leading to oxidative DNA damage (Ayala et al., 2014 and papers there in; Zhang et al., 2018). This mechanism was already suggested in coelomocytes exposed to a pollutant (Zhang et al., 2018). However, the exposure of TiO₂ NPs (1, 10, and 100 µg mL⁻¹) with GFSk-S1 cells (primary cell line from goldfish skin) produced slight DNA damage. The same exposure to UVA increased significantly the toxicity (Hu et al., 2010; Reeves et al., 2008; Zhang et al., 2018). Hu et al. (2010) showed the same relation between ROS and DNA damage when the earthworms were exposed to 1 g TiO₂ NPs and ZnO NPs Kg⁻¹ soil in earthworms (Hu et al., 2010). Moreover, Zhu et al. (2020) suggested that long exposure to TiO₂ NPs can affect the carbohydrates, lipids and proteins synthesis (Zhu et al., 2020).

Remarkably, the results obtained for CuO NPs and CuSO₄ exposures confirmed Ayala et al. (2014) and paper there in. They suggested that the interaction of MDA with the nucleosides lead to the formation of the MDA-DNA adducts that can produce mutations or DNA damage (Ayala et al., 2014 and papers there in). It was observed that CuSO₄ exerted stronger DNA damage than the CuO NPs themselves (Figure 23 C). The Cu⁺² ions from CuSO₄ were more toxic than the same amount of Cu⁺² ions from CuO NPs. Similar

Chapter 5. Final Discussion

results were also observed in the study where trout erythrocytes were exposed to CuSO_4 and CuO NPs (Isani et al., 2013). Yang et al. (2017) observed that there was dose-response effects when MWCNTs were exposed to earthworms. They also suggested that comet assay was enough sensitive to detect DNA damages in coelomocytes (Yang et al., 2017). Similar results were also observed by Yirsaw et al. (2016). Yirsaw and colleagues observed the dose-response but also they suggested that the radicals generated during the Fenton-like redox were the precursors of the DNA damage (Yirsaw et al., 2016). The results (Figure 23) were in concordance with Mincarelli et al. (2016) and Yang et al. (2017). They observed dose-response effect when coelomocytes were exposed to H_2O_2 (Mincarelli et al., 2016). The genotoxicity was also observed in other metal NPs (nanomagnetite) exposed to A549 alveolar cells (Valdeiglesias et al., 2015, and papers there in). Different studies suggested that DNA damage is a sensitive endpoint for genotoxicity as the thesis results also showed (Mincarelli et al., 2016; Yang et al., 2017; Yirsaw et al., 2016).

TiO_2 NPs exposure did not show any statistically significant changes in phagocytic activity compared to control amoebocytes. The results observed (Figure 24 A) with TiO_2 NPs were in concordance with Bigorgne et al. (2012) results. They reported there were no changes in phagocytic activity after being exposed to 1, 2, 19, and $25 \mu\text{g mL}^{-1}$ TiO_2 NPs (Bigorgne et al., 2012). Although phagocytic activity was not suppressed, Bigorne and colleagues showed TiO_2 NPs inside the cytoplasm of coelomocytes so that the coelomocytes phagocytosed the TiO_2 NPs (Bigorgne et al., 2012). Gupta et al. (2014) suggested that the engulfment of ZnO NPs could be done through phagocytosis, macropinocytosis or scavenger receptors. However, they observed that there is still a lack of knowledge of the engulfment process in earthworms. They also showed that 50 nm size of NPs were engulfed faster than 100 nm size, which showed a relation between size NPs and their engulfment (Gupta et al., 2014). Brown et al. (2007) also suggested the size dependency because 20 nm nanotubes were easily phagocytosed while over 20 to 120 nm nanotubes were not entirely phagocytosed. However, RAW 264.7 cell line and mouse bone marrow derived macrophages showed a depletion of their phagocytic activity when they were exposed to $100 \mu\text{g mL}^{-1}$ TiO_2 NPs after 24 h (Chen et al., 2018).

Through the exposure of coelomocytes to TiO_2 NPs, CuO NPs and CuSO_4 , it observed that the phagocytic activity of the coelomocytes was mainly performed by the amoebocytes population (Bigorgne et al., 2012, 2011; Hayashi et al., 2012; Semerad et al., 2020). Furthermore, our results showed that only HAs exposed to the high concentration ($100 \mu\text{g Cu mL}^{-1}$) of CuO NPs and , HAs and GAs exposed to $100 \mu\text{g Cu mL}^{-1}$ of CuSO_4 caused a decrease in the phagocytic activity (Figure 24 A.2, A.3 and B.3). Similarly, Gautam and colleagues observed depletion of phagocytic activity at 14 days exposure to CuO NPs and CuSO_4 with *Metaphire postuma* (Gautam et al., 2018). They also observed there was no dose-response effect while our results showed that the greatest concentration of CuO NPs and CuSO_4 caused the largest decrease of phagocytic activity in coelomocytes (Gautam et al., 2018). Sémerad et al. (2020) observed that GAs were

Chapter 5. Final Discussion

sensitive to the ferric irons causing the depletion of the phagocytic activity in GAs. Further, exposure of coelomocytes to CuO NPs resulting in the suppression of their ability to phagocyte may be a severe problem as the defence mechanism against other potential pathogens may be blocked.

It is suggested that a cell death programme, also called apoptosis, could be developed due to ROS and NO species (Homa et al., 2016). It is known that exacerbated ROS species are able to damage the host cell (**5.5.1 ROS and NO production**), stimulating the apoptotic activity (Fuller-Espie et al., 2011; Homa et al., 2016; Tumminello and Fuller-espie, 2013). In the case of TiO₂ NPs, there were no statistical differences between control amoebocytes and the different exposures. However, it was detected remarkably higher percentage of HAs in early apoptosis than that of GAs (Figure 25 A.1 and B.1). The differences between HAs and GAs were not strongly observed in the late apoptosis until 24 h exposure (Figure 26 A.1 and B.1). In addition TiO₂ NPs did not cause oxidative stress (Figures 19 and 21). It corroborated the previous suggestion that oxidative stress could induce apoptosis (Fuller-Espie et al., 2011; Homa et al., 2016). Wu et al. (2010) also suggested that the type of TiO₂ NPs (anatase or rutile) could undergo to apoptosis or necrosis. Apoptotic PC12 cells occurred in the exposure to rutile TiO₂ NPs while apoptotic and necrotic PC12 cells happened in exposure to anatase TiO₂ NPs (Wu et al., 2010). Although TiO₂ NPs used in the thesis were anatase and rutile (4:1), neither necrotic nor apoptotic coelomocytes happened during the different times exposure.

Furthermore, Homa et al. (2016) suggested that the stimulation with fungi and bacteria products stimulated coelomocytes to undergo apoptotic pathways rather than disintegration (necrosis). Moreover, they observed an inverse relationship between the antioxidative system and the apoptotic pathway (Homa et al., 2016).

In the case of CuO NPs exposure, it was detected that the amoebocyte populations (HAs and GAs) tend to the disintegration (necrosis, Figure 27 A.2 and B.2) more than the apoptotic pathway. Then, it may be that pollutants like NPs or heavy metals could affect amoebocytes differently than fungi or bacteria products. Thus, the coelomocytes could behave differently according to the type of product they are exposed to, being apoptotic pathways to fungi and bacteria and disintegration for pollutants (NPs, heavy metals, chemical substances). Homa et al. (2016) showed the correlation between low NO and high apoptotic activity when coelomocytes were exposed to LPS. Thus, the observed late apoptosis and necrosis in the exposure to CuO NPs, and CuSO₄ were correlated to the ROS and MDA production (Figures 19 A2-3 and B.2-3 and 21 B-C). However, differences between HAs and GAs were observed where a higher percentage of HAs underwent late apoptosis than GAs (Figure 26 A.2-3 and B.2-3). While necrosis of HAs and GAs increased along the exposure time (Figure 27 A.2-3 and B.2-3), the late apoptosis decreased similarly (Figure 26). Sémerad et al. (2020) also showed that only the ferric ions induced the apoptosis in HAs and

Chapter 5. Final Discussion

GAs. Similarly to our results with CuO NPs and CuSO₄, Fuller-Espie et al. (2011) showed that phagocytosis and apoptosis were induced by oxidative stress. Sémerad et al. (2020) also corroborated this affirmation because they demonstrated the potential negative effect of ferric ion. Sémerad and colleagues showed the induction oxidative stress produced by ferric ion induced the depletion of phagocytosis and the increased of apoptosis in HAs and GAs (Semerad et al., 2020).

Amongst the immune biomarkers, phenoloxidase activity was carried out in coelomocytes exposed to 5 mg Ag Kg⁻¹ soil from Ag₂S NPs. It is one of the predominant immunology biomarkers shared between invertebrates (i.g. *Porcellio scaber*; Swartzwelter et al., 2021 and papers there in). The importance of this activity is the end product, melanin (**1.4.3.1. Cellular response**). Melanin and lipofuscein have been suggested as substances produced by coelomocytes to scavenge the free radicals released (Homa et al., 2013; Valembois et al., 1994). Valembois et al. (1994) showed that the brown bodies and the melanin product were formed by the encapsulation of foreign materials (i.e. aggregation of coelomocytes around foreign material like bacteria), which was confirmed by Homa et al (2016). The brown bodies were also observed during the cultivation of coelomocytes with CuO NPs (Figure 31).

After the exposure of coelomocytes to Ag₂S NPs, no NO production was detected, leading to non-activated phenoloxidase activity due to absence of free radicals to be eliminated. Compared with arthropods, PO is produced in a low amount and requires more time to be assessed (Procházková et al., 2006b). The results from measurement of phenoloxidase activity are in concordance with NO production. As no free radicals were produced, the prophenoloxidase cascade and the end product melanin were not produced because it was not needed to scavenge excessive free radicals that could damage the coelomocytes (**1.4 Earthworms Eisenia andrei**). Nevertheless, *Metaphire posthuma* earthworms increased the phenoloxidase activity after being exposed to CuO NPs and CuSO₄ (Gautam et al., 2018). They also observed increased production of NO, so then, it confirmed the association of the free radicals and phenoloxidase activity (Gautam et al., 2018). Thus, Ag₂S NPs could be eliminated in another way, or the immune system was not affected. Probably, the low solubility of Ag₂S NPs and the subsequently slow release of Ag⁺ ions lead to no production of NO (Figure 20) and no production of phenoloxidase activity (Figure 29).

5.7 mRNA analyses

Molecular studies have brought a new level of knowledge into the effects of pollutants on earthworms. Bodó et al. (2018) showed which molecules were highly expressed between amoebocytes and eleocytes. For example, there are molecules produced indistinctly by both populations of coelomocytes (metallothioneins, Fet/Lys, and CAT), but others are expressed only by amoebocytes (MnSOD, CuZnSOD,

Chapter 5. Final Discussion

lumbricin, MEKKI, PKC I; Bodó et al., 2018). Each relevant molecule assessed through the mRNA levels is associated with different functions: metal detoxification and metal stress (metallothioneins; Reinecke et al., 2006), suppression of oxidative stress (CAT, MnSOD, CuZnSOD), heavy metal detoxification (phytochelatin), immune molecules (Fet/Lys, CCF, lumbricin), and also related to earthworm cell homeostasis (MEKK I and PKC I; **1.4.3.1 Cellular response**). Interestingly, metal oxide NPs (TiO₂ NPs and CuO NPs) shared the upregulation of the metallothioneins after their exposure to cells at 1 and 10 µg mL⁻¹ concentrations. The metallothionein results observed after the exposure of cells to CuO NPs (Table 6) agreed with Mincarelli et al. (2019) who observed an increase of metallothioneins mRNA levels after 6 and 9 days of exposure. Moreover, TiO₂ NPs results (Table 5) were in concordance with Bigorgne et al. (2012; Hayashi et al., 2016; Oberdörster et al., 2006). They observed an increase of metallothioneins mRNA levels in cells exposed to 10 and 25 µg mL⁻¹ TiO₂ NPs after 12 h. In this case, coelomocytes were immunostimulated with LPS (500 ng mL⁻¹) for 5 h before the addition of TiO₂ NPs (Bigorgne et al., 2012). Moreover, after the upregulation of metallothioneins after 12 h, they also observed a decrease of metallothioneins after 24 h for 10 µg mL⁻¹ (Bigorgne et al., 2012). Our results with 10 µg mL⁻¹ TiO₂ NPs showed the same tendency. The upregulation of metallothioneins at 6 h after the cell exposure to TiO₂ NPs was followed by subsequent decrease at 24 h (Table 5).

Regarding the antioxidative system, 1 and 10 µg Cu mL⁻¹ CuO NPs exposure downregulated CAT and MnSOD, respectively (Table 6), while 10 µg mL⁻¹ TiO₂ NPs exposure downregulated MnSOD after 6 h (Table 5). MnSOD protects mitochondria and ATP production from oxidative stress, as demonstrated with macrophage RAW 264.7 cell line and primary rat hepatocytes (Bigorgne et al., 2012; Candas and Li, 2014; Chen et al., 2018; Natarajan et al., 2015). TiO₂ NPs may target mitochondria by inducing their malfunction (Chen et al., 2018).

In the case of CuSO₄, the effects were greater than in CuO NPs (Table 7). Although CAT and MnSOD protect macromolecules against free radicals, it did not observe their upregulation. Qui et al. (2018) and Roubalová et al. (2018) suggested that they are usually activated when the oxidative stress is caused by pollutants. Mincarelli et al. (2019) also observed that the cell exposure to Cu did not activate the earthworm's antioxidative system. Thus, the inactivated antioxidative system may force coelomocytes to undergo apoptosis or disintegration (Homa et al., 2016). The CAT is more effective in eliminating ROS produced by earthworms (Qi et al., 2018) and SOD is not the most suitable to eliminate the activated oxidative stress produced by metals and heavy metals pollutants (Honsi et al., 1999; Roubalová et al., 2018). The CAT can also scavenge the free radicals, but in the CuO NPs case, the Fenton-like copper redox may probably generate exacerbated free radicals that finally CAT could not eliminate.

Among the antioxidative stress molecules assessed, metallothioneins seem to be more efficient enzyme eliminating or detoxifying metal pollutants (NPs or not) compared to the antioxidative system. Thus, the

Chapter 5. Final Discussion

high earthworms' tolerance to metal pollutants could be derived from the activation and increased production of these enzymes (Ećimović et al., 2018; Hayashi et al., 2012; Hsin et al., 2008; Pham et al., 2013).

The mRNA levels of assorted AMPs assessed in cells exposed to CuO NPs were not altered. Exposure of cells to $10 \mu\text{g mL}^{-1}$ TiO₂ NPs led to the the induction of Fet/Lys, and lumbricin mRNA levels after 6 h, was in concordance with Bigorgne et al. (2012). They detected an upregulation of fetidin after being exposed to $10 \mu\text{g mL}^{-1}$ TiO₂ NPs for 12 h (Bigorgne et al., 2012). Mincarelli et al. (2019) also suggested that the exposure to Cu developed the induction of AMPs through the activation of the signalling cascade and the induction of TLR (Figure 6). Contrary to Mincarelli et al. (2019) TLR induction, Bigorne et al. (2012) showed CCF suppression after coelomocytes exposure to $10 \mu\text{g mL}^{-1}$ TiO₂ NPs after 4 h (PRR; Figure 26). However, TLR or CCF mRNA levels were not assessed after the exposure to TiO₂ NPs and CuO NPs in this thesis. The reason is that there were no LPS-free NPs, so then, it could not guarantee that induction or suppression of the AMPs and the PRRs were caused by NPs themselves.

Remarkably, the higher statistical differences in the mRNA levels of immunologically relevant molecules were observed after the exposure to Cu⁺² ions from control (CuSO₄) than by NPs themselves (Table 6 and 7). Therefore, it could hypothesize that some pollutants (indistinctly if they are NPs) could act as AMPs (lumbricin, Fet/Lys) inducers, as demonstrated by Mincarelli et al. (2019). Hayashi and colleagues already showed upregulation of PKC 1 (signal transducer; **1.4.3.1 Cellular response**) by exposure of coelomocytes to Ag NPs which was contrary to our results from the exposure to CuO NPs, Cu⁺² ions control, and $10 \mu\text{g mL}^{-1}$ TiO₂ NPs showing downregulation (Table 5-7; Hayashi et al., 2016). In the case of exposure with $10 \mu\text{g mL}^{-1}$ TiO₂ NPs, the PKC 1 downregulation was observed after 6 and 24 h (Table 5). The PKC 1 is associated with cellular homeostasis and cell proliferation signalling cascade (Bodó et al., 2018; Homa et al., 2013). Thus, the observed PKC 1 downregulation would suggest that coelomocytes had destabilized homeostasis after the exposure with TiO₂ NPs. MEKK 1 was upregulated upon the exposure to 1 and $10 \mu\text{g mL}^{-1}$ TiO₂ NPs after 24 and 6 h, respectively (Table 5). MEKK 1 is related to the MAP cascade, and it participates in cellular processes, including stress signalling (Bodó et al., 2018; Hayashi et al., 2012) .

Nevertheless, mRNA analyses were not performed during the exposure with Ag₂S NPs, but it was focused on the phenoloxidase activity related to the recognition of foreign material by CCF, which leads to the encapsulation and elimination (Figure 6). In the end, the molecular analyses supported the cellular studies performed along with the thesis work. However, there is still a lack of knowledge regarding downstream signalling in earthworms and their immune system.

Noteworthy, the molecular techniques bring a new perspective to toxicity assessment. So, the toxicity of the pollutants could be related to the induction of AMP and activation/suppression of the immune and antioxidative systems. In conclusion, it was observed that although strong effects like growth or mortality

Chapter 5. Final Discussion

did not occur, it does not mean that the earthworm is healthy and other lethal or sub-lethal may not occur in the long term. Some processes like phagocytosis, DNA damages, activation of antioxidative system could be undergoing on behalf, and these new biomarkers could bring up the information needed to understand the toxicity mechanisms.

5.8 Weight loss and mortality

During *in vivo* exposure there was no mortality after 14 days of exposure to 5 mg Ag Kg⁻¹ from Ag₂S NPs. The results were in agreement with Baccaro et al. (2018), who could not demonstrate mortality. Apart from the mortality, weight changes were detected. The control earthworms were the only ones that increased their weight after 14 days (Figure 30). The earthworms exposed to Ag₂S NPs had decreased their weight after 14 days of exposure which was in line with another study where the metal oxide NPs (CuO NPs) had a similar effect (Tatsi et al., 2018). However, not every metal oxide NPs decreases the weight of earthworms' *in vivo* experiments. There are others like SnO₂ (346.6 ± 18.2 mg Kg⁻¹ dry food) and CeO₂ (26.1 ± 2.9 mg Kg⁻¹ dry food) that do not exert any adverse effect (Carbone et al., 2016). Reproduction test neither mortality was observed when *Eisenia fetida* earthworms were exposed to CeO₂ NPs (41, 102, 256, 640, 1600, 4000 and 10 000 mg Ce Kg⁻¹ soil) while LC₅₀ survival was established for the cerium nitrate (Ce ions control) at 317.82 ± 314.7 mg Ce Kg⁻¹ soil and LC₅₀ reproduction was 294.6 ± 72.095 mg Ce Kg⁻¹ soil (Lahive et al., 2014). This could explain our results and the results of decreased weight reported by Curieses et al. (2017). Remarkably, the control ions AgNO₃ used to observe whether the effects were from Ag⁺ ions or NPs (Figure 30) did not decrease the earthworm's weight. Then, it could suggest that the weight loss from Ag₂S NPs was coming from the NPs effect. Moreover, another study suggested that no growth or production in earthworms would not mean the earthworm is healthy (Zhu et al., 2020). Thus, they showed that there were transcriptomic and metabolic changes occurring in the earthworm during the exposure (Zhu et al., 2020).

5.9 Possible observed route of toxicity

Along the thesis, It was assessed the different toxicity mechanisms that lead to toxicity inside the cells, either *in vitro* or *in vivo*, with different metallic NPs. One interesting mechanism observed is related to oxidative stress, as it could observe clearly through the exposure to CuO NPs. The transmission and scanning electron microscope (TEM and SEM) showed that coelomocytes were able to engulf the CuO NPs due to their size, observed through the TEM image (Figure 8 B), where CuO NPs were detected at 2 h exposure. Thus, phagocytes play an essential role due to their ability of uptaking foreign material (fungi, bacteria, pollutants) and excreting it from earthworms. Although some NPs could be toxic, like Ag and Cd NPs, others can be potentially toxic only at higher concentrations (Fe, Zinc, Cu; Sukhanova et al., 2018 and

Chapter 5. Final Discussion

papers there in). Still, the predominant role of toxicity is the degradation of NPs (oxidation, dissolution processes) that would leak the ions.

Cornelis et al. and paper there in (2014) suggested that pH could be essential in the dissolution of metallic NPs. Thus, the NPs engulfed by phagocytic cells may cause the Trojan-horse effect (Figure 33), and due to the changes in pH in the cell, the metallic ions may be released. The example is seen in the study of CuO NPs; after 2 h of exposure, coelomocytes uptook the CuO NPs and several damages were observed. It can start as lipid peroxidation which can be generated through the free radicals derived from Fenton-like redox copper (Wang et al., 2013). Then, the MDA may develop the subsequent damages observed (DNA damages, high apoptosis, and necrosis). It was analysed that $100 \mu\text{g Cu mL}^{-1}$ CuO NPs required up to 24 h to release the metallic ions. Thus, the metallic ions (Cu^{+2}) may trigger the observed oxidative stress and the upcoming damage.

After the exposure to CuO NPs, coelomocytes upregulated the mRNA levels of metallothioneines. However, the upregulation was not enough to suppress the oxidative metal stress leading to lipid peroxidation and DNA damages.

The HAs and GAs, whose function is to phagocytose, are the most sensitive cells to metal NPs. According to this sensitiveness, the immune system may be compromised. Although the Trojan-horse effect (Figure 33) could occur in metallic NPs, not all of them are susceptible. TiO_2 and Ag_2S NPs had low solubility and limited ions released resulting in lower toxic potential. TiO_2 NPs showed no oxidative stress, and so adverse effects were not observed. Studies with different NPs suggested that the main precursors of adverse effects of NPs comes from free radicals produced during the NPs exposure with the cells (Boraschi et al., 2020 and papers there in; Curieses Silvana et al., 2017; Gautam et al., 2018; Reeves et al., 2008; Swartzwelter et al., 2021 and papers there in). The free radicals are exerted when the cells are under stress.

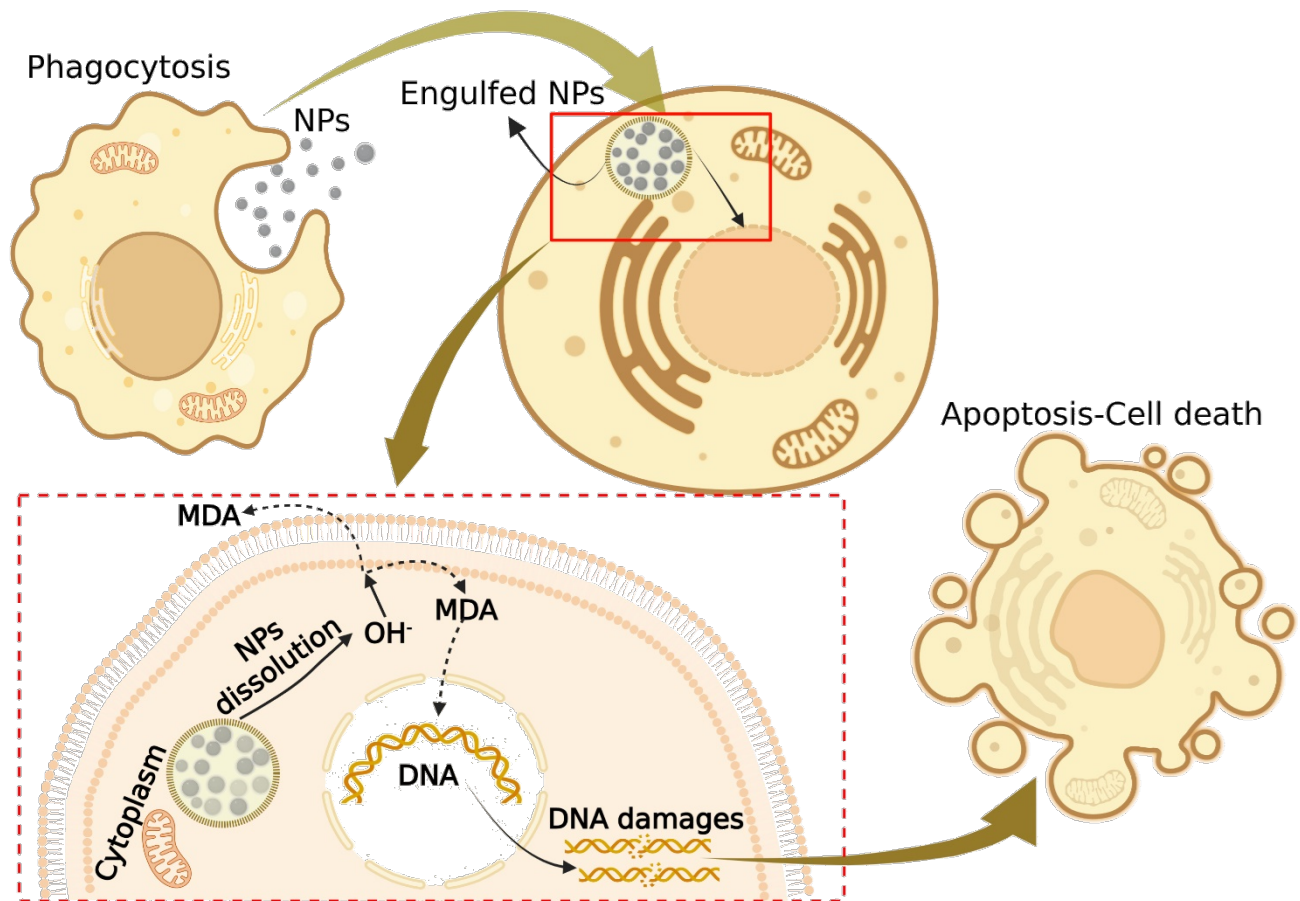


Figure 33. Trojan-horse effect. Described image of Trojan-Horse effect caused by the ingested NPs in the coelomocytes. The Trojan-horse was caused by oxidative stress damages. Created with BioRender.com

To sum up, the toxicity of metallic NPs probably should be taken carefully. The medium they are exposed to, the conditions (irradiation, pH, DOM, etc.), and processes such as dissolution, oxidation, and sulfidation can influence the toxicity. Like Sukhanova et al. (2018) it was observed that the released ions seem to be the likely precursors to the observed toxicity and subsequent damage in earthworm cells. However, the appearance of the "Trojan horse effect" opens a new way to understand internal exposure and toxicity and reveals the importance of combining *in vitro/in vivo* studies. Consequently, the knowledge of the various processes that occur in the earthworm before assuring whether NP are toxic or not should be improved.

5.10 Future perspectives

Immunotoxicity seems to be an important avenue to understand pollutant effects on earthworms. When the immune system is compromised, animals could die due to their incapacity to eliminate other potential

Chapter 5. Final Discussion

pathogens that would injure the animal. Then, the combination of *in vitro/in vivo* testing leads to new opportunities to discerning between direct toxic effects or pathogen-mediated effects in the animal in real-time. The *in vitro* approach is focused on understanding each cell and its function, which could vary, being some of the more sensitive (HAs) than the others (GAs). Thus, how the cells behave (molecular and cellular level) and how the earthworm behaves would broaden the comprehension of toxicity. Further studies regarding coelomocytes, their function and their use as new toxicity biomarkers should be considered.

Hence, the NP risk assessment should include these new biomarkers to better comprehend earthworms' responses in the environment. During this PhD thesis, it was observed that earthworms' mortality did not occur although coelomocytes were strongly affected by the pollutants assessed, e.g. CuO NPs. Therefore, biomarkers related to coelomocytes assessment should be added to have a broader understanding of pollutant hazards.

Chapter 6



Conclusions

6. Conclusions

The main conclusions that can be drawn from this thesis are:

1. The cultivation medium for coelomocytes is RPMI 1640 with adjusted osmolarity (R-RPMI 1640), including 5% FBS, 1 M HEPES, 100 mM Na-pyruvate, 100 mg mL⁻¹ gentamycin and antibiotic-antimycotic solution. The optimal culture conditions are darkness and 20 °C.
2. Among the battery of biomarkers used, the most reliable and sensitive ones are reactive oxygen species (ROS) production, malondialdehyde production (MDA), phagocytic activity, apoptosis, and phenoloxidase activity.
3. HA and GA subpopulations showed different sensitiveness in the phagocytic activity and ROS production. HAs were the most sensitive ones in these assays when they were exposed to the chosen NPs.
4. The main defence mechanisms of HAs and GAs include the provision of several enzymes shutting down the ROS species and other free radicals. Remarkably, metallothioneins seem to be promising proteins helping the cells in overcoming the excess production of ROS and other free radicals caused by the metal pollutants and metal NPs.
5. Assessment of the battery of cellular and molecular biomarkers revealed that the earthworms are resistant against NPs. However, in some cases, the NPs may behave as a "Trojan-horse" (**5.9 Possible observed route of toxicity**), leading to more considerable damage of the earthworms' cells and thus, the whole animal.. In these toxicity mechanisms, oxidative stress seems to be the precursor.
6. The risk in the earthworm's immune system would rely on coelomocytes' ability to phagocyte the foreign material. Then, phagocytic coelomocytes are the main target of metal NPs leading to the suppression of the earthworm immune system and, indirectly, the death of the earthworms.

Chapter 6. Conclusions

7. Environmentally relevant concentrations of NPs may affect the earthworms if there is bioaccumulation of these NPs in their tissues. The studies performed here included short-term exposure periods, so long term exposures may aggravate bioaccumulation and risks for soil organisms.

Overall we can conclude that metal oxide NPs and their transformation products affect earthworm coelomocytes, being HAs and GAs target coelomocytes. Therefore, the no-harmful effects observed is mostly related to the physicochemical characteristics of the NPs. However, further studies should be performed to observe if the prolonged exposures in the soil and cultivation medium would allow the slow release of ions, which seem to be the precursors of the observed damage in ROS, MDA, and DNA.

Chapter 7



References

7. References

- Abbas, A.K., Lichtman, A.H., Pillai, S., 2021. Cellular and Molecular Immunology, 10th Edition. ed. Elsevier.
- Abbas, Q., Yousaf, B., Amina, Ali, M.U., Munir, M.A.M., El-Naggar, A., Rinklebe, J., Naushad, M., 2020. Transformation pathways and fate of engineered nanoparticles (ENPs) in distinct interactive environmental compartments: A review. *Environ. Int.* 138, 105646. <https://doi.org/10.1016/j.envint.2020.105646>
- Aggarwal, B.B., Kohr, W.J., Hass, P.E., Moffat, B., Spencer, S.A., Henzel, W.J., Bringman, T.S., Nedwin, G.E., Goeddel, D. V, Harkins, R.N., 1985. Human tumor necrosis factor. Production, purification, and characterization. *J. Biol. Chem.* 260, 2345–2354.
- Alijagic, A., Benada, O., Kofroňová, O., Cigna, D., Pinsino, A., 2019. Sea Urchin Extracellular Proteins Design a Complex Protein Corona on Titanium Dioxide Nanoparticle Surface Influencing Immune Cell Behavior. *Front. Immunol.* <https://doi.org/10.3389/fimmu.2019.02261>
- Alijagic, A., Gaglio, D., Napodano, E., Russo, R., Costa, C., Benada, O., Kofroňová, O., Pinsino, A., 2020. Titanium dioxide nanoparticles temporarily influence the sea urchin immunological state suppressing inflammatory-related gene transcription and boosting antioxidant metabolic activity. *J. Hazard. Mater.* <https://doi.org/10.1016/j.jhazmat.2019.121389>
- Alijagic, A., Pinsino, A., 2017. Probing safety of nanoparticles by outlining sea urchin sensing and signaling cascades. *Ecotoxicol. Environ. Saf.* <https://doi.org/10.1016/j.ecoenv.2017.06.060>
- Ayala, A., Muñoz, M.F., Argüelles, S., 2014. Lipid peroxidation: Production, metabolism, and signaling mechanisms of malondialdehyde and 4-hydroxy-2-nonenal. *Oxid. Med. Cell. Longev.* 2014. <https://doi.org/10.1155/2014/360438>
- Azhdarzadeh, M., Saei, A.A., Sharifi, S., Hajipour, M.J., Alkilany, A.M., Sharifzadeh, M., Ramazani, F., Laurent, S., Mashaghi, A., Mahmoudi, M., 2015. Nanotoxicology: advances and pitfalls in research methodology. *Nanomedicine (Lond)*. 10, 2931–2952. <https://doi.org/10.2217/nnm.15.130>
- Baccaro, M., Undas, A.K., De Vriendt, J., Van Den Berg, J.H.J., Peters, R.J.B., Van Den Brink, N.W., 2018. Ageing, dissolution and biogenic formation of nanoparticles: How do these factors affect the uptake kinetics of silver nanoparticles in earthworms? *Environ. Sci. Nano* 5, 1107–1116. <https://doi.org/10.1039/c7en01212h>
- Barhoum, A., García-Betancourt, M.L., Jeevanandam, J., Hussien, E.A., Mekkawy, S.A., Mostafa, M., Omran, M.M., S Abdalla, M., Bechelany, M., 2022. Review on Natural, Incidental, Bioinspired, and Engineered Nanomaterials: History, Definitions, Classifications, Synthesis, Properties, Market, Toxicities, Risks, and Regulations. *Nanomater. (Basel, Switzerland)* 12. <https://doi.org/10.3390/nano12020177>

Chapter 7. References

- Beschin, A., Bilej, M., Hanssens, F., Raymakers, J., Van Dyck, E., Revets, H., Brys, L., Gomez, J., De Baetselier, P., Timmermans, M., 1998. Identification and cloning of a glucan- and lipopolysaccharide-binding protein from *Eisenia foetida* earthworm involved in the activation of prophenoloxidase cascade. *J. Biol. Chem.* 273, 24948–24954. <https://doi.org/10.1074/jbc.273.38.24948>
- Beschin, A., Bilej, M., Magez, S., Lucas, R., De Baetselier, P., 2004. Functional convergence of invertebrate and vertebrate cytokine-like molecules based on a similar lectin-like activity. *Prog. Mol. Subcell. Biol.* 34, 145–163. https://doi.org/10.1007/978-3-642-18670-7_6
- Bigorgne, E., Foucaud, L., Caillet, C., Giambérini, L., Nahmani, J., Thomas, F., Rodius, F., 2012. Cellular and molecular responses of *E. fetida* coelomocytes exposed to TiO₂ nanoparticles. *J. Nanoparticle Res.* 14. <https://doi.org/10.1007/s11051-012-0959-5>
- Bigorgne, E., Foucaud, L., Lapied, E., Labille, J., Botta, C., Sirguy, C., Falla, J., Rose, J., Joner, E.J., Rodius, F., Nahmani, J., 2011. Ecotoxicological assessment of TiO₂ byproducts on the earthworm *Eisenia fetida*. *Environ. Pollut.* 159, 2698–2705. <https://doi.org/10.1016/j.envpol.2011.05.024>
- Bilej, M., Procházková, P., Šilerová, M., Josková, R., 2010. Earthworm immunity. *Adv. Exp. Med. Biol.* https://doi.org/10.1007/978-1-4419-8059-5_4
- Bilej, M., Rossmann, P., Šinkora, M., Hanušová, R., Beschin, A., Raes, G., De Baetselier, P., 1998. Cellular expression of the cytolytic factor in earthworms *Eisenia foetida*. *Immunol. Lett.* 60, 23–29. [https://doi.org/https://doi.org/10.1016/S0165-2478\(97\)00127-2](https://doi.org/https://doi.org/10.1016/S0165-2478(97)00127-2)
- Bodó, K., Boros, Á., Rumpler, É., Molnár, L., Böröcz, K., Németh, P., Engelmann, P., 2019. Identification of novel lumbricin homologues in *Eisenia andrei* earthworms. *Dev. Comp. Immunol.* 90, 41–46. <https://doi.org/10.1016/j.dci.2018.09.001>
- Bodó, K., Ernszt, D., Németh, P., Engelmann, P., 2018. Distinct immune-and defense-related molecular fingerprints in separated coelomocyte subsets of *Eisenia andrei* earthworms. *Invertebr. Surviv. J.* 15, 338–345.
- Bondarenko, O., Juganson, K., Ivask, A., Kasemets, K., Mortimer, M., Kahru, A., 2013. Toxicity of Ag, CuO and ZnO nanoparticles to selected environmentally relevant test organisms and mammalian cells *in vitro*: a critical review. *Arch. Toxicol.* 87, 1181–1200. <https://doi.org/10.1007/s00204-013-1079-4>
- Boraschi, D., Aljagic, A., Auguste, M., Barbero, F., Ferrari, E., Hernadi, S., Mayall, C., Michelini, S., Navarro Pacheco, N.I., Prinelli, A., Swart, E., Swartzwelter, B.J., Bastús, N.G., Canesi, L., Drobne, D., Duschl, A., Ewart, M.-A., Horejs-Hoeck, J., Italiani, P., Kemmerling, B., Kille, P., Prochazkova, P., Puentes, V.F., Spurgeon, D.J., Svendsen, C., Wilde, C.J., Pinsino, A., 2020. Addressing Nanomaterial Immunosafety by Evaluating Innate Immunity across Living Species. *Small* 16, e2000598. <https://doi.org/10.1002/smll.202000598>

Chapter 7. References

- Bouché, M.B., 1977. Strategies lombriciennes. *Ecol. Bull.* 122–132.
- Brown, D.M., Kinloch, I.A., Bangert, U., Windle, A.H., Walter, D.M., Walker, G.S., Scotchford, C.A., Donaldson, K., Stone, V., 2007. An *in vitro* study of the potential of carbon nanotubes and nanofibres to induce inflammatory mediators and frustrated phagocytosis. *Carbon N. Y.* 45, 1743–1756. <https://doi.org/10.1016/j.carbon.2007.05.011>
- Bruhn, H., Winkelmann, J., Andersen, C., Andrä, J., Leippe, M., 2006. Dissection of the mechanisms of cytolytic and antibacterial activity of lysenin, a defence protein of the annelid *Eisenia fetida*. *Dev. Comp. Immunol.* 30, 597–606. <https://doi.org/https://doi.org/10.1016/j.dci.2005.09.002>
- Candas, D., Li, J.J., 2014. MnSOD in oxidative stress response-potential regulation via mitochondrial protein influx. *Antioxidants Redox Signal.* 20, 1599–1617. <https://doi.org/10.1089/ars.2013.5305>
- Carbone, S., Hertel-aas, T., Joner, E.J., Oughton, D.H., 2016. Chemosphere Bioavailability of CeO₂ and SnO₂ nanoparticles evaluated by dietary uptake in the earthworm *Eisenia fetida* and sequential extraction of soil and feed. *Chemosphere* 162, 16–22. <https://doi.org/10.1016/j.chemosphere.2016.07.044>
- CE, 2012. Second Regulatory Review on Nanomaterials. Types and uses of nanomaterials, including safety aspects.
- Chen, Q., Wang, N., Zhu, M., Lu, J., Zhong, H., Xue, X., Guo, S., Li, M., Wei, X., Tao, Y., Yin, H., 2018. TiO₂ nanoparticles cause mitochondrial dysfunction, activate inflammatory responses, and attenuate phagocytosis in macrophages: A proteomic and metabolomic insight. *Redox Biol.* 15, 266–276. <https://doi.org/10.1016/j.redox.2017.12.011>
- Cho, J.H., Park, C.B., Yoon, Y.G., Kim, S.C., 1998. Lumbricin I, a novel proline-rich antimicrobial peptide from the earthworm: purification, cDNA cloning and molecular characterization. *Biochim. Biophys. Acta* 1408, 67–76. [https://doi.org/10.1016/s0925-4439\(98\)00058-1](https://doi.org/10.1016/s0925-4439(98)00058-1)
- Çiğerci, İ.H., Ali, M.M., Kaygısız, Ş.Y., Liman, R., 2016. Genotoxicity assessment of cobalt chloride in *Eisenia hortensis* earthworms coelomocytes by comet assay and micronucleus test. *Chemosphere* 144, 754–757. <https://doi.org/10.1016/j.chemosphere.2015.09.053>
- Cook, S.R., Sperratore, M.M., Fuller-espie, S.L., 2015. Nitric oxide production in celomocytes of the earthworm *Eisenia hortensis* following bacterial challenge 46–65.
- Cornelis, G., Hund-Rinke, K., Kuhlbusch, T., Van Den Brink, N., Nickel, C., 2014. Fate and Bioavailability of Engineered Nanoparticles in Soils: A Review. Interactions within natural soils have often been neglected when assessing fate and bioavailability of engineered nanomaterials (ENM) in soils. This review combines patchwise ENM resea. *Crit. Rev. Environ. Sci. Technol.* 44, 2720–2764.

Chapter 7. References

<https://doi.org/10.1080/10643389.2013.829767>

Courtois, P., Rorat, A., Lemiere, S., Guyoneaud, R., Attard, E., Levard, C., Vandembulcke, F., 2019. Ecotoxicology of silver nanoparticles and their derivatives introduced in soil with or without sewage sludge: A review of effects on microorganisms, plants and animals. *Environ. Pollut.* 253, 578–598. <https://doi.org/10.1016/j.envpol.2019.07.053>

Curieses Silvana, P., García-Velasco, N., Urionabarrenetxea, E., Sáenz María, E., Bilbao, E., Di Marzio Walter, D., Soto, M., 2017. Responses to silver nanoparticles and silver nitrate in a battery of biomarkers measured in coelomocytes and in target tissues of *Eisenia fetida* earthworms. *Ecotoxicol. Environ. Saf.* 141, 57–63. <https://doi.org/10.1016/j.ecoenv.2017.03.008>

Davidson, S.K., Stahl, D.A., 2006. Transmission of nephridial bacteria of the earthworm *Eisenia fetida*. *Appl. Environ. Microbiol.* 72, 769–775. <https://doi.org/10.1128/AEM.72.1.769-775.2006>

Dvořák, J., Mančíková, V., Pižl, V., Elhottová, D., Silerová, M., Roubalová, R., Skanta, F., Procházková, P., Bilej, M., 2013. Microbial environment affects innate immunity in two closely related earthworm species *Eisenia andrei* and *Eisenia fetida*. *PLoS One* 8, e79257–e79257. <https://doi.org/10.1371/journal.pone.0079257>

Ečimović, S., Velki, M., Vuković, R., Štolfa Čamagajevac, I., Petek, A., Bošnjaković, R., Grgić, M., Engelmann, P., Bodó, K., Filipović-Marijić, V., Ivanković, D., Erk, M., Mijošek, T., Lončarić, Z., 2018. Acute toxicity of selenate and selenite and their impacts on oxidative status, efflux pump activity, cellular and genetic parameters in earthworm *Eisenia andrei*. *Chemosphere* 212, 307–318. <https://doi.org/https://doi.org/10.1016/j.chemosphere.2018.08.095>

Engelmann, P., Hayashi, Y., Bodó, K., Ernszt, D., Somogyi, I., Steib, A., Orbán, J., Pollák, E., Nyitrai, M., Németh, P., Molnár, L., 2016. Phenotypic and functional characterization of earthworm coelomocyte subsets: Linking light scatter-based cell typing and imaging of the sorted populations. *Dev. Comp. Immunol.* 65, 41–52. <https://doi.org/10.1016/j.dci.2016.06.017>

Fuller-Espie, S.L., Bearoff, F.M., Minutillo, M.A., 2011. Exposure of coelomocytes from the earthworm *Eisenia hortensis* to Cu, Cd, and dimethylbenz[a]anthracene: An *in vitro* study examining reactive oxygen species production and immune response inhibition. *Pedobiologia (Jena)*. 54, S31–S36. <https://doi.org/10.1016/j.pedobi.2011.09.009>

Garcia-Velasco, N., Gandariasbeitia, M., Irizar, A., Soto, M., 2016. Uptake route and resulting toxicity of silver nanoparticles in *Eisenia fetida* earthworm exposed through Standard OECD Tests. *Ecotoxicology* 25, 1543–1555. <https://doi.org/10.1007/s10646-016-1710-2>

Garcia-Velasco, N., Irizar, A., Urionabarrenetxea, E., Scott-Fordsmand, J.J., Soto, M., 2019. Selection of an

Chapter 7. References

- optimal culture medium and the most responsive viability assay to assess Ag NPs toxicity with primary cultures of *Eisenia fetida* coelomocytes. *Ecotoxicol. Environ. Saf.* 183, 109545. <https://doi.org/10.1016/j.ecoenv.2019.109545>
- Gautam, A., Ray, A., Mukherjee, S., Das, Santanu, Pal, K., Das, Subhadeep, Karmakar, P., Ray, M., Ray, S., 2018. Immunotoxicity of copper nanoparticle and copper sulfate in a common Indian earthworm. *Ecotoxicol. Environ. Saf.* 148, 620–631. <https://doi.org/10.1016/j.ecoenv.2017.11.008>
- Gupta, S., Kushwah, T., Yadav, S., 2014. Earthworm coelomocytes as nanoscavenger of ZnO NPs. *Nanoscale Res. Lett.* 9, 259. <https://doi.org/10.1186/1556-276X-9-259>
- Gupta, S.M., Tripathi, M., 2011. A review of TiO₂ nanoparticles. *Chinese Sci. Bull.* 56, 1639–1657. <https://doi.org/10.1007/s11434-011-4476-1>
- Hayashi, Y., Engelmann, P., Foldbjerg, R., Szabó, M., Somogyi, I., Pollák, E., Molnár, L., Autrup, H., Sutherland, D.S., Scott-Fordsmand, J., Heckmann, L.-H., 2012. Earthworms and humans *in vitro*: characterizing evolutionarily conserved stress and immune responses to silver nanoparticles. *Environ. Sci. Technol.* 46, 4166–4173. <https://doi.org/10.1021/es3000905>
- Hayashi, Y., Miclaus, T., Engelmann, P., Autrup, H., Sutherland, D.S., Scott-Fordsmand, J.J., 2016. Nanosilver pathophysiology in earthworms: Transcriptional profiling of secretory proteins and the implication for the protein corona. *Nanotoxicology* 10, 303–311. <https://doi.org/10.3109/17435390.2015.1054909>
- Hayashi, Y., Miclaus, T., Scavenius, C., Kwiatkowska, K., Sobota, A., Engelmann, P., Scott-Fordsmand, J.J., Enghild, J.J., Sutherland, D.S., 2013. Species differences take shape at nanoparticles: Protein corona made of the native repertoire assists cellular interaction. *Environ. Sci. Technol.* 47, 14367–14375. <https://doi.org/10.1021/es404132w>
- Homa, J., Stalmach, M., Wilczek, G., Kolaczkowska, E., 2016. Effective activation of antioxidant system by immune-relevant factors reversely correlates with apoptosis of *Eisenia andrei* coelomocytes. *J. Comp. Physiol. B.* 186, 417–430. <https://doi.org/10.1007/s00360-016-0973-5>
- Homa, J., Zorska, A., Wesolowski, D., Chadzinska, M., 2013. Dermal exposure to immunostimulants induces changes in activity and proliferation of coelomocytes of *Eisenia andrei*. *J. Comp. Physiol. B Biochem. Syst. Environ. Physiol.* 183, 313–322. <https://doi.org/10.1007/s00360-012-0710-7>
- Honsi, T.G., Hoel, L., Stenersen, J. V., 1999. Non-inducibility of antioxidant enzymes in the earthworms *Eisenia veneta* and *E. fetida* after exposure to heavy metals and paraquat. *Pedobiologia (Jena)*. 43, 652–657.
- Hsin, Y.-H., Chen, C.-F., Huang, S., Shih, T.-S., Lai, P.-S., Chueh, P.J., 2008. The apoptotic effect of nanosilver

Chapter 7. References

is mediated by a ROS- and JNK-dependent mechanism involving the mitochondrial pathway in NIH3T3 cells. *Toxicol. Lett.* 179, 130–139. <https://doi.org/https://doi.org/10.1016/j.toxlet.2008.04.015>

Hu, C.W., Li, M., Cui, Y.B., Li, D.S., Chen, J., Yang, L.Y., 2010. Toxicological effects of TiO₂ and ZnO nanoparticles in soil on earthworm *Eisenia fetida*. *Soil Biol. Biochem.* 42, 586–591. <https://doi.org/10.1016/j.soilbio.2009.12.007>

Huerta-García, E., Pérez-Arizti, J.A., Márquez-Ramírez, S.G., Delgado-Buenrostro, N.L., Chirino, Y.I., Iglesias, G.G., López-Marure, R., 2014. Titanium dioxide nanoparticles induce strong oxidative stress and mitochondrial damage in glial cells. *Free Radic. Biol. Med.* 73, 84–94. <https://doi.org/https://doi.org/10.1016/j.freeradbiomed.2014.04.026>

Isani, G., Falcioni, M.L., Barucca, G., Sekar, D., Andreani, G., Carpenè, E., Falcioni, G., 2013. Comparative toxicity of CuO nanoparticles and CuSO₄ in rainbow trout. *Ecotoxicol. Environ. Saf.* 97, 40–46. <https://doi.org/https://doi.org/10.1016/j.ecoenv.2013.07.001>

Josková, R., Silerová, M., Procházková, P., Bilej, M., 2009. Identification and cloning of an invertebrate-type lysozyme from *Eisenia andrei*. *Dev. Comp. Immunol.* 33, 932–938. <https://doi.org/10.1016/j.dci.2009.03.002>

Kaegi, R., Voegelin, A., Ort, C., Sinnet, B., Thalmann, B., Krismer, J., Hagendorfer, H., Elumelu, M., Mueller, E., 2013. Fate and transformation of silver nanoparticles in urban wastewater systems. *Water Res.* 47, 3866–3877. <https://doi.org/10.1016/j.watres.2012.11.060>

Kah, M., Kookana, R.S., Gogos, A., Bucheli, T.D., 2018. A critical evaluation of nanopesticides and nanofertilizers against their conventional analogues. *Nat. Nanotechnol.* 13, 677–684. <https://doi.org/10.1038/s41565-018-0131-1>

Keller, A.A., Adeleye, A.S., Conway, J.R., Garner, K.L., Zhao, L., Cherr, G.N., Hong, J., Gardea-Torresdey, J.L., Godwin, H.A., Hanna, S., Ji, Z., Kaweeteerawat, C., Lin, S., Lenihan, H.S., Miller, R.J., Nel, A.E., Peralta-Videa, J.R., Walker, S.L., Taylor, A.A., Torres-Duarte, C., Zink, J.I., Zuverza-Mena, N., 2017. Comparative environmental fate and toxicity of copper nanomaterials. *NanoImpact* 7, 28–40. <https://doi.org/https://doi.org/10.1016/j.impact.2017.05.003>

Keller, A.A., Lazareva, A., 2014. Predicted Releases of Engineered Nanomaterials: From Global to Regional to Local. *Environ. Sci. Technol. Lett.* 1, 65–70. <https://doi.org/10.1021/ez400106t>

Knies, U.E., Behrendorf, H.A., Mitchell, C.A., Deutsch, U., Risau, W., Drexler, H.C., Clauss, M., 1998. Regulation of endothelial monocyte-activating polypeptide II release by apoptosis. *Proc. Natl. Acad. Sci. U. S. A.* 95, 12322–12327. <https://doi.org/10.1073/pnas.95.21.12322>

Chapter 7. References

- Koziol, B., Markowicz, M., Kruk, J., Plytycz, B., 2006. Riboflavin as a Source of Autofluorescence in *Eisenia fetida* Coelomocytes. *Photochem. Photobiol.* 82, 570. <https://doi.org/10.1562/2005-11-23-ra-738>
- Lahive, E., Jurkschat, K., Shaw, B.J., Handy, R.D., Spurgeon, D.J., Svendsen, C., 2014. Toxicity of cerium oxide nanoparticles to the earthworm *Eisenia fetida*: Subtle effects. *Environ. Chem.* 11, 268–278. <https://doi.org/10.1071/EN14028>
- Liang, J., Xia, X., Zhang, W., Zaman, W.Q., Lin, K., Hu, S., Lin, Z., 2017. The biochemical and toxicological responses of earthworm (*Eisenia fetida*) following exposure to nanoscale zerovalent iron in a soil system. *Environ. Sci. Pollut. Res. Int.* 24, 2507–2514. <https://doi.org/10.1007/s11356-016-8001-6>
- Limbach, L.K., Wick, P., Manser, P., Grass, R.N., Bruinink, A., Stark, W.J., 2007. Exposure of engineered nanoparticles to human lung epithelial cells: influence of chemical composition and catalytic activity on oxidative stress. *Environ. Sci. Technol.* 41, 4158–4163. <https://doi.org/10.1021/es062629t>
- Liu, R., Lal, R., 2015. Potentials of engineered nanoparticles as fertilizers for increasing agronomic productions. *Sci. Total Environ.* 514, 131–139. <https://doi.org/10.1016/j.scitotenv.2015.01.104>
- Lund, M., Kjeldsen, K., Schramm, A., 2014. The earthworm—Verminephrobacter symbiosis: an emerging experimental system to study extracellular symbiosis. *Front. Microbiol.* 5. <https://doi.org/10.3389/fmicb.2014.00128>
- Magdolenova, Z., Bilaniová, D., Pojana, G., Fjellsbø, L.M., Hudecova, A., Hasplova, K., Marcomini, A., Dusinska, M., 2012. Impact of agglomeration and different dispersions of titanium dioxide nanoparticles on the human related *in vitro* cytotoxicity and genotoxicity. *J. Environ. Monit.* 14, 455–464. <https://doi.org/10.1039/c2em10746e>
- Mincarelli, L., Tiano, L., Craft, J., Marcheggiani, F., Vischetti, C., 2019. Evaluation of gene expression of different molecular biomarkers of stress response as an effect of copper exposure on the earthworm *Eisenia andrei*. *Ecotoxicology* 28, 938–948. <https://doi.org/10.1007/s10646-019-02093-3>
- Mincarelli, L., Vischetti, C., Craft, J., Tiano, L., 2016. DNA damage in different *Eisenia andrei* coelomocytes sub-populations after *in vitro* exposure to hydrogen peroxide. *Springerplus* 5, 302. <https://doi.org/10.1186/s40064-016-1950-x>
- Müllerová, I., 2001. Imaging of specimens at optimized low and very low energies in scanning electron microscopes. *Scanning* 23, 379–394. <https://doi.org/10.1002/sca.4950230605>
- Natarajan, V., Wilson, C.L., Hayward, S.L., Kidambi, S., 2015. Titanium dioxide nanoparticles trigger loss of function and perturbation of mitochondrial dynamics in primary hepatocytes. *PLoS One* 10, 1–19. <https://doi.org/10.1371/journal.pone.0134541>

Chapter 7. References

- Navarro Pacheco, N.I., Roubalova, R., Dvorak, J., Benada, O., Pinkas, D., Kofronova, O., Semerad, J., Pivokonsky, M., Cajthaml, T., Bilej, M., Prochazkova, P., 2021a. Understanding the toxicity mechanism of CuO nanoparticles: the intracellular view of exposed earthworm cells. *Environ. Sci. Nano* 8, 2464–2477. <https://doi.org/10.1039/D1EN00080B>
- Navarro Pacheco, N.I., Roubalova, R., Semerad, J., Grasserova, A., Benada, O., Kofronova, O., Cajthaml, T., Dvorak, J., Bilej, M., Prochazkova, P., 2021b. *In Vitro* Interactions of TiO₂ Nanoparticles with earthworm coelomocytes: Immunotoxicity Assessment. *Nanomater.* (Basel, Switzerland) 11. <https://doi.org/10.3390/nano11010250>
- Oberdörster, E., Zhu, S., Blickley, T.M., McClellan-Green, P., Haasch, M.L., 2006. Ecotoxicology of carbon-based engineered nanoparticles: Effects of fullerene (C60) on aquatic organisms. *Carbon N. Y.* 44, 1112–1120. <https://doi.org/10.1016/j.carbon.2005.11.008>
- OECD, 2016. Test No. 222: Earthworm Reproduction Test (*Eisenia fetida/Eisenia andrei*). <https://doi.org/https://doi.org/https://doi.org/10.1787/9789264264496-en>
- OECD, 2010. Guidance manual for the testing of manufactured nanomaterials: OECD's Sponsorship Programme; First revision. Development 1–92.
- OECD, 1984. "Earthworm, Acute Toxicity Tests." OECD Guid. Test. Chem. 207, 2–8.
- Olive, P.L., Banáth, J.P., 2006. The comet assay: A method to measure DNA damage in individual cells. *Nat. Protoc.* 1, 23–29. <https://doi.org/10.1038/nprot.2006.5>
- Peixoto, S., Khodaparast, Z., Cornelis, G., Lahive, E., Green Etxabe, A., Baccaro, M., Papadiamantis, A.G., Gonçalves, S.F., Lynch, I., Busquets-Fite, M., Puentes, V., Loureiro, S., Henriques, I., 2020. Impact of Ag₂S NPs on soil bacterial community - A terrestrial mesocosm approach. *Ecotoxicol. Environ. Saf.* 206, 111405. <https://doi.org/10.1016/j.ecoenv.2020.111405>
- Pham, A.N., Xing, G., Miller, C.J., Waite, T.D., 2013. Fenton-like copper redox chemistry revisited: Hydrogen peroxide and superoxide mediation of copper-catalyzed oxidant production. *J. Catal.* 301, 54–64. <https://doi.org/10.1016/j.jcat.2013.01.025>
- Poon, W.L., Lee, J.C.Y., Leung, K.S., Alenius, H., El-Nezami, H., Karisola, P., 2020. Nanosized silver, but not titanium dioxide or zinc oxide, enhances oxidative stress and inflammatory response by inducing 5-HETE activation in THP-1 cells. *Nanotoxicology* 14, 453–467. <https://doi.org/10.1080/17435390.2019.1687776>
- Procházková, P., Roubalova, R., Dvorak, J., Navarro Pacheco, N.I., Bilej, M., 2020. Pattern recognition receptors in annelids. *Dev. Comp. Immunol.* 102, 103493. <https://doi.org/10.1016/j.dci.2019.103493>
- Prochazkova, P., Roubalova, R., Skanta, F., Dvorak, J., Pacheco, N.I.N., Kolarik, M., Bilej, M., 2019.

Chapter 7. References

- Developmental and Immune Role of a Novel Multiple Cysteine Cluster TLR From *Eisenia andrei* Earthworms. *Front. Immunol.* 10, 1277. <https://doi.org/10.3389/fimmu.2019.01277>
- Procházková, P., Šilerová, M., Felsberg, J., Josková, R., Beschin, A., De Baetselier, P., Bilej, M., 2006a. Relationship between hemolytic molecules in *Eisenia fetida* earthworms. *Dev. Comp. Immunol.* 30, 381–392. <https://doi.org/https://doi.org/10.1016/j.dci.2005.06.014>
- Procházková, P., Šilerová, M., Stijlemans, B., Dieu, M., Halada, P., Josková, R., Beschin, A., De Baetselier, P., Bilej, M., 2006b. Evidence for proteins involved in prophenoloxidase cascade *Eisenia fetida* earthworms. *J. Comp. Physiol. B Biochem. Syst. Environ. Physiol.* 176, 581–587. <https://doi.org/10.1007/s00360-006-0081-z>
- Qi, S., Wang, D., Zhu, L., Teng, M., Wang, C., Xue, X., Wu, L., 2018. Effects of a novel neonicotinoid insecticide cycloxaprid on earthworm, *Eisenia fetida*. *Environ. Sci. Pollut. Res.* 25, 14138–14147. <https://doi.org/10.1007/s11356-018-1624-z>
- Reeves, J.F., Davies, S.J., Dodd, N.J.F., Jha, A.N., 2008. Hydroxyl radicals (OH) are associated with titanium dioxide (TiO₂) nanoparticle-induced cytotoxicity and oxidative DNA damage in fish cells. *Mutat. Res. Mol. Mech. Mutagen.* 640, 113–122. <https://doi.org/https://doi.org/10.1016/j.mrfmmm.2007.12.010>
- Reinecke, F., Levanets, O., Olivier, Y., Louw, R., Semete, B., Grobler, A., Hidalgo, J., Smeitink, J., Olckers, A., Van Der Westhuizen, F.H., 2006. Metallothionein isoform 2A expression is inducible and protects against ROS-mediated cell death in rotenone-treated HeLa cells. *Biochem. J.* 395, 405–415. <https://doi.org/10.1042/BJ20051253>
- Reynolds, G.S., 1963. Potency of Conditioned Reinforcers Based on Food and on Food and Punishment. *Science* 139, 838–839. <https://doi.org/10.1126/science.139.3557.838>
- Ritchie, N., Davis, J.M., Newbury, D.E., 2008. DTSA-II: A New Tool for Simulating and Quantifying EDS Spectra - Application to Difficult Overlaps. *Microsc. Microanal.* 14, 1176–1177. <https://doi.org/DOI:10.1017/S143192760808361X>
- Roch, P., 1979. Protein analysis of earthworm coelomic fluid: 1) polymorphic system of the natural hemolysin of *Eisenia fetida andrei*. *Dev. Comp. Immunol.* 3, 599–608. [https://doi.org/10.1016/s0145-305x\(79\)80055-5](https://doi.org/10.1016/s0145-305x(79)80055-5)
- Roubalová, R., Dvořák, J., Procházková, P., Škanta, F., Navarro Pacheco, N.I., Semerád, J., Cajthaml, T., Bilej, M., 2018. The role of CuZn- and Mn-superoxide dismutases in earthworm *Eisenia andrei* kept in two distinct field-contaminated soils. *Ecotoxicol. Environ. Saf.* 159, 363–371. <https://doi.org/https://doi.org/10.1016/j.ecoenv.2018.04.056>

Chapter 7. References

Roubalová, R., Procházková, P., Dvořák, J., Škanta, F., Bilej, M., 2015. The role of earthworm defense mechanisms in ecotoxicity studies. *Invertebr. Surviv. J.* 12, 203–213.

Schlich, K., Klawonn, T., Terytze, K., Hund-Rinke, K., 2013. Effects of silver nanoparticles and silver nitrate in the earthworm reproduction test. *Environ. Toxicol. Chem.* 32, 181–188. <https://doi.org/10.1002/etc.2030>

Schultz, C.L., Gray, J., Verweij, R.A., Busquets-Fité, M., Puentes, V., Svendsen, C., Lahive, E., Matzke, M., 2018. Aging reduces the toxicity of pristine but not sulphidised silver nanoparticles to soil bacteria. *Environ. Sci. Nano* 5, 2618–2630. <https://doi.org/10.1039/C8EN00054A>

Sekine, R., Brunetti, G., Donner, E., Khaksar, M., Vasilev, K., Jämting, Å.K., Scheckel, K.G., Kappen, P., Zhang, H., Lombi, E., 2015. Speciation and Lability of Ag-, AgCl-, and Ag₂S-Nanoparticles in Soil Determined by X-ray Absorption Spectroscopy and Diffusive Gradients in Thin Films. *Environ. Sci. Technol.* 49, 897–905. <https://doi.org/10.1021/es504229h>

Semerád, J., Čvančarová, M., Filip, J., Kašlík, J., Zlotá, J., Soukupová, J., Cajthaml, T., 2018. Novel assay for the toxicity evaluation of nanoscale zero-valent iron and derived nanomaterials based on lipid peroxidation in bacterial species. *Chemosphere* 213, 568–577. <https://doi.org/10.1016/j.chemosphere.2018.09.029>

Semerád, J., Moeder, M., Filip, J., Pivokonský, M., Filipová, A., Cajthaml, T., 2019. Oxidative stress in microbes after exposure to iron nanoparticles: analysis of aldehydes as oxidative damage products of lipids and proteins. *Environ. Sci. Pollut. Res.* 26, 33670–33682. <https://doi.org/10.1007/s11356-019-06370-w>

Semerad, J., Pacheco, N.I.N., Grasserova, A., Prochazkova, P., Pivokonsky, M., Pivokonska, L., Cajthaml, T., 2020. *In Vitro* Study of the Toxicity Mechanisms of Nanoscale Zero-Valent Iron (nZVI) and Released Iron Ions Using Earthworm Cells. *Nanomater.* (Basel, Switzerland) 10. <https://doi.org/10.3390/nano10112189>

Šíma, P., 1994. Annelid coelomocytes and haemocytes: roles in cellular immune reactions, in: *Immunology of Annelids*. CRC Press Boca Raton, pp. 115–165.

Škanta, F., Procházková, P., Roubalová, R., Dvořák, J., Bilej, M., 2016. LBP/BPI homologue in *Eisenia andrei* earthworms. *Dev. Comp. Immunol.* 54, 1–6. <https://doi.org/10.1016/j.dci.2015.08.008>

Škanta, F., Roubalová, R., Dvořák, J., Procházková, P., Bilej, M., 2013. Molecular cloning and expression of TLR in the *Eisenia andrei* earthworm. *Dev. Comp. Immunol.* 41, 694–702. <https://doi.org/10.1016/j.dci.2013.08.009>

Sukhanova, A., Bozrova, S., Sokolov, P., Berestovoy, M., Karaulov, A., Nabiev, I., 2018. Dependence of Nanoparticle Toxicity on Their Physical and Chemical Properties. *Nanoscale Res. Lett.* 13, 44. <https://doi.org/10.1186/s11671-018-2457-x>

Chapter 7. References

Swartzwelter, B.J., Mayall, C., Alijagic, A., Barbero, F., Ferrari, E., Hernadi, S., Michelini, S., Navarro Pacheco, N.I., Prinelli, A., Swart, E., Auguste, M., 2021. Cross-Species Comparisons of Nanoparticle Interactions with Innate Immune Systems: A Methodological Review. *Nanomater.* (Basel, Switzerland) 11. <https://doi.org/10.3390/nano11061528>

Tatsi, K., Shaw, B.J., Hutchinson, T.H., Handy, R.D., 2018. Copper accumulation and toxicity in earthworms exposed to CuO nanomaterials: Effects of particle coating and soil ageing. *Ecotoxicol. Environ. Saf.* 166, 462–473. <https://doi.org/10.1016/j.ecoenv.2018.09.054>

Thiagarajan, V., Ramasubbu, S., 2021. Fate and Behaviour of TiO₂ Nanoparticles in the Soil: Their Impact on Staple Food Crops. *Water, Air, Soil Pollut.* 232. <https://doi.org/10.1007/s11270-021-05219-8>

Tortella, G.R., Rubilar, O., Durán, N., Diez, M.C., Martínez, M., Parada, J., Seabra, A.B., 2020. Silver nanoparticles: Toxicity in model organisms as an overview of its hazard for human health and the environment. *J. Hazard. Mater.* 390, 121974. <https://doi.org/10.1016/j.jhazmat.2019.121974>

Tumminello, R.A., Fuller-espie, S.L., 2013. Heat stress induces ROS production and histone phosphorylation in celomocytes of *Eisenia hortensis*. *Invertebrate Survival Journal.* 50–57.

Vaillier, J., Cadoret, M.A., Roch, P., Valembois, P., 1985. Protein analysis of earthworm coelomic fluid. III. Isolation and characterization of several bacteriostatic molecules from *Eisenia fetida andrei*. *Dev. Comp. Immunol.* 9, 11–20. [https://doi.org/10.1016/0145-305x\(85\)90055-2](https://doi.org/10.1016/0145-305x(85)90055-2)

Valdeiglesias, V., Kiliç, G., Costa, C., Fernández-Bertólez, N., Pásaro, E., Teixeira, J.P., Laffon, B., 2015. Effects of Iron Oxide Nanoparticles: Citotoxicity, Genotoxicity, Developmental Toxicity, and Neurotoxicity. *Environ. Mol. Mutagen.* 56, 125–148. <https://doi.org/10.1002/em>

Valembois, P., Seymour, J., Lassègues, M., 1994. Evidence of lipofuscin and melanin in the brown body of the earthworm *Eisenia fetida andrei*. *Cell Tissue Res.* 277, 183–188. <https://doi.org/10.1007/BF00303095>

Wang, P., Menzies, N.W., Lombi, E., Sekine, R., Blamey, F.P.C., Hernandez-Soriano, M.C., Cheng, M., Kappen, P., Peijnenburg, W.J.G.M., Tang, C., Kopittke, P.M., 2015. Silver sulfide nanoparticles (Ag₂S-NPs) are taken up by plants and are phytotoxic. *Nanotoxicology* 9, 1041–1049. <https://doi.org/10.3109/17435390.2014.999139>

Wang, T., Liu, W., 2022. Emerging investigator series: metal nanoparticles in freshwater: transformation, bioavailability and effects on invertebrates. *Environ. Sci. Nano.* <https://doi.org/10.1039/D2EN00052K>

Wang, Z., von dem Bussche, A., Kabadi, P.K., Kane, A.B., Hurt, R.H., 2013. Biological and Environmental Transformations of Copper-Based Nanomaterials. *ACS Nano* 7, 8715–8727. <https://doi.org/10.1021/nn403080y>

Chapter 7. References

- Wu, J., Sun, J., Xue, Y., 2010. Involvement of JNK and P53 activation in G2/M cell cycle arrest and apoptosis induced by titanium dioxide nanoparticles in neuron cells. *Toxicol. Lett.* 199, 269–276. <https://doi.org/10.1016/j.toxlet.2010.09.009>
- Yang, Y., Xiao, Y., Li, M., Ji, F., Hu, C., Cui, Y., 2017. Evaluation of complex toxicity of carbon nanotubes and sodium pentachlorophenol based on earthworm coelomocytes test. *PLoS One* 12. <https://doi.org/10.1371/journal.pone.0170092>
- Yirsaw, B.D., Mayilswami, S., Megharaj, M., Chen, Z., Naidu, R., 2016. Effect of zero valent iron nanoparticles to *Eisenia fetida* in three soil types. *Environ. Sci. Pollut. Res.* 23, 9822–9831. <https://doi.org/10.1007/s11356-016-6193-4>
- Zhang, C., Zhu, L., Wang, Jun, Wang, Jinhua, Du, Z., Li, B., Zhou, T., Cheng, C., Wang, Z., 2018. Evaluating subchronic toxicity of fluoxastrobin using earthworms (*Eisenia fetida*). *Sci. Total Environ.* 642, 567–573. <https://doi.org/10.1016/j.scitotenv.2018.06.091>
- Zhang, Z., Trautmann, K., Schluesener, H.J., 2005. Microglia activation in rat spinal cord by systemic injection of TLR3 and TLR7/8 agonists. *J. Neuroimmunol.* 164, 154–160. <https://doi.org/10.1016/j.jneuroim.2005.03.014>
- Zhu, Y., Wu, X., Liu, Y., Zhang, J., Lin, D., 2020. Integration of transcriptomics and metabolomics reveals the responses of earthworms to the long-term exposure of TiO₂ nanoparticles in soil. *Sci. Total Environ.* 719, 137492. <https://doi.org/10.1016/j.scitotenv.2020.137492>

Annexes



Annex I

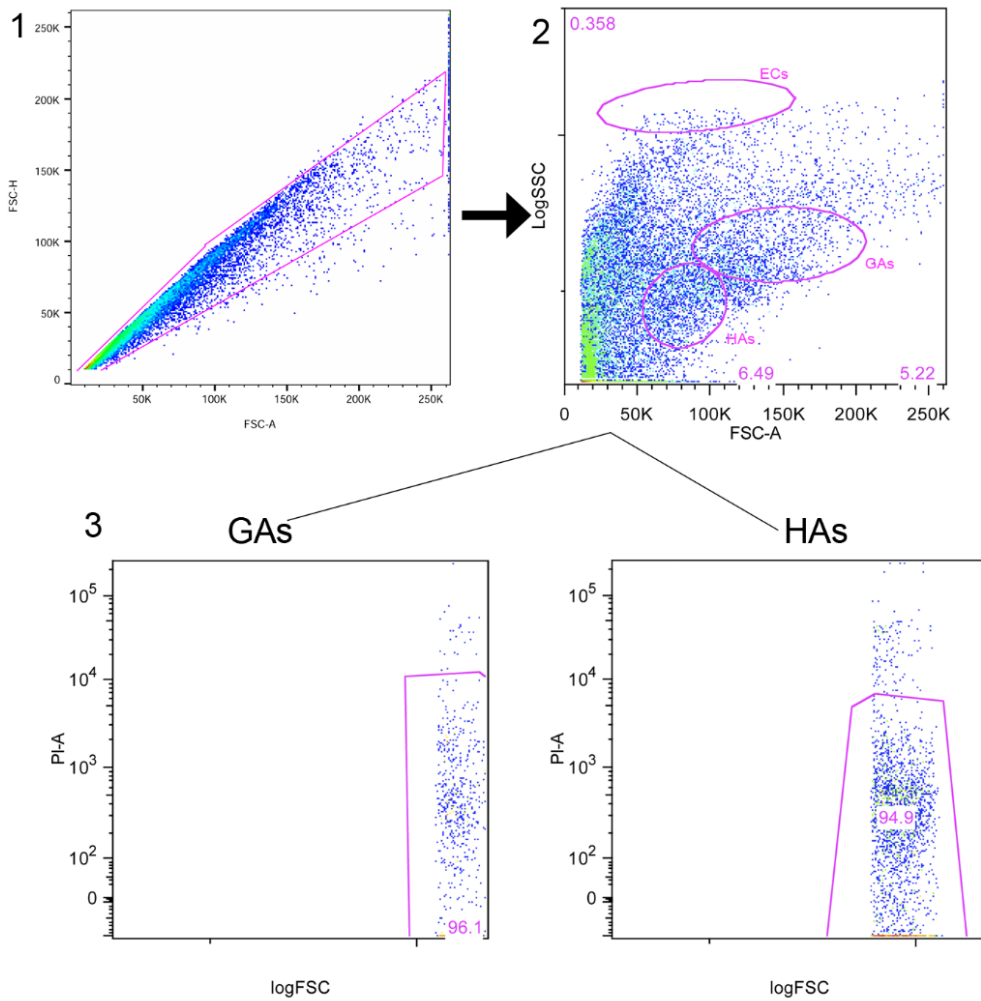


Figure 34. Illustrative image of FACS analyses. 1. The singlets. 2. Subpopulations detection. 3. Cellular viability stained with PI. Images are from control samples at 2 h incubation.

At Figure 34, it was described the steps prior to analyse ROS, phagocytosis and apoptosis. Step 1. Singlets was the step of detection of one cell. The events out of the pink box meant that there was double cells stucked together so the cytometer discarded them for the analyses. From the selected singlet, at the step 2, we detected the different subpopulations (ECs, HAs and GAs). The combination of the log SSC and the FSC aided to detect the different subpopulations. Then, at each subpopulation, the viability with PI staining was analysed (step 3; Figure 34). Dead cells were found over 10⁴ in PI axis. However, every study included no PI staining to accurate the boxes and assure the right selections. Probably, more than 3000 thousand samples were carried out during the thesis in the flow cytometer. ROS and phagocytosis were analysed based on the viable cells determined in Figure 34. The gating process could be observed through Figure 34, 35 and 36. Every assay contained triplicates of the non-staining cells. Negative controls were also included in the analyses performed. The negative controls (100 mM H₂O₂) affected the cells producing

high quantity of ROS (Figure 35 A) or a high decrease of phagocytic activity (Figure 35 B). At the case of phagocytosis (Figure

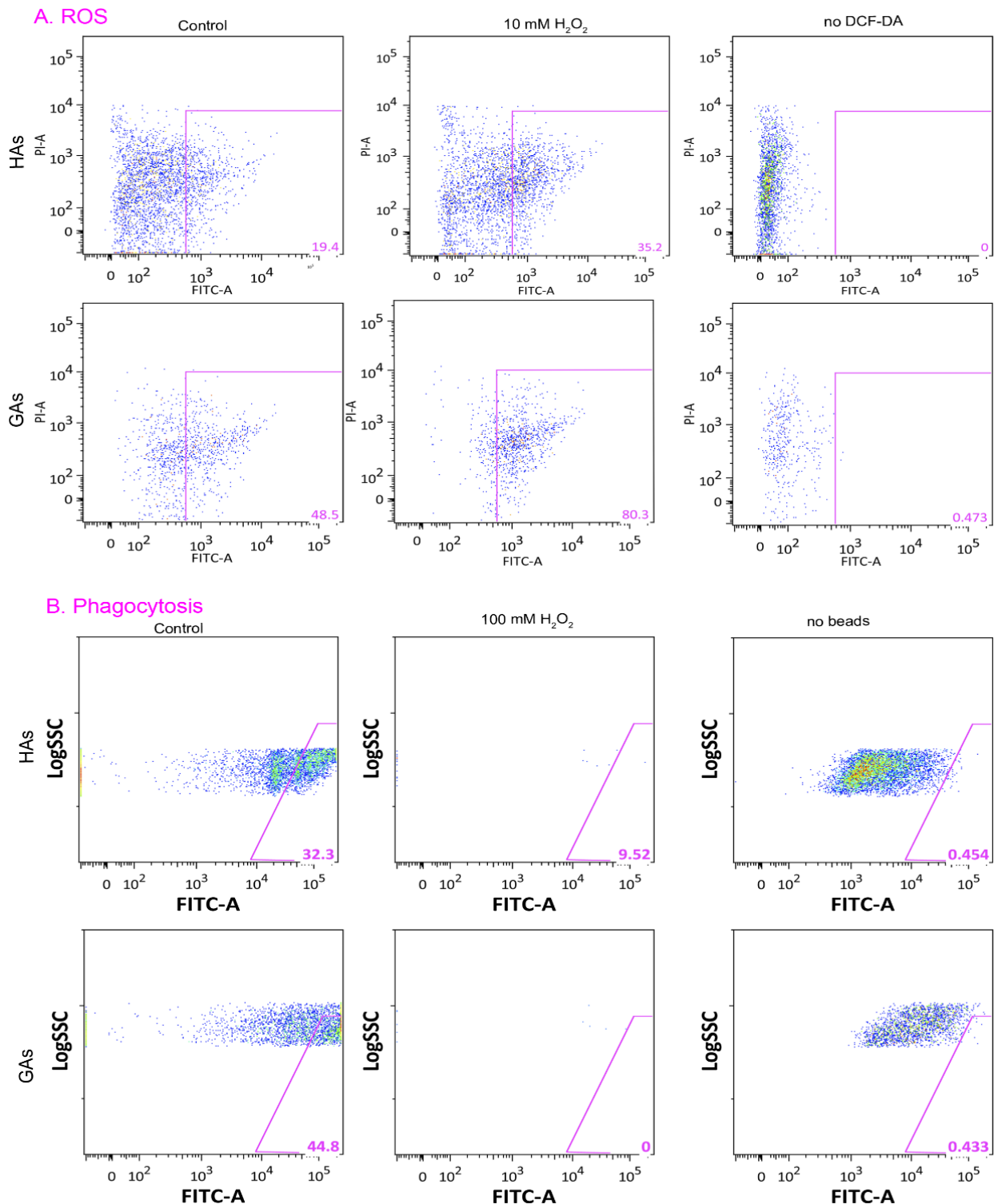


Figure 35. Illustrative image of ROS and phagocytosis. A) ROS activity detected in HAS and GAS for control, 10 mM H₂O₂ and no DCF-DA staining. B) the phagocytic activity detected in HAS and GAS for control, 100 mM H₂O₂ and no beads. The data was collected after 2 h of incubation.

35 no beads) and apoptosis (Figure 36, PI and no Annexin V). The values observed were subtracted from the controls and NPs data to eliminate the background noise.

The apoptosis was performed by the staining of Alexa 647-Annexin V staining. The illustrative image showed the necrosis, late apoptosis, early apoptosis and viable coelomocytes (Figure 36). The determination of the gates was associated with the laser emission so if the coelomocytes were positive to PI and Annexin V, then it was late apoptosis. If they were only positive to Annexin V, they were undergoing into early apoptosis. The viability was determined when coelomocytes were negative to Annexin V and PI. The necrosis was only positive to PI. Alexa 647-Annexin V staining was in a different wavelength than PI. Positive to PI or Annexin V meant that the coelomocytes emitted fluorescences in both wavelengths were PI and Alexa 647-Annexin V were.

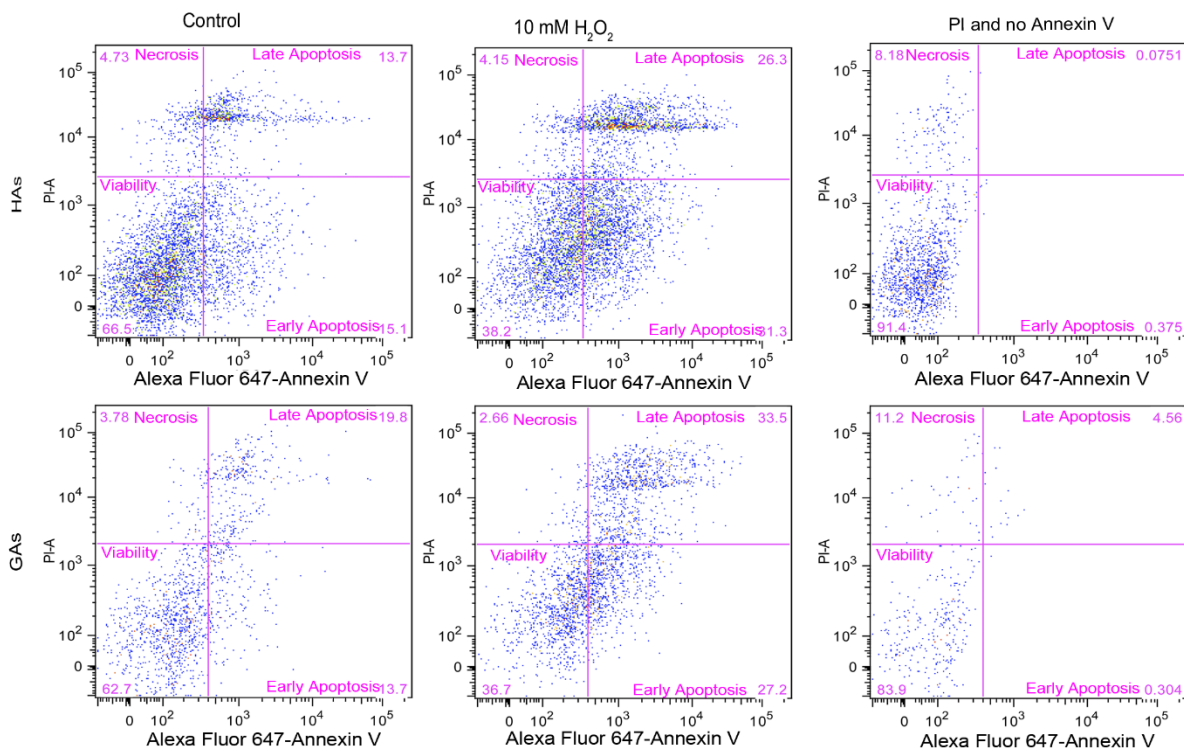


Figure 36. Illustrative image of apoptosis. Apoptosis was analysed in HAs and GAs in the control, 10 mM H₂O₂ and, the PI and no Annexin V. The data was obtained after 2 h of incubation.

Annex II. Chemicals and Instruments

Name	Manufacturer	Country
0,4 % Trypan blue solution	Sigma-Aldrich	Steinheim, Germany
1 M HEPES	Sigma-Aldrich	Gillingham, UK
2',7'-dichlorofluorescein diacetate (DCF-DA)	Sigma-Aldrich	Steinheim, Germany
2-hydroxyethyl agarose (LMA)	Sigma-Aldrich	Steinheim, Germany
5 μ L capillary Bran™ Blaubrand® micropipettes	Sigma-Aldrich	Wertheim, Germany
Aeroxide TiO ₂ P25 NPs	Evonik Degussa	Essen, Germany
Ag ICP standards	Merck	Darmstadt, Germany
Ag ₂ S NPs	Applied Nanoparticles S.L	Barcelona, Spain
Ag ₂ S NPs stabilized in 1 mg mL ⁻¹ 55kDA Polyvinylpyrrolidone (PVP)	Applied Nanoparticles S.L.	Barcelona, Spain
AgNO ₃	Sigma-Aldrich	Steinheim, Germany
Alexa Fluor 647-Annexin V	Thermo Fisher Scientific	Eugene, OR, USA
Annexin V binding buffer	Thermo Fisher Scientific	Eugene, OR, USA
Antibiotic-antimycotic solution	Sigma-Aldrich	Steinheim, Germany
Carbon coated 400 mesh copper grids (G400)	SPI Supplies, Structure Probe Inc.	West Chester, PA, USA
Carbon stabilized 200-mesh copper grids	Ted-Pella Inc.	Redding, CA, USA
CuO NPs	Promethean Particles Ltd.	Nottingham, United Kingdom
CuSO ₄	Sigma-Aldrich	Steinheim, Germany
Dopamine hydrochloride	Sigma-Aldrich	Steinheim, Germany
EDTA	Sigma-Aldrich	Steinheim, Germany
Epoxy resin (EMBed-812 Embedding kit)	Electron Microscopy Sciences	Hatfield, PA, USA
Fetal Bovine Serum (FBS)	Life Technologies	Carlsbad, CA, USA
Fluoresbrite® Plain YG	Polysciences Inc.	Warrington, PA, US
Gentamicin	Sigma-Aldrich	Steinheim, Germany
Guaiacol glyceryl ether (GGE)	Sigma-Aldrich	Steinheim, Germany

H ₂ O ₂	Sigma-Aldrich	Steinheim, Germany
HCl	Pentachemicals	Prague, Czech Republic
HNO ₃	Pentachemicals	Prague, Czech Republic
L-Arginine	Sigma-Aldrich	Steinheim, Germany
LUFA soil 2.1	LUFA Speter	Speyer, Germany
NaCl	Lachner	Neratovice, Czech Republic
N-alpha-naphtyl-ethylenediamine	Sigma-Aldrich	Steinheim, Germany
NaNO ₂	Sigma-Aldrich	Steinheim, Germany
NaOH	Sigma-Aldrich	Steinheim, Germany
Oligo (dT)12-18 primer	Life Technologies	Carlsbad, CA, USA
PBS	MP Biologicals	Illkirch-Graffenstaden, France
Phosphoric acid	Sigma-Aldrich	Steinheim, Germany
Propidium iodide (PI)	Sigma-Aldrich	Steinheim, Germany
RNAqueous® Micro Kit	Invitrogen	Vilnius, Lithuania
RPMI 1640 with ultramine glutamine	Lonza BioWhitaker®	Belgium
Sodium dodecyl sulfate (SDS)	Serva	Heidelberg, Germany
Sulphanilamide	Sigma-Aldrich	Steinheim, Germany
Superscript IV Reverse Transcriptase	Life Technologies	Carlsbad, CA, USA
Thermanox Plastic Coverslips	Nunc, Thermo Fisher Scientific	Roskilde, Denmark
Ti-grids	SPI Supplies, Structure Probr Inc.	West Chester, PA, USA
Tris	AppliChem	Darmstadt, Germany
Triton X-100	Sigma-Aldrich	Steinheim, Germany

Table 8. Chemicals and reagents

Name	Manufacturer	Country
Agilent Cary 60 UV-Vis Spectrophotometer	Agilent Technologies	Santa Clara, CA, USA
Ametek® EDAX Octane Plus SDD detector	AMETEK B.V.	Tilburg, The Netherlands
Bürker chamber	The Paul marienfield GmbH&Co	Lauda-Königshofen, Germany
CFX96 Touch™ Real-Time PCR detection System	Bio-Rad Laboratories Inc.	Hercules, CA, USA
Confocal Microscope Olympus FV1000 TIRF	Olympus Life Sciences	Hamburg, Germany
Fast Prep 24	MP Biomedicals	Santa Ana, CA, USA
FEI Nova NanoSEM	FEI	Brno, Czech Republic
Fiel-emission scanning electron microscope (FE-SEM) Hitachi SU6600	Hitachi High-Tech Corporation	Tokyo, Japan
Flow cytometer (LSR II)	BD Biosciences	San Jose, CA, USA
Flowjo (9.9.4 version)	BD Biosciences	San Jose, CA, USA
GraphPad Prism (8.3.1 versio)	GraphPad software	San Diego, CA, USA
High-performance liquid chromatography with fluorescence detection (HPLC-FLD)	Alliance Waters HPLC system	Prague, Czech Republic
Image J software	NIH	Bethesda, Maryland, USA
Inductively coupled plasma optical emission spectrophotometer (ICP-OES, 5110 Series)	Agilent Technologies	USA
Inkscape	Inkscape software	USA
iTEM software	EMSIS GmbH	Muenster, Germany
JEOL F200 electron microscope with HAADF detector and JED-2300 X-Ray	JEOL Ltd.	Akishima, Tokyo, Japan
K850 Critical Point Dryer	Quorum Technologies Ltd.	Rignmer, UK

Lucia Comet Assay Software	Laboratory Imaging Ltd.	Prague, Czech Republic
Malvern Zetasizer Nano ZS90 analyzer	Malvern Instruments Ltd.	Worcestershire, UK
MARS 5	CEM Corporaion	USA
Nanodrop 2000c spectrpphotometer	Thermo Scientific™	Willmington, DE, USA
NIST DTSA Software	NIST	Gaithersburg, USA
Origin Lab software 2019b	OriginLab Corporation	Northampton, MA,USA
Philips CM100 Electron Microscope	Philips EO	Eindhoven, Netherlands
TEAM™ EDS Analyses Systems	AMETEK B.V.	Tilburg, The Netherlands
TECAN 200 Pro plate Reader	Tecan Trading AG	Männedorf, Switzerland
TECAN Infinite M200 PRO	Tecan Trading AG	Männedorf, Switzerland
Turbo-Pumped Sputter Coater Q150T	Quorum Technologies Ltd.	Rignmer, UK
Veleta-slow scan CCD camera	EMSIS GmbH	Muenster,Germany
Zetasizer Ultra	Malvern Panalytical	UK

Table 9. Instruments



Natividad Isabel Navarro Pacheco

Email: nanapa@alumni.uv.es

ORCID: 0000-0001-9064-0666

ResearchID: AAG-6783-2019

Scopus: 57219848097

LinkedIn: Natividad Navarro

Dirección de trabajo:

Instituto CAVanilles de Biodiversidad y Biología Evolutiva, Universida de Valencia, c/Catedrático José Beltrán 2, 46980 Paterna, Valencia, Spain

Conferencias

PhD Conference in Immunology, Prague, Czech Republic, 2019

12th International Particle Toxicology Conference en Salzburgo, Austria, 2019

Interaction of the innate immune system with nanoparticles: perspectives for understanding environmental and human adaptation and health, Salzburgo, Austria, 2019

Food, Microbiota and Immunity. For strong immunity - feed your microbiota well, 2017

EXPERIENCIA LABORAL

2021-2022	<p><u>Área:</u> Instituto Cavanilles de Biodiversidad y Biología Evolutiva</p> <p><u>Proyecto:</u> Efecto de las nanopartículas en el sistema inmune de la lombriz <i>Eisenia andrei</i>.</p> <p><u>Funciones:</u> colaboración en el laboratorio, aprendizaje de nuevas técnicas y participación en mesocosmos.</p>
2019-2021	<p><u>Área:</u> Laboratorio de inmunología celular y molecular. Laboratorio de Biotecnología Ambiental en el Institute of Microbiology of the CAS (Praga, República Checa).</p> <p><u>Proyecto:</u> Efecto de las nanopartículas en el sistema inmune de la lombriz <i>Eisenia andrei</i>.</p> <p><u>Funciones:</u> colaboración con el laboratorio de biotecnología ambiental mediante la aplicación de la metodología optimizada y desarrollada para <i>Eisenia andrei</i> (lombriz de tierra) y análisis con otro tipo de compuestos diferentes a las nanopartículas.</p> <p><u>Referencias:</u> Jefe del laboratorio prof. RNDr. Tomas Cajthaml y RNDr. Petra Procházková, Ph.D. Institute of Microbiology of the CAS, v. v. i. Vídeňská 1083,142 20, Prague (Czech Republic).</p>
2016-2021	<p>ITN Programme en H2020 Marie Skłodowska- Curie.</p> <p><u>Área:</u> Laboratorio de inmunología celular y molecular Probing safety of nano-objects by defining immune responses of environmental organisms (PANDORA project).</p> <p><u>Proyecto:</u> Efecto de las nanopartículas en el sistema inmune de la lombriz <i>Eisenia andrei</i>.</p> <p><u>Funciones:</u> Optimización de cultivo celular de células inmune de <i>E. andrei</i>, ensayos de fagocitosis, apoptosis, estrés oxidativo ,genotoxicidad y caracterización de nanopartículas.</p>
2014-2015	<p>Prácticas de empresa en el Instituto Tecnológico de Transporte, Embalaje y Logística (ITENE). Paterna, Valencia. Departamento de Seguridad.</p> <p><u>Área:</u> Sector plástico y alimentación/ I+D</p> <p><u>Puesto:</u> Ayudante en proyectos de I+D en el área de Nanoseguridad.</p> <p><u>Funciones:</u> Apoyo a proyectos I+D dentro de la línea de seguridad de nanomateriales, identificación de propiedades fisicoquímicas, toxicológicas y ecotoxicológicas. Redacción de informes, recopilación y actualización bibliográfica de la base de datos REACHnano.</p> <p><u>Referencias:</u> Carlos Fito López. Responsable del Departamento de Seguridad. Coordinador de proyectos en la Línea tecnológica de Nanoseguridad y riesgos</p>

<p>PhD Conference in Immunology, Praga, República Checa, 2017</p> <p>Cursos y seminarios</p> <p>Comunicación al público en general y comunicación de riesgos, Salzburgo (Austria), 2019</p> <p>El Sistema inmune de las plantas. University of Tübingen, Tübingen, Alemania, 2018</p> <p>Habilidades de comunicación científica y redacción de subvenciones., Nápoles, 2018</p> <p>Inmunidad de invertebrados terrestres. Evaluación del impacto de los NP en las células inmunes de invertebrados: un enfoque de toxicología sistémica, Cardiff, UK, 2017</p> <p>Investigación e innovación responsable desde el laboratorio, Barcelona, España, 2017</p> <p>Capacidades y competencias:</p> <p>Idioma nativo: Castellano y valenciano (C1)</p> <p>Otros idiomas: Inglés (Advanced, CAE, C1)</p> <p>Ofimática: Competente en todo el paquete Office. Carnet de conducir: Disponible (Permiso B).</p> <p>Curso de Introducción a la Gestión de proyectos. (5 semanas; Noviembre 2015)</p> <p>Carnet de usuario profesional de productos fitosanitarios (Generalitat Valenciana; Octubre 2015)</p> <p>Voluntariado en International Valencia Hockey World League Semi-Final Spain en Valencia desarrollando labores de bienvenida y guía a oficiales de la federación en el aeropuerto y ayudante con los grupos de otros países y de recepción (10 días; Junio 2015)</p> <p>Acreditación ABET de la carrera Ingeniero Agrónomo (Septiembre 2014)</p> <p>Segundo Premio de la IV edición del Premio Ideas Comerciales, "Innovación y Excelencia Comercial" de la Cátedra CONSUM (Noviembre 2011).</p> <p>Curso de formación sobre medio ambiente: El Suelo y los Incendios Forestales. Font Roja, Alcoy (14 horas; Julio 2010).</p>	<p>2013-2014</p> <p>Instituto de Ingeniería del Agua y Medio Ambiente (IIAMA). Departamento de Química y Microbiología del Agua.</p> <p><u>Área:</u> I+D</p> <p><u>Puesto:</u> Ayudante en tareas de Investigación en Laboratorio de Microbiología</p> <p><u>Funciones:</u> Técnicas moleculares FISH y DVC-FISH, tratamiento y análisis microbiológico de aguas residuales, utilización de sondas y microscopios de fluorescencias, recopilación bibliográfica y trabajo rutinario de un laboratorio de microbiología tanto en preparación de material como en desarrollo de los ensayos.</p>
<p>ESTUDIOS</p>	
<p>2021-2022</p> <p>Universidad de Valencia.</p> <p>Doctorado en contaminación, toxicología y sanidad ambientales.</p> <p><u>Supervisores:</u> Andreu Rico. Codirectores: Tomás Cajthmal, Petra Prochazkova. Tutor: Antonio Camacho</p> <p>2016-2021</p> <p>Charles University en Praga (República Checa), 1º Facultad de Medicina</p> <p>Doctorado en Inmunología</p> <p>Field of study: Immunology (YMUI9)</p> <p><u>Proyecto:</u> El efecto de las nanopartículas en el sistema inmune de las lombrices <i>Eisenia andrei</i> Supervisora: Petra Prochazkova, PhD.</p> <p>2014-2015</p> <p>Universidad de Valencia</p> <p>Máster en Contaminación, Toxicología y Sanidad Ambiental.</p> <p>Estudiante de master en el Instituto Tecnológico de Transporte, Embalaje y Logística (ITENE) en Valencia (España).</p> <p>Trabajo Fin de Máster: Análisis comparativo de la toxicidad ambiental de nanopartículas de óxidos de aluminio y hierro para su uso en formulaciones de tintas conductivas.</p> <p><u>Supervisores:</u> Carlos Fito López and Dr. Óscar Andreu Sánchez.</p> <p>2012-2013</p> <p>Estancia de ERASMUS en la Universidad de Gante (Bélgica) UNIVERSITEIT GENT</p> <p>Master of Science in Environmental Sanitation/Master of Science in Physical Land Resources</p>	

Diploma del curso: Ingeniero Consultor. Organizado por Grupo Typsa y la Escuela Técnica Superior de Ingeniería Agronómica y Medio Natural (ETSIAMN) (14 horas; Octubre 2009)	2007-2014 Universidad Politécnica de Valencia Ingeniero Agrónomo Especialidad: Recursos ambientales Trabajo final de carrera: Estudio de Comunidades Microbianas complejas mediante la técnica DVC-FISH en MBRs y fangos de depuradora <u>Supervisores:</u> Dr. José Luis Alonso Molina and Dra. Yolanda Moreno Trigos.
	EXPERIENCIA TÉCNICA
	<p><u>Biología molecular:</u> extracción y aislamiento de ARN, PCR, qPCR, electroforesis, electroforesis unicelular (ensayo del cometa alcalino), cultivos celulares</p> <p><u>Técnicas básicas de inmunología:</u> citometría de flujo</p> <p><u>Bases de datos:</u> Pubmed, science direct</p> <p><u>Interpretación y presentación de resultados:</u> MS Office, GraphPad Prism, Bio-Rad CFZ Manager, SPSS, LUCIA comet assay software, Matlab.</p> <p><u>Microscopía:</u> confocal, microscopio de fluorescencia, microscopía electrónica.</p> <p><u>Caracterización de nanopartículas:</u> Malvern Z Sizer (MADLS, Zeta Potential)</p> <p><u>Programas de fotografía:</u> Photoshop AutoCAD</p> <p><u>Experimentos <i>in vivo</i>:</u> trabajo de suelos, preparación para la correcta humedad, manejo con las normas OECD 222, OECD 207.</p>
	INTERCAMBIO ACADÉMICO
	Comparación de métodos y datos en <i>E. foetida</i> , Natural Environmental Research Council, Wallingford, UK, 2018 Desarrollo de metodología en Ljubljana, (Univerza v Ljubljana), Ljubljana, Eslovenia. Research group for nanobiology and nanotoxicology at the Biotechnical faculty, 14 días, 2018
PUBLICACIONES	
<p><u>Effects of silver sulfide nanoparticles on the earthworm <i>Eisenia andrei</i>.</u> Navarro Pacheco, et al., Comp. Biochem. Physiol. Part C Toxicol. Pharmacol. 2022.. 257, 109355. https://doi.org/https://doi.org/10.1016/j.cbpc.2022.109355 . IF: 4.16</p> <p><u>Understanding the toxicity mechanism of CuO nanoparticles: the intracellular view of exposed earthworm cells.</u> Navarro Pacheco NI et al., Environmental Science: Nano. 2021 https://doi.org/10.1039/D1EN00080B. IF: 8.06</p> <p><u>Cross-Species Comparisons of Nanoparticle Interactions with Innate Immune Systems: A Methodological Review.</u> Swartzwelter BJ et al., Nanomaterials. 2021; 11(6):1528. https://doi.org/10.3390/nano11061528. IF: 4.921</p> <p><u><i>In Vitro</i> Interactions of TiO₂ Nanoparticles with Earthworm Coelomocytes: Immunotoxicity Assessment.</u> Navarro Pacheco NI et al., Nanomaterials. 2021; 11(1):250. https://doi.org/10.3390/nano11010250. IF: 4.921</p> <p><u><i>In Vitro</i> Study of the Toxicity Mechanisms of Nanoscale Zero-Valent Iron (nZVI) and Released Iron Ions Using Earthworm Cells.</u> Semerad J et al., Nanomaterials. 2020; 10(11):2189. https://doi.org/10.3390/nano10112189. IF: 5.4</p>	

PUBLICACIONES

Addressing Nanomaterial Immunosafety by Evaluating Innate Immunity across Living Species. Boraschi D et al., Small 2020, 16, 2000598. <https://doi.org/10.1002/sml.202000598>. IF: 13.281

Pattern recognition receptors in annelids. Prochazkova P. et al., Dev. Comp. Immunol. 2020, 102, 103493. doi: 10.1016/j.dci.2019.103493. IF: 3.49

Developmental and immune role of a novel multiple cysteine cluster TLR from *Eisenia Andrei* Earthworms. Prochazkova P. et al., Front. Immunol. 2019, 10. doi: 10.3389/fimmu.2019.01277 IF: 6.429

The role of CuZn- and Mn-superoxide dismutases in earthworm *Eisenia andrei* kept in two distinct field contaminated soils. Roubalová R. et al., Ecotoxicol. Environ. Saf. 2018, 159,363–371. doi: 10.1016/j.ecoenv.2018.04.056. IF: 4.527

Contribution of *Eisenia andrei* earthworms in pathogen reduction during vermicomposting. Procházková P. et al., Environ. Sci. Pollut. Res. 2018, 25, 26267–26278. doi: 10.1007/s11356-018-2662-2. IF: 2.914

Annelida: Environmental Interactions and Ecotoxicity in Relation to the Earthworm Immune System. Roubalová R. et al., In: Cooper E. (eds) Advances in Comparative Immunology. Springer, Cham. 2018 Doi: 10.1007/978-3-319-76768-0_27.

